EFFECTS OF COASTAL TRANSITIONS ON CLOUD-TO-GROUND LIGHTNING

A Thesis

by

AARON MARK STUDWELL

Submitted to the Office of Graduate Studies of
Texas A&M University
in partial fulfillment of the requirements for the degree of

MASTER OF SCIENCE

August 1995

Major Subject: Meteorology

EFFECTS OF COASTAL TRANSTIONS ON

CLOUD-TO-GROUND LIGHTNING

A Thesis

by

AARON MARK STUDWELL

Submitted to Texas A&M University
in partial fulfillment of the requirements
for the degree of

MASTER OF SCIENCE

Approved as to style and content by:

Richard E. Orville
(Chair of Committee)

John W. Nielsen-Gammon
(Member)

Juan B. Valdes
(Member)

Edward J. Zipser
(Head of department)

August 1995

Major Subject: Meteorology

ABSTRACT

Effects of Coastal Transitions on Cloud-to-Ground Lightning. (August 1995)
Aaron Mark Studwell, B.S.Eng., University of Michigan
Chair of Advisory Committee: Dr. Richard Orville

This study examined the characteristics of the cloud-to-ground (CG) lightning in twenty-three storms as they moved from over land to over water or vice versa. The data were categorized according to the storms' generation mechanism and divided into fifteen minute intervals through the storms. The data were then examined for trends in the CG flash rate, median first stroke peak current and mean multiplicity after the storm crossed the coastline. Linear and logarithmic correlations were calculated for different combinations of the parameters before and after the storm crossed the coastline.

The positive and negative CG flash rate changed in a more predictable manner for airmass storms than in frontal storms. In the single airmass storm which moved onshore, the flash rate increased, while in the storms which moved offshore, the negative CG flash rates had a decreasing trend in four of the five cases. The positive CG flash rate decreased in all three cases. In the storms caused by the passage of fronts, the negative CG flash rate was more variable. The negative CG flash rate for frontal storms had an increasing trend in 43% of the cases, while it was decreasing in 57% of the storms. The positive CG flash rate had an increasing trend in 25% of the cases, while it was decreasing in 63% of the cases. The positive CG flash rate remained the same in 12% of the cases.

The negative CG flash rate and the mean negative multiplicity were positively correlated in 13 of 16 periods. This is consistent with previous findings. An unexpected result was that the negative CG flash rate and first stroke peak current were positively correlated during the early part of the storms and negatively correlated during the latter part of the storms for 11 of the 13 periods.

Both airmass and frontal storms which had less than 10% changes in the negative CG flash rate exhibited consistent changes in the mean negative multiplicity. The median first stroke peak current also decreased in 83% of the storms.

DEDICATION

I dedicate this work to my wife, Jennie, for all of the love and support she has given me in pursuing this goal. Without her help, my meteorology career could not have started.

I also include my parents, Allan and Dorothea, for encouraging me to pursue a career in the sciences.

ACKNOWLEDGEMENTS

I would like to express my sincere appreciation to many people for their help and suggestions without which this effort would not have succeeded.

First and foremost, I am grateful to my committee chairman, Dr. Richard E. Orville, for his initial inspiration of my research and his encouragement throughout the past two years. His guidance and assistance were an invaluable asset. I would also like to thank him for the opportunity to work with the Cooperative Institute for Applied Meteorological Studies. I wish to express my gratitude to Dr. John Nielsen-Gammon for focusing my research and providing key answers to my questions. I would also like to thank my other committee members, Dr. Juan Valdes and Dr. Ralph Wurbs, for their time and assistance.

I am very grateful to additional individuals who made important contributions to this effort: Mr. Daniel Austin and Mr. Steve Barnaby for computer assistance, Mr. Matt Gilmore and Mr. Tony Perez for developing XLIGHT, without which this research may not have been possible, and to my fellow graduate students for their friendship and support. I offer special thanks to my close friends, Mr. Charlie O'Brien, Mr. Scott Sheridan, and Mr. Alan Silver, for help in both professional and technical matters.

I also want to express my thanks to Dr. Edward Zipser, Dr. Michael Biggerstaff, and Dr. Louis Wicker for their support and suggestions throughout my time at Texas A&M University.

Finally, I would like to offer my heartfelt thanks to my loving wife and chief editor, Jennie, for her constant support, patience and understanding.

TABLE OF CONTENTS

LIST OF FIGURES

CHAPTER I

INTRODUCTION

The subject of a coastal transition, when a thunderstorm traverses from land to sea or vice versa, and its effect of the storm's associated lightning characteristics has not been previously studied. While examinations of land-sea breeze-driven convection (Atkinson 1981; Blanchard and Lopez 1985; Nicholls et al. 1991; Reible et al. 1993), coastal processes (Colucci 1976; Bell and Bosart 1988; Lapenta and Seaman 1990, 1992), and extensive lightning research in coastal regions (Dirks et al. 1988; Biswas and Hobbs 1990; Orville 1990a; Dodge and Burpee 1993; Reap 1994; Samsury and Orville 1994) have been independently conducted, a complete study of the lightning characteristics of a coastal transition has not been performed. A synthesis of previous research with the new data and ideas derived through this research will provide a better understanding of the effects of the change in the ambient environment on thunderstorms.

A sharp contrast in lightning activity between continental and marine area is detected by satellites. Vorphal et al. (1970) published the first reports of the use of satellite instrumentation in the detection of lightning. The data came from instrumentation aboard the orbiting solar observatory OSO-2 satellite. They noted that between 35°N and 35°S there were ten times as many lightning storms occurring over land areas as over the sea. More recently, data from the Defense Meteorological Satellite Program (DMSP) satellite series, shown in Fig. 1, has provided a global distribution of midnight lightning activity between September 1977 and August 1978 (Orville and Henderson 1986). They reported that the land-ocean lightning ratio ranges from 2.2 in September to 4.2 in July. To account for a land-ocean area ratio of $(2.4)^{-1}$, an adjustment of the ratios is necessary. This adjustment yields values from 5.3 in September to 10.1 in July. Since there is a marked difference between lightning occurrences between the land and the oceans, some process must be occurring to suppress marine lightning activity.

As thunderstorms pass through coastal regions, the storms experience a change in surface conditions that influence their ambient environment. The change in the thunderstorm's ambient environment may cause changes in the storm's, specifically the

---

The style is that of the *Monthly Weather Review*.

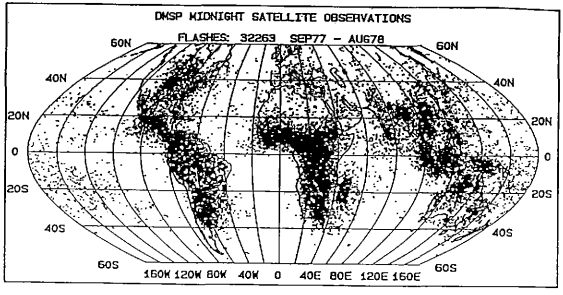

Figure 1: Global distribution of midnight lightning locations between September 1977 and August 1978 detected by the DMSP satellite. Adapted from Orville and Henderson (1986).

lightning, characteristics. For the lightning, the parameters of interest are:

- Cloud-to-ground (CG) flash rate,
- Percent positive,
- First stroke peak current, and
- Multiplicity.

This study considered two categories of formation: 1) Non-frontal, i.e. land-sea breeze effects (predominant in the summer along coastal regions) and convection due to surface warming with possible enhancement from upper-level disturbances, and 2) Frontal passages.

The areas of interest for this study were:

- The Gulf of Mexico coast from Brownsville, Texas to Key West, Florida
- The Atlantic Ocean coast from Key West, Florida to 35°N latitude.

These areas included the entire Florida peninsula. This allowed for the potential to study a thunderstorm which makes landfall on the Gulf of Mexico coast, passes over the peninsula and moves over the Atlantic Ocean. This research disregarded the area north of 35°N latitude due to the irregular geography of the areas of Pamlico Sound, North Carolina and the Chesapeake Bay. A storm passage through a region of irregular geography, where a storm could be over different areas of land with a dividing area of water, may affect the storm in a undefinable manner.

The data collected by the National Lightning Detection Network (NLDN) were categorized according to the storm's generation mechanism. Changes in the lightning parameters due to a coastal passage may be specific to a storm's method of formation. By considering changes in lightning parameters, changes in the storm's structure that occur during a coastal passage could be explained.

The data were divided into fifteen minute intervals through the storms. It was then examined for patterns in the CG flash rates after the storm crossed the coastline. The trends of the parameters were also examined individually and compared to those of the CG flash rates. This data were categorized into files for before and after the storm moved over the coastline. Linear and logarithmic correlations were calculated for different combinations of the parameters. For correlation coefficients of greater than 0.400, the patterns of the correlations were noted and examined.

Between the period of 1 December 1993 to 30 November 1994, there were twenty-three cases suitable for analysis. There were four storms which moved from

sea to land and nineteen which moved from land to sea. The geographic area of the storms ranged from Galveston, Texas to Wilmington, North Carolina. Of the sea to land storms, there was only one formed by an non-frontal mechanism. The remaining three were generated by frontal systems. Of these nineteen storms which moved from land to sea, five were generated by non-frontal processes.

The negative CG flash rate changed in more predictable manner for non-frontal storms than in frontal storms. In the non-frontal storm which moved onshore, the flash rate increased, while in the storms which moved offshore, the flash rate decreased in 80% of the cases. In the storms caused by the passage of fronts, the negative CG flash rate was more variable. The negative CG flash rate increased in 43% of the cases, while it decreased in the remaining 57% of the cases. This variability is because the storms may be in different stages of their life cycles. So the variability seen in the negative CG flash rate is associated with the natural variability of the storm.

The negative multiplicity did not show a strong relationship with the negative CG flash rate for a majority of the storms. There may be a lag in the multiplicity with regards to the flash rate because the magnitude of charge in the charge centers may not be depleted or replenished fast enough to keep pace with the change in flash rate.

Similar to the negative multiplicity, the negative first stroke peak current did not show a strong relationship with the negative CG flash rate for most of the storms. The same argument used for multiplicity may apply to the first stroke peak current. Changes in the magnitude of the current may have a time lag behind changes in the flash rate.

The positive CG flash rate also changed in more predictable manner for non-frontal storms than in frontal storms. However, the decrease in the CG flash rate was not expected. An increase would be expected because as an non-frontal storm moves over water, the storm starts to dissipate. The occurrence of positive CG lightning has been associated with the end of electrically active storms (Williams 1989). However, the positive activity is typically located within the stratiform region. In non-frontal storms, there is not typically a large stratiform region. In the storms caused by the passage of fronts, the positive CG flash rate was more variable. This variability is because the storms may not necessarily dissipate as it moves offshore. Different storms would be in various stages of development. So the variability seen in the positive CG flash rate is associated with the natural variability of the storm. The positive multiplicity did not show a strong relationship with the positive CG flash rate.

Similar to the multiplicity, the positive first stroke peak current did not show a strong relationship with the positive CG flash rate.

The negative CG flash rate and the mean negative multiplicity were positively correlated in 81% of the intervals with correlation coefficients greater than 0.400. This is consistent with previous findings (Goodman and MacGorman 1986). In 85% of the intervals with correlation coefficients greater than 0.400, the negative CG flash rate and the first stroke peak current were positively correlated during the early part of the storm and negatively correlated during the latter periods of the storm. As a storm dissipates, the CG flash rate decreases. The increase in the peak current results from fewer flashes using the mid-level charge centers which may not be dissipating as quickly as the flash rate.

The non-frontal storms which had changes in the negative CG flash rate less than 10% exhibited decreases in the mean negative multiplicity for all cases. The frontal storms which had less than 10% changes in the negative CG flash rate also exhibited consistent changes in the mean multiplicity. However, the consistency for the mean multiplicity is different than what was seen for the non-frontal storms. For 75% of the cases, the mean negative multiplicity followed the trend of the negative CG flash rate or did not change.

Considering both non-frontal and frontal storms, the median first stroke peak current decreased in six of the seven cases. There is not enough known about the mechanisms which govern the magnitude of the peak current to determine why changes are occurring. However, there has to be some kind of change to alter the currents in such a consistent manner.

CHAPTER II

BACKGROUND

An understanding of the parameters which may vary during a coastal transition is essential to interpreting the results of this study. For this reason, a review of the mechanisms which cause the generation of coastal storms, the theories considering cloud charge separation and the subsequent initiation of lightning, and the lightning parameters detailed in the Introduction is provided for the reader.

1. Generation of coastal storms

The initiation of the formation of towering cumulus clouds, which may lead to thunderstorms, can be caused by both non-frontal and frontal mechanisms. Non-frontal mechanisms include land / sea breeze convergence and buoyant thermals (Cotton 1990). The topic of buoyant thermals and upper-level disturbances will be discussed in a single section entitled "Airmass Formation." The formation of towering cumulus along a frontal system is due to lifting of warm air converging along the cold frontal boundaries, outflow boundaries from existing thunderstorms, and mesoscale ascent ahead of the frontal system.

a) Non-frontal mechanisms

1) Land-Sea breeze driven formation

During the summer, the mesoscale meteorology of coastal areas is often controlled by the daytime differential heating of the land and sea surfaces (Reible et al. 1993). Since water has a higher specific heat than soil, the land warms up at a faster rate than the water during the summer (Atkinson 1981). Therefore, the air over land warms up quicker than the air over water. The vertical pressure gradient is greater in the cooler air over the water than in the warmer air over the land because of hydrostatic conditions. This situation yields a mesohigh over the water and a mesolow over the land. Initially, ageostrophic flow develops from the mesohigh towards the mesolow. This is the sea-breeze branch of the circulation cycle. The resulting onshore wind advects cool, moist air inland, modifies local winds, causes cumulus cloud formation, and occasionally yields precipitation (Reible et al. 1993). In the middle latitudes, the onshore flow veers because of the Coriolis effect, such that later during the day the flow becomes parallel to the coast (Atkinson 1981). Conversely, at night, because of

the differences in specific heat, the water cools slower than the land. Thus, the flow reverses and a land breeze develops. Similar to the daytime pattern, cumulus cloud formation and precipitation may occur offshore.

Nicholls et al. (1991) conducted a two-dimensional numerical analysis of the interaction between sea-breeze fronts and the resulting convection over the Florida peninsula. Due to Florida's geography, sea-breeze fronts from each coast propagate inland and interact. This interaction results in the development of convective cells. Blanchard and Lopez (1985) identify three categories in land-sea breeze generated convection over peninsular Florida. Type 1 yields major convection development along both coasts due to low-level uplift. Type 2 favors convection over the western half of the peninsula because the east coast sea-breeze front moves inland quicker than the west coast sea-breeze front. Type 3 is the opposite of Type 2 causing convection to be predominately in the eastern half of Florida. It is shown by Nicholls et al. (1991) that the synoptic wind profile is responsible for determining which type of convection will occur.

2) Airmass formation

During the late spring and summer in the southeastern United States, airmass thunderstorms occur. Solar heating causes surface warming. The warming of the ground causes the atmospheric parcels above them to rise because of hydrostatic instability. The rising columns of air are called thermals. The height of the column may exceed the lifted condensation level (LCL) causing cloud formation. The entrianment of cooler and drier environmental air into the cloud produces thorough mixing above the boundary layer. Additionally, evaporation takes place at the edges of the cloud yielding cooling. The entrainment coupled with the evaporation causes a decay of the cloud. This cooling also results in sinking motions called downdrafts.

The net upward motion in the convective clouds is offset by subsidence and the downdrafts. The subsidence reduces the amount of convection in the area between the clouds. The thermals now preferentially form in the vertical columns of old thermals as they are advected along by the mean 1000-850 mb flow. The air is moister in the columns of the old thermals, because of earlier evaporation, so subsequent evaporation is reduced. This reduction in evaporation allows for enhanced growth of towering cumulus.

This cycle continues until either the source of heating is removed (because of nightfall or the thermal moving over a cooler surface, i.e., water) or the height of the

towering cumulus exceeds the level of free convection (LFC). The lifted air in the thermal is positively buoyant above the LFC and upward parcel acceleration occurs until the parcel reaches its equilibrium level. Within the towering cumulus cloud, droplet formation may yield precipitation. Charge separation processes may also occur which could initiate CG lightning activity.

Airmass formation of thunderstorms is further enhanced by the presence of an upper-level trough. In this situation, the atmosphere into which the thermal is penetrating is more unstable because of cold air advection aloft. The LFC is lower resulting in reduced convective instability (CIN). The lower value of CIN results in additional convection because more cumulus exceed the LFC. The convection may also be more intense because additional convective available potential energy (CAPE) would be available.

b) Frontal mechanisms

A front can be defined as the confluence line which is the boundary between a rather homogeneous warm air mass and a region of strong thermal contrast between the warm air mass and the colder air (Wallace and Hobbs 1977, 116). Fronts are important because of their role in warm air and moisture advection. They also result in organized ascending and descending motion.

To understand their role in forming thunderstorms, there are two mechanisms which work in concert. In the classical Norwegian model, uplifting takes place when the denser cold air acts as a wedge and lifts the less dense warm air ahead of the front. If the atmosphere ahead of the front is unstable, the clouds formed in this lifting will become convective. In a manner similar to that discussed in previous section, the uplifted parcel will condense and form convective towering cumulus.

The second mechanism is shown in Fig. 2. The low level jet (LLJ) transports warm, moist air into the warm sector of the cyclone. There is an increase in the wet bulb potential temperature (Θ_w) which makes the air mass in front of the cold front more unstable. The region east of the trough in the polar jet (PJ) is characterized by upper-level divergence in the horizontal winds. This upper-level divergence yields ascending motion in the troposphere. Additional upper-level divergence will occur in the region if the subtropical jet (SJ) is present (as shown in Fig. 2). The moisture advection coupled with the upward motion increases the depth of the moist layer. The

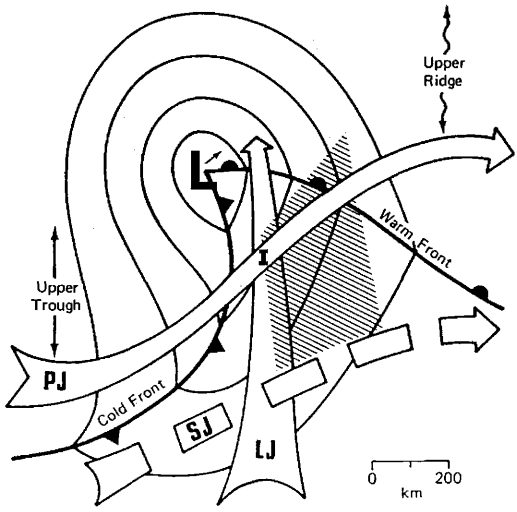

FIG. 2. Idealized sketch of a middle-latitude, synoptic scale situation favorable to the formation of severe thunderstorms. The thin lines are sea-level isobars around a low pressure center with cold and warm fronts. The broad arrows denote the polar jet (PJ) in the upper troposphere, the subtropical jet (SJ) at a higher level of the upper troposphere, and the low-level jet (LJ). Adapted from Barnes and Newton (1986).

uplifting may lift the air above the LFC causing convective storms. Severe storms may break out near the intersection I of the PJ and the LLJ. These storms will advance with the cold front (Barnes and Newton 1986).

The difference between the storms generated by non-frontal and frontal mechanisms is that non-frontal storms lose their generation source, surface heating, as they move over the water. Frontal storms that move over the water will tend to remain intact because either the uplifting due to the advancing cold air or the synoptic structure described above, or both mechanisms, will continue as the system moves offshore. By examining the changes in lightning parameters as a storm moves offshore, comparisons can be made between the devolution of non-frontal storms and the continuation of frontal storms into a marine environment.

2. Cloud charge separation

Within a thunderstorm, the separation of electric charge by liquid or solid particles is dominated by the transfer of electrons or ions during collisions between asimilar ice particles (Williams et al. 1991). Further separation of the particles carrying opposite charge occurs because of differential fall speeds between particles of different sizes and densities (Dong and Hallett 1992).

The charge transfer is dependent upon the method of the droplet's or rimer's growth. There are two fundamental parameters which appear to control the growth, and therefore the charging process: liquid water content (LWC) and the temperature. If we examine the relationship between LWC and temperature, there are three regions which are associated with their respective growth mechanisms. These methods of growth are: wet growth, dry growth by sublimation, and dry growth by deposition (Williams et al. 1991). The calculated boundaries between wet growth and dry growth by sublimation and between dry growth by sublimation and deposition are shown in Figure 3.

As the graupel falls, it has a surface temperature greater than the ambient environment. A steady-state uniform temperature of the graupel will be established in order to provide an equilibrium between the latent heat release due to freezing and the release of heat to the environment by thermal and vapor transfer (Williams et al. 1991). When the graupel temperature is greater than 0°C, wet growth occurs as the graupel falls through a region of LWC larger than the value required for wet growth. Even though the liquid graupel surface is evaporating, it is experiencing net growth by accretion. During the wet growth, the graupel undergoes positive charging. When the

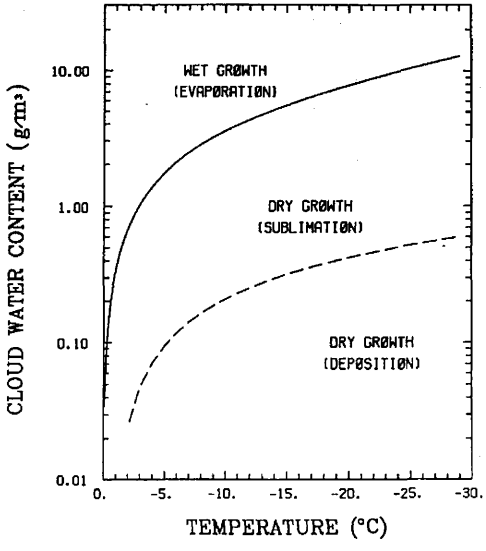

FIG. 3. Calculated boundaries between wet growth by accretion and dry growth with sublimation and between dry growth with sublimation and deposition for the hydrometeor. Adapted from Williams et al. (1991).

graupel's temperature is less than 0°C, it will begin to undergo sublimation. The sublimation will occur because the graupel's temperature is larger than to the ambient environment's temperature, and the rimer is subsaturated. However, net growth will occur because of accretion of supercooled droplets. When the graupel is undergoing dry growth with sublimation, it accumulates negative charge. The region of dry growth by deposition occurs because the graupel collides with supercooled droplets and undergoes vapor deposition. In this region of dry growth by deposition, the graupel undergoes positive charging.

The combination of the charging methods described above yields a dipolar (or possibly tripolar) structure within the cloud. In the upper region of the cloud, there will be positive charge due to dry growth by deposition. Through the lower to middle part of the cloud, dry growth with sublimation occurs yielding negative charging. A region of positive charge may occur on the base of the cloud because of two reasons. First (and probably predominantly), positive ions generated by cosmic rays are attracted to the main negative charge in the lower part of the cloud forming what is called a screening layer (Krehbiel 1986). Additionally, a region of positive charge may occur in the base of the cloud because of the positive charging of the graupel due to wet growth. By examining Figure 3, it can be seen that for a specific level of LWC there is a temperature at which the hydrometeors will begin to experience wet growth. The temperature is referred to as the charge reversal temperature. As a hydrometeor descends through the cloud, it will pass this temperature level and begin to undergo wet growth. As the graupel accumulates positive charge, the magnitude of the existing negative charge on the graupel is reduced. If a level of zero charge is met and the graupel is still undergoing wet growth, a net positive charge occurs.

3. Initiation of lightning

Cloud-to-ground lightning typically begins with a process known as preliminary or dielectric breakdown (Krider 1986). Breakdown may begin in a region of high potential gradient between upper positive and negative charge regions. The concentration of negative charge is typically between -10°C and -20°C. The dielectric breakdown occurs when potential gradient is about 3000 kV m^{-1} in dry air and about 1000 kV m^{-1} in the presence of water drops 1 mm in radius (Wallace and Hobbs 1977, 206-209). Typically, measurements of the electric field within storms yield maximum values between 100 and 200 kV m^{-1} (Krider 1986). Winn et al. (1974) reported one measurement of 400 kV m^{-1}. Since the typical measured potential gradient values are

five to ten times less than those measured in the laboratory for dielectric breakdown to occur, a rapid, almost instantaneous increase in the potential gradient has to occur for the initiation of lightning.

This breakdown initiates an intermittent, highly branched discharge which propagates horizontally and downward (Krider 1986). This discharge begins the stepped leader which lowers charge to ground. The stepped leader advances in segments which are 30 to 90 m in length and have intervals of 20 to 100 μs. As the tip of the stepped leader approaches the ground, the electric field gradient becomes very large and one or more upward discharges will occur. Once contact between the upward discharge and the stepped leader occurs, the first return stroke begins.

The return stroke is a positive wave of ionization that propagates back up the leader channel at a speed of approximately one-third to one-half the speed of light (Krider 1986). It carries ground potential upward and neutralizes most of the leader channel and a portion of the cloud charge. After a 40 to 80 ms interval, most CG flashes produce a dart leader which travels down the previous return stroke channel. This will initiate a subsequent return stroke. The subsequent strokes affect different volumes of cloud charge (Krider 1986; Krehbiel et al. 1979). Occasionally, the dart leader forges a new path to ground which yields the forked appearance generally associated with CG lightning.

4. Lightning parameters

a) Cloud-to-ground flash rate

The CG flash rate varies within the life cycle of an individual storm. Typically as a storm intensifies, the CG flash rate increases. Similarly, as the storm matures and starts to dissipate, the CG flash rate decreases. The increase in the CG flash rate is correlated with a strong updraft which leads to the presence of a large mixed-phase region (high radar reflectivities) at 7-9 km (MacGorman 1993). Also, a strengthening updraft above the -20°C level is associated with an increase in the CG flash rate (MacGorman et al. 1989). However, when there is a combination of a stronger, deep updraft core and a resulting weak echo region, there is a delay in CG activity. These correlations do not necessarily mean cause and effect, but may only be indicative of underlying relationships.

The updraft keeps negatively charged particles suspended at an optimal level within the storm. Zipser and Lutz (1994) proposed a threshold of 6-7 m s^{-1} average updraft between the 0°C and -20°C levels to suspend hydrometeors at the level required

to provide rapid electrification. The increase in electrification occurs because of increased hydrometeor collisions which generates additional negative charge in the mid-levels of the storm. This rapid electrification initiates CG lightning. A peak value of 10-12 m s^{-1} was suggested, beyond which electrification occurs at higher levels in the storm leading to a decrease in CG flash rates.

During the evolution of smaller storms, the negative charged region remains at a relatively constant height, while the positively charged region ascends in height. The increase in height is due to the updraft which leads to upward transport of the small, positively charged cloud particles (Lhermitte and Williams 1985). Since less charge is required to produce a given electric field when the two charge centers are closer together, as the center move apart, an increase in the negative charge is required to produce the electric field (MacGorman et al. 1989). An increase in the magnitude of the charge in the negative charge center results from the increased updraft, as the storm grows.

In the case where there is a strong, deep updraft core and an accompanying weak echo region, there is a suppression of CG flashes (MacGorman 1994). The stronger updraft keeps negatively charged particles higher in the storm. The strong updraft lifts all but the largest hydrometeors to the upper levels of the storm. Since there would be a short residence time at any given level, there would be fewer collisions between cloud particles. By having fewer collisions, there would be little net charging at the lower levels. This situation increases the amount of negative charge required for electric field breakdown because of the greater distance between the negatively charged region of the storm and the positively charge ground.

However, the intercloud (IC) flash rate would increase in this situation because the regions of positively and negatively charged particles are closer together (MacGorman 1994). The increase in the IC flash rate would enhance the decrease of the CG flash rate because it would reduce the amount of negative charge available for CG flashes. As the intensity of the updraft begins to decrease, the negatively charged regions move closer to the ground. The CG flash rate will begin to increase again as the negative and positive regions begin to separate (MacGorman et al. 1989).

Samsury and Orville (1994) examined the pre- and post-landfall total CG flash rates in two Atlantic hurricanes. Hurricane Hugo experienced a decrease in total CG flash rate, from 2.3 hr^{-1} to 1.3 hr^{-1}, as it made a coastal transition. As Hurricane Jerry made landfall, the total CG flash rate increased from 27.8 hr^{-1} to 43.7 hr^{-1}. These

contradictory results for the effects of a coastal transition on total CG flash rate were a topic of investigation during this research.

b) Percent positive

Two theories have been proposed for the occurrence of positive CG lightning. The first postulates that the cloud is in a pattern referred to as a tilted dipole. A tilted dipole occurs when the upper positive charge is laterally displaced by upper level winds from above the lower negative charge center (Engholm et al. 1990). Rutledge and MacGorman (1988) proposed that the rearward advection of positive charge on small ice particles from the upper levels of convective cells occurs due to storm relative winds. Brook et al. (1982) stated that a value for vertical wind shear of greater than 1.5 m s^{-1} km^{-1} appears to be necessary for the initiation of positive CG lightning. Orville (1988) associated the tilted dipole concept to mesoscale systems. In these situations, the dipole is aligned with the geostrophic wind. Samsury and Orville (1994) theorized that enhanced vertical shear of the horizontal wind upon landfall increases the horizontal separation of the electrically charged regions, thus enabling positive charge to be lowered to the ground due to the tilted dipole structure.

The second theory suggests an *in situ* charging mechanism in the stratiform region. Similar patterns have been noticed between the occurrence of winter and summer positive lightning: upright convection above the melting level, differential particle motion and vertical wind shear (Engholm et al. 1990). They also noted that there were positive CG strikes within a video integrator and processor (VIP) 2 level. This leads to their belief that there may be local charge generation within the stratiform area. The presence of supercooled liquid water was linked to the role of noninductive charging in the stratiform region (Rutledge and Petersen 1994). This noninductive charging may play a role in the electrification of the stratiform region. The positive CG flashes are associated with local enhancements in vertical velocities, i.e., embedded convection. Rutledge and Petersen (1994) presented some evidence against the advection of charged particles: 1) Turbulent mixing would decrease charge densities below the level required for the initiation of CG lightning, 2) Advection does not account for the occurrence of negative lightning unless negative charge is also advected, and 3) Cases have been studied in which there was no front to rear flow, yet there was positive CG lightning.

Typical percent positive values for the East Coast are less than 4% for the summer and about 20% during the winter (Orville 1993). However, values up to

100% have been measured during individual storms. Investigations have been made by Samsury and Orville (1994) into the percent positive exhibited by two Atlantic hurricanes before and after the storms made a coastal transition. Hurricane Hugo's percent positive decreased from 30% to 20% after landfall. The percent positive in Hurricane Jerry increased from 7% to 27% after landfall. Similar to the examination of negative CG flash rate, there are contradictory results in the percent positive.

c) Multiplicity

Multiplicity is defined as the number of return strokes in a single CG flash of lightning. Krehbiel et al. (1979) studied the location of charge centers associated with individual strokes in a flash. In this study, the charge centers for successive strokes occurred over a large horizontal distance (up to 8 km). These centers were at a relatively constant level in the storm. The charge centers were typically located from four to six kilometers above ground level. It was noted that for one case, the charged regions which supported the subsequent strokes were collocated with the strongest radar echoes. Strong radar echoes at mid-levels are indicative of the mixed-phase region; the mixed-phase region is the source of a large amount of negatively charged cloud particles. However, even as a storm undergoes extensive vertical development, the vertical distribution of the charge centers does not change much.

Between the successive strokes, the electric field change is called the interstroke or J process. This is due to a "junction" breakdown which links the top of the previous stroke with "fresh" regions of negative charge (Malan and Schonland 1951). The interstroke activity transports negative charge away from the source region of the stroke and in the direction of the first stroke's source volume (Krehbiel et al. 1979). Additional interstroke activity may fully discharge previously discharged regions and continue to transport negative charge away from adjacent cloud volumes. This process may continue to cover distances up to 8 km. Continuing current discharges also progress horizontally through the cloud. In cases of continuing current, it appears that the interstroke process may continue independent of the continuing current.

Reap and MacGorman (1989) conducted a climatological study with the National Severe Storms Laboratory lightning detection network for the 1985-86 warm season (April - September). The study shows that, for both positive and negative lightning flashes, as the monthly flash count increases, there is an increase in the multiplicity. Similarly, Studwell and Orville (1995) note for a winter storm in the southern United States that during times of increased negative CG flashes, there is a

corresponding increase in multiplicity. Krehbiel (1986) notes that CG flashes with low multiplicity values occur in the beginning stages of thunderstorms.

For mesoscale convective complexes (MCCs), the most active electrical period (± 2 h of the peak flash rate) is characterized by the highest multiplicity (Goodman and MacGorman 1986). They also noted that during the first hour of MCC development, there was a greater fraction of single stroke discharges than any other time during the storm. During storm initiation for a specific case, only 5% of all flashes had a multiplicity of greater than three. The percentage increased to 62% of all flashes during the MCC's maximum extent and decreased to 35% during termination. A problem with this study is that Goodman and MacGorman failed to consider positive and negative multiplicity separately. As storms become more electrically active, the percent positive decreases (Orville 1983; Orville et al. 1987). Reap and MacGorman (1989) showed that over 70% of positive flashes have a multiplicity of 1, while 70% of the negative flashes have a multiplicity of less than 4. A decrease in the amount of positive flashes would lead to a higher mean multiplicity value. This may be the effect shown in the Goodman and MacGorman study.

These mesoscale and synoptic scale results are consistent with the field observations and subsequent discussion of Krehbiel et al. (1979). As the negative CG flash rate increases, it is implied that the amount of negative charge available has also increased. If there is a greater amount of negative charge, it would increase the likelihood that interstroke activity would occur. The larger electric field would decrease the potential gradient required for field breakdown for either interstroke or CG activity.

Similar to this research, Samsury and Orville (1994) examined the magnitude of multiplicity between two Atlantic hurricanes before and after the storms made landfall. The multiplicity for Hurricane Hugo increased from 1.5 to 2.0 upon landfall. They hypothesized that this is a result of the storm coming into the range of the regional direction finders (DF), thereby allowing weaker flashes to be detected. However, the results for Hurricane Hugo may not be significant due its low total CG flash count (42 flashes over 18 hours). For Hurricane Jerry, the multiplicity decreased upon landfall from 2.8 to 2.5. They believe that this decrease may be associated with an increase in the vertical wind shear due to increased frictional effects over land. Orville et al. (1987) noted a decrease in multiplicity during the winter. In winter thunderstorms, an increased sheared environment has been noted which may be associated with the decrease. Similarly, the increase in shear due to frictional forces during the landfall of Hurricane Jerry may be associated with a decrease in multiplicity.

Samsury and Orville (1994) also compared Atlantic hurricanes Hugo and Jerry over an 18-hour time period, Jerry had a mean multiplicity of 2.6, while Hugo had a mean multiplicity of 1.7. During these 18 hours, Hugo had 42 CG flashes while Jerry had 835 CG flashes. This compares to a similar pattern seen by Goodman and MacGorman (1989) and Studwell and Orville (1995) that showed when the hourly flash count is higher, the multiplicity is higher. Contrary to this, the decrease in multiplicity in Jerry after landfall is opposite to this pattern because the pre-landfall flash count was 179 and the post-landfall flash count was 656.

While there are significant data showing that the mean multiplicity of the CG flashes increases as the flash rate increases, there is some evidence that this may not hold during a coastal transition.

d) First stroke peak current

The magnitude of the first stroke peak current has been studied through climatological studies in the southern Plains of the United States (Reap and MacGorman 1989) and the continental United States (Silver and Orville 1995), studies of individual storms in northern Australia (Petersen and Rutledge 1992) and hurricanes in the southeastern United States (Samsury and Orville 1994).

Reap and MacGorman (1989) noted that the minimum hourly mean peak signal strength for positive CG flashes are about equal to the maximum value for negative CG flashes. The highest values for the mean peak current, both positive and negative, were seen in the early morning. They believe that these peaks may be associated with nocturnal convection. Relating peak current to multiplicity for negative CG flashes, the trend in signal strength and the percentage of CG having a multiplicity of one are generally out of phase. Similarly, Rakov et al. (1994) noted that the initial electric field peak was lower when the flashes had a multiplicity of one in a study conducted near Tampa, Florida.

Typical winter values for the median first stroke peak current range from 37 kA to 44 kA for negative CG flashes and 61 kA to 69 kA for positive CG flashes (Silver and Orville 1995). For the summer, typical values for the median first stroke peak current range from 28 kA to 30 kA for negative flashes and 33 kA to 41 kA for positive flashes .

Petersen and Rutledge (1992) observed that positive peak current maxima occurred primarily in the trailing stratiform region, while the minima were located mostly in the convective region. The positive peak current maxima occurred during the

time of largest areal extent of the stratiform region. This is another piece of evidence which suggests an *in situ* charging mechanism for positive CG lightning in the stratiform region. For negative CG flashes, there was no distinct pattern for the location of the peak current maxima or minima. For tropical and mid-latitude storms, both extremes occurred in the convective region.

Orville (1990b) noted a latitudinal variation in the peak currents, ranging from 20-25 kA in New England to 40-45 kA in Florida. He observed that the average cloud-top height was greater in Florida (16.2 km) than in New England (12.5 km). This increase in the cloud-top height would increase the total volume of the cloud which would lead to a larger charge volume and an elevated main charge center. The increase in charge volume makes more charge available for transport to ground. The increased height of the charge center results in a longer current channel to ground. This leads to an increase in charge residing on the channel, and hence a larger peak current (Orville 1990; Petersen and Rutledge 1992).

Samsury and Orville (1994) noted that for Hurricane Hugo, the median negative peak current was 49 kA and the mean positive peak current was 62 kA. For Hurricane Jerry, the median negative peak current was 40 kA and the mean positive peak current was 52 kA. There were no comparisons made between pre- and post-landfall for the hurricanes.

Typically, the first stroke of a multistroke flash will, on average, have the largest peak current. However, Rakov et al. (1994) noted that for strokes with a multiplicity of greater than one, 33% (15 of 46 flashes) had at least one subsequent stroke where the peak current was higher than in the first return stroke. This may bring a degree of uncertainty of using peak current as a lightning parameter in any study.

More uncertainty may occur due to the method through which the peak current is determined. The first stroke peak current is determined through the measurement of the peak magnetic field caused by a CG flash. The peak current, i_{peak}, is directly related to the peak magnetic field, B_{peak}

$$i_{peak} = (2\pi cr / \mu_o v) B_{peak} \qquad (1)$$

where c is the speed of light (m s^{-1}), r is the range from the detector to the ground strike point of the CG flash (km), μ_o is the conductivity of free space ($4\pi \times 10^{-7}$ N a^{-2}), and v is the velocity of the return stroke (m s^{-1}). The velocity of the return stroke is assumed to be 1.5×10^8 m s^{-1}.

A study was conducted in New Mexico to measure various parameters of triggered lightning (Idone et al. 1984). They measured the mean return stroke propagation speed to be 1.2 x 10^8 m s^{-1} with values ranging from 6.7 x 10^7 to 1.7 x 10^8 m s^{-1}. The standard deviation was 2.7 x 10^7 m s^{-1}. These values compare favorably with those measured for natural lightning during the Thunderstorm Research International Program (TRIP). Idone and Orville (1982) reports a mean return stroke velocity of 1.1 x 10^8 m s^{-1} with values ranging from 2.9 x 10^7 to 2.4 x 10^8 m s^{-1}.

The return stroke velocity values for the natural lightning reported in Idone and Orville (1982) may be underestimated. The values for return stroke velocity were calculated using two-dimensional length measurements. Idone et al. (1984) compared the three-dimensional lengths to the two-dimensional lengths of the lightning observed. The three-dimensional lengths ranged from 5% to 20% longer than the two-dimensional measurements. This implies that the two-dimensional velocities measured for natural lightning may be 5% to 20% greater than reported. The mean return stroke velocity values obtained during TRIP (1.15 to 1.32 x 10^8 m s^{-1}, with length correction) and the three-dimensional measurements (1.2 x 10^8 m s^{-1}) are about 20% less than the value (1.5 x 10^8 m s^{-1}) currently being used for the calculation of first stroke peak current in (1).

Based on theoretical work, Lundholm (1957) and Wagner (1963) proposed the following relationship between the return stroke propagation speed, V_{rs}, and the first stroke peak current, I_p:

$$V_{rs} = c\,(1 + W/I_p)^{-1/2} \qquad (2)$$

where W is a constant (900 kA). The subsequent observational work conducted by Idone (1984) revised the value for W to 40 kA. The altered value reflects the higher conductivities present in lightning channels due to the propagation of the lightning leaders along the channel. Using the new value for W, 70% of the data fell within the standard error of estimate of 2 x 10^7 m s^{-1}. Additional data collected on triggered lightning (Hubert and Mouget 1981) was reasonably fit to the new value of W (Idone et al. 1984).

It is very relevant that this work comparing return stroke velocities and first stroke peak current was conducted on triggered lightning. Unfortunately, no data has been published relating the relationship between the return stroke propagation speed and the first stroke peak current for natural lightning. If the relationship revised by

Idone (1984) holds for natural lightning, it would have important implication on the data collected by the NLDN, since i_{peak} and return stroke velocity could no longer be considered independent.

A calibration study was conducted by Orville (1991) using simultaneous measurements from six DFs on triggered lightning near Kennedy Space Center, Florida. The return stroke peak currents were measured through a coaxial shunt on the rocket which triggered the lightning. This measurement technique can yield errors of up to 10%. The data from the six DFs were plotted and correlated versus the *in situ* measurements. The correlation coefficients r^2 varied from 0.28 to 0.86. Additionally, the range-normalized values were plotted and correlated versus the *in situ* data. The resulting correlation coefficients r^2 was 0.79 with a standard deviation of 6.1 kA. The standard deviation represents 10% of the highest peak current, 60 kA, measured *in situ*.

The above discussion combined with the previous discussion on the percentage of subsequent strokes which have a higher peak current than the first stroke casts some doubt on the validity of the present values of peak current generated by the NLDN.

CHAPTER III

NATIONAL LIGHTNING DETECTION NETWORK

All CG lightning data used in this research was collected by the National Lightning Detection Network (NLDN). The NLDN is a system of approximately 105 lightning direction finders (DF) throughout the contiguous United States (Kraus and Canniff 1995). The NLDN uses a combination of magnetic direction finders (MDF) and a time-of-arrival (TOA) system. This network is the evolution of combining the MDF network, which was operated by GeoMet Data Services, and the TOA system which was operated by Atmospheric Research Systems, Incorporated.

An individual MDF unit uses two orthogonal magnetic-loop antennas to detect the magnetic field generated by a return stroke. The induced signal provides the information necessary to determine:

- Current in the first stroke.
- Azimuth to the stroke.
- Multiplicity of the flash.

By combining the azimuth of the first stroke from the DF with azimuths from one or more other DFs, the location of the ground contact point can be determined. In addition to the loop antennas, a flat plane antenna is used as an electric field detector to determine the polarity of the flash.

An individual TOA unit uses a single whip antenna to detect the electric pulse generated by the return stroke (Holle and Lopez 1993). Each CG flash is assigned a time of arrival of the peak amplitude. The central analyzer computes the difference in the time of arrival of the signal between pairs of stations. The difference in the time of arrival can be represented by a hyperbolae that passes between the two stations and has both stations as its foci. The location of the ground contact point lies anywhere along derived hyperbolae. To obtain an unambiguous ground strike location, three TOA DFs must be used. The three TOA DFs will yield two non-redundant hyperbolas. The intersection of these hyperbola will yield the ground contact point. If there are two overlapping points between the hyperbolas, it requires the use of a fourth DF.

There are some limitations with the NLDN data. First, the network does not have a 100% detection efficiency. Work by Orville (1993) for a blizzard in the southern United States assumed a detector efficiency of 70%. Recent work by GeoMet

Data Services have estimated that the 70% efficiency extends over most of the United States (Pyle 1995). The area east of the Mississippi River has an estimated efficiency of greater than 90%. Second, the nominal range of a direction finder is 400 km because the radiation field inversely varies with range (Orville 1990). This causes the network efficiency to decrease rapidly over the Gulf of Mexico and the Atlantic Ocean (Pyle 1995).

A computer program called XLIGHT (Gilmore and Perez 1994) was used to interpret the data from the NLDN. XLIGHT uses the Interactive Data Language to graphically interpret the location of CG flashes and calculate flash densities. XLIGHT also includes a statistical package to calculate mean multiplicity and median current for a given time period.

CHAPTER IV

PROCEDURE

1. Data search and reduction

This research examined lightning data from 1 December 1993 through 30 November 1994. This allowed for the opportunity to examine thunderstorms generated by a variety of mechanisms and propagating through different environments. The first step was to identify a coastal passage of a thunderstorm. Individual storms were identified through a combination of examining hourly radar summaries and lightning displays on XLIGHT, an Interactive Data Language (IDL) program.

For a thunderstorm to be included in the data set, it must have existed for at least one hour before a coastal passage. It must have also possessed elevated VIP levels (VIP $\geq$ 3), indicating strong convection, for the entirety of the case. Typically, the storms that were studied were single cell events ranging from 25 km to 75 km along their major axis at their widest point. The largest case that was investigated was 200 km along its major axis. This case was associated with a cold front that crossed the South Carolina coast and elevated reflectivity levels existed along the length of the front.

The daily search involved the use of the listed FORTRAN programs:

- Coastal - For a single day of lightning data, the program selected flashes within 150 km of the Gulf Coast from Brownsville, Texas to Key West, Florida and the Atlantic coast from Key West, Florida to Cape Lookout, North Carolina.
- Narrow - For the data isolated by Coastal, it isolated the flashes in one hour segments.
- Latlon - For any given time period of lightning data, the program isolated flashes within a box bounded by specified latitude and longitude ranges.

For a majority of the period of study, the lightning was examined on a daily basis. For time periods that had not been analyzed on a daily basis, this research involved downloading individual day's lightning data from the files provided by GeoMet Data Services.

After the lightning of a potential case was identified, Narrow was used to divide the file into one hour segments. The data were not limited to the 300 km wide file

developed by Coastal. These hour long segments were displayed using XLIGHT. Using the National Radar Summaries, lightning activity was compared versus the radar identified locations of storm cells. If the CG flashes were collocated with elevated VIP levels, the lightning activity for the storm during that hour was isolated into a file.

XLIGHT contains a function which allows the user to zoom into the region of a particular storm. The latitude and longitude coordinates of the region were noted and the program Latlon was used to put the CG flashes within in the region into a separate file. This process was repeated for each hour of the storm and the individual files were concatenated. This new file contained the CG activity of the case for the entirety of the storm.

2. Data analysis

The data analysis consisted of examining the appropriate data for temporal and spatial patterns in median first stroke peak current, mean multiplicity, total CG flash count, and percent positive. This research considered the entire spatial extent of the storm. XLIGHT includes a statistical package which was used to calculate mean multiplicity and median current for a given time period (Gilmore et al. 1994).

Special FORTRAN programs were also designed to analyze the data. These programs are:

- Geocent - For a file generated by Coastal, it determined the geographic center of the positive and negative lightning and calculated the mean multiplicity for each fifteen minute interval.
- Median - For a file generated by Coastal, it calculated the median first stroke peak current, mean multiplicity, total CG flash count, and percent positive.

For each thunderstorm, the geographic center of the lightning activity was determined every fifteen minutes. A similar technique was used in analysis by Engholm et al. (1990) and Samsury and Orville (1994). The time of coastal transition was designated as the time when the geographic center of the lightning passed over the coastline. All lightning parameters were separated into onshore and offshore categories and analyzed using XLIGHT and Median.

Two perspectives in changes of lightning parameters were considered as a storm made a coastal transition:

- No significant change in flash rate ($\pm$ 10%) may associate changes in other lightning parameters with changes in the environment.

• If there is a significant change in flash rate, then a corresponding change in other lightning parameters could be associated with changes in the flash rate or changes in the environment.

The data were categorized according to the storm's generation mechanism. Changes in the lightning parameters due to a coastal passage may be specific to a storm's method of formation. By considering changes in lightning parameters, changes in microphysical processes that might occur during a storm's coastal passage could be implied.

3. Analysis techniques

The analysis consisted of three segments. First, the parameters were examined using the Macintosh application Cricket Graph. The fifteen minute values of the parameters were plotted versus the time until (or since) the coastal crossing. Positive lightning parameters were not plotted if greater than 50% of the time periods had less than three flashes for the fifteen minute interval. Trends in the fifteen minute CG flash rate, mean multiplicity, median first stroke peak current (I_p) and percent positive were examined for just prior to and immediately after the coastal crossing. Double Y-axis plots were also employed to examine if there was a commonality in trends between the fifteen minute CG flash rate and the remaining parameters.

Second, the individual cases were divided into two files based on the time the geographic center of lightning crossed the coastline. The Macintosh statistical analysis application StatWorks was applied to the "Before" and "After" datasets to determine the correlation coefficients between the following parameter combinations (the first parameter is defined as the independent value):

1) Flash rate versus percent positive,
2) Flash rate versus I_p,
3) Flash rate versus mean multiplicity, and
4) Mean multiplicity versus I_p.

The correlation coefficient for multiple regressions were also calculated for the following combinations (the first parameters are defined as the independent values):

5) Flash rate and mean multiplicity versus Ip, and
6) Flash rate and Ip versus mean multiplicity.

Both positive and negative CG flashes were used in combinations 2-6. The determination of the level of correlation between the fifteen minute positive CG flash rate and the percent positive would not yield a meaningful value. Correlation coefficients were calculated if there were five or more data points for the parameters.

The correlation coefficients were calculated for both linear and logarithmic regressions using the method of least squares. A logarithmic regression was considered because it could reflect the physical mechanism being modeled better than a linear regression. Some of the parameters being examined, e.g., first stroke peak current and multiplicity, may be limited, regardless of the flash rate. A linear fit implies that as the flash rate increases, the parameters could increase (or decrease) without limitation, depending on whether the value is positively or negatively correlated. With a logarithmic regression, the projected dependent values may not increase as quickly as they would with a linear regression. The use of a logarithmic regression may be more representative of the physical mechanisms of CG lightning activity. In the calculations of Lundholm (1957), Wagner (1963) and Idone (1984), a power fit ($x^{-1/2}$) was used in correlating return stroke velocity and the first stroke peak current. It is necessary to take the logarithm of the dependent and independent variables to use a $x^{-1/2}$ regression. The logarithm of equation (3) is equation (4).

$$y = x^{-1/2} + C \tag{3}$$

$$\ln y = -0.5 \ln x + \ln C \tag{4}$$

where x is the independent variable, y is the dependent variable and C is a constant. It is easier to use the statistical package on (4) to determine the best linear fit on the logarithmic data.

Third, the program Median was then applied to the "Before" and "After" files to determine the total number of positive and negative CG flashes which occurred before (or after) the coastal crossing, the mean multiplicity, the median first stroke peak current, and the percent positive for those flashes. From the total number of flashes, a one minute flash rate was calculated. The flash rate values and other parameters were compared for before and after the storm crossed the coast.

CHAPTER V

DATA

During the period of 1 December 1993 to 30 November 1994, there were twenty-three cases suitable for analysis. The geographic area covered ranged from Galveston, Texas to Wilmington, North Carolina. Table 1 shows the case number assigned to each storm, the date and time of the storm's crossing, the general location of the storm's crossing, the direction of the crossing, and the generation mechanism of the storm. Case numbers were assigned based on the chronological order of the storm's crossing. Case 4 was removed from the data set after further examination showed it did not meet the geographic criteria.

Of the four sea to land storms, there was only one storm formed by non-frontal mechanisms. This storm occurred in the mid-September along the Texas coast near Galveston. The remaining three storms were caused by frontal systems. These frontal storms occurred in early February, mid-August, and mid-October. The first and third storms were caused by cold fronts making landfall along the Gulf coast of Florida. The second storm was caused by a coastal front along the South Carolina coast.

There are three reasons for the low number of sea to land transitions. First, there is a relatively small length of shoreline, the western coast of Florida, which would be exposed to an eastward moving frontal system. Second, there was a seeming infrequency of coastal fronts in the region of the study. These fronts may not be identified or initiate severe convective activity. Third, non-frontal storms that form offshore rarely move onshore. Case 19 is the only non-frontal case detailed in the study. The proposed formation and movement of the case will be detailed during the analysis of this case and in Appendix B.

The remaining nineteen storms moved from land to sea. Five of these storms were created by non-frontal mechanisms. These non-frontal storms crossed along the Gulf coast of Florida and the Atlantic coast from southern Florida to the Georgia - South Carolina border. The non-frontal storms occurred between mid-April and mid-November.

The thirteen frontal storms made their coastal crossings predominantly along the Atlantic seaboard between Florida and North Carolina. One storm (Case 17) moved north to south near the Texas - Louisiana border. Similar to the previously mentioned Case 19, the storm's formation and movement will be explained in Appendix B.

Table 1. The date, time, and location of the crossing of the lightning's geographic center, the direction of the crossing and the generation mechanism for each case.

Case	Date / Time (UTC)	Location	Direction	Generation
19	14 Sep / 1930	Texas	Sea to Land	Non-frontal
2	6 Feb / 2300	Gulf coast of Florida	Sea to Land	Frontal
14	11 Aug / 0645	South Carolina	Sea to Land	Frontal
22	11 Oct / 1800	Gulf coast of Florida	Sea to Land	Frontal
8	16 Apr / 2245	Atlantic coast of Florida	Land to Sea	Non-frontal
12	11 Jun / 2315	Atlantic coast of Florida	Land to Sea	Non-frontal
13	17 Jul / 2230	Gulf coast of Florida	Land to Sea	Non-frontal
18	9 Sep / 0215	GA/SC border	Land to Sea	Non-frontal
20	18 Sep / 0000	Georgia	Land to Sea	Non-frontal
1	6 Feb / 2000	Atlantic coast of Florida	Land to Sea	Frontal
3	14 Mar / 0700	South Carolina	Land to Sea	Frontal
5	25 Mar / 0745	South Carolina	Land to Sea	Frontal
6	14 Apr / 2130	Atlantic coast of Florida	Land to Sea	Frontal
7	14 Apr / 2130	Atlantic coast of Florida	Land to Sea	Frontal
9	2 May / 0130	South Carolina	Land to Sea	Frontal
10	4 May / 1115	South Carolina	Land to Sea	Frontal
11	18 May / 2115	Atlantic coast of Florida	Land to Sea	Frontal
15	22 Aug / 0030	Atlantic coast of Florida	Land to Sea	Frontal
16	2 Sep / 2215	South Carolina	Land to Sea	Frontal
17	7 Sep / 0200	TX/LA border	Land to Sea	Frontal
21	18 Sep / 2200	NC/SC border	Land to Sea	Frontal
23	30 Oct / 1645	Georgia	Land to Sea	Frontal
24	11 Nov / 0715	Georgia	Land to Sea	Frontal

CHAPTER VI

RESULTS

The examination of the cases considered the trends in the lightning parameters over fifteen minute time intervals, the correlation coefficients (r^2) among the lightning parameters, and the values of the parameters before and after the storm crossed the coast. The notation used for the analysis of the fifteen minute time intervals was:

T-15 – Interval 15 to 30 minutes before the crossing of the storm's center,

T- 0 – Interval zero to 15 minutes before the crossing of the storm's center,

T+15 – Interval zero to 15 minutes after the crossing of the storm's center.

Correlation coefficients were calculated if there were five or more data points for the parameters. Additionally, correlation calculations were not conducted on lightning parameters if greater than 50% of the time periods had less than three flashes for the fifteen minute interval. The correlation coefficients were provided if either the linear or logarithmic regression values of r^2 were greater than or equal to 0.400. The equations associated with these regressions are in Appendix A.

1. Sea to land transitions

a) Non-frontal

1) Case 19

Case 19 was the only non-frontal storm to move from over the water to over land. It happened along the Texas coast near Galveston on 14 September. The first CG stroke associated with this case was at 1639 UTC. (Hereafter, all time references are in UTC.) The geographic center of the lightning made landfall at 1930. The last CG flash occurred at 2028. The synoptic overview is in Appendix B.

As the storm moved onshore, the negative CG flash rate increased sharply (Fig. 4a). This increase was a continuation of the increases experienced during the 45 minutes prior to landfall. During T-0, there were 23 negative CG flashes. The negative CG flash rate increased 91% to 44 during T+15. The negative multiplicity decreased from 3.6 to 2.5, a reduction of 31% (Fig. 4b). The negative first stroke peak current, I_p, decreased 15% from 49.4 kA to 42.2 kA as the storm made landfall (Fig 4c). During T+30, the negative CG flash rate continued to increase to 63, an increase of 43%. The mean negative multiplicity increased 32% to 3.3. The first stroke peak

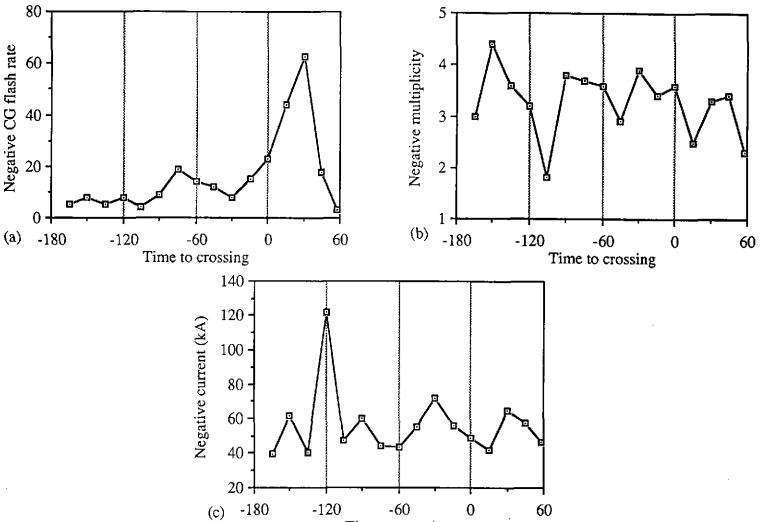

FIG. 4. For Case 19, the lightning parameters (a) 15 minute negative CG flash rate, (b) mean negative multiplicity and (c) median negative first stroke peak current in kA, for the preceding 15 minute period versus the amount of time until/since the geographic center of the CG lightning activity crossed the coastline.

current increased from 42.2 kA to 64.6 kA. The storm dissipated over the remaining 28 minutes, with fifteen minutes flash rate of 18 and 3, respectively. Similarly, both multiplicity and I_p lessened through the end of the storm. Positive CG lightning was not examined because there was not enough data to provide a significant statistical basis.

There were no correlations determined between any of the parameters before the storm made landfall. No correlations could be calculated for the storm over the land because there were only four fifteen minute intervals of data after the storm made landfall. However, I_p and multiplicity followed the same pattern after the storm made landfall.

The total and negative CG flash rates increased as the storm made landfall. While the storm was over the water, the total CG flash rate was 0.83 min^{-1} and the negative CG flash rate was 0.76 min^{-1}. After landfall, the total CG flash rate increased to 2.28 min^{-1} and the negative CG flash rate increased to 2.21 min^{-1}. The percent positive decreased from 7.8% to 3.0%. The mean negative multiplicity decreased from 3.4 to 3.0 and the median negative I_p decreased from 52.0 kA to 49.5 kA.

b) Frontal

1) Case 2

Case 2 occurred along the Gulf coast of Florida north of Tampa on 6 and 7 February. The first CG stroke associated with this case was at 2204. The geographic center of the lightning made landfall at 2300 on 6 February. The last CG flash occurred at 0104 on 7 February. The synoptic overview is in Appendix B.

As the storm approached the coast, the negative CG flash rate decreased (Fig. 5a). During T-15, there were 4 negative CG flashes. The negative CG flash rate decreased to 1 during T-0. As the storm crossed the coast, the negative CG flash rate increased to 3. The negative multiplicity decreased from 3.0 to 2.3, a decrease of 23% (Fig. 5b). The negative I_p increased from 93.7 kA to 94.4 kA as the storm made landfall (Fig. 5c). During T+30, the negative CG flash rate increased to 5. The mean negative multiplicity increased 4% to 2.4. The first stroke peak current decreased from 94.4 kA to 78.8 kA. The storm continued to intensify as it moved inland. The negative CG flash rate peaked at 8 during between 0015 and 0030 (T+75). The storm dissipated after this peak and CG activity ceased at 0104. Positive CG lightning was not examined because there was not enough data to provide a significant statistical basis.

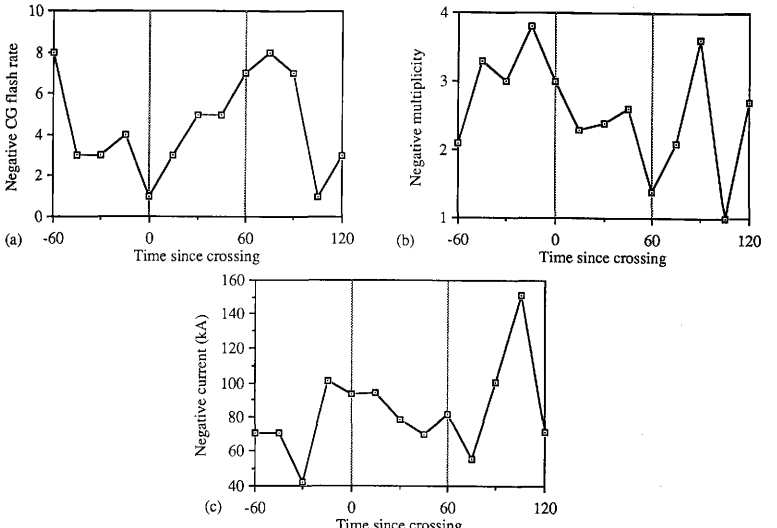

FIG. 5. Same as Fig. 4, except for Case 2.

No correlations were calculated for the storm over the water because there were only four fifteen minute intervals of data before the storm made landfall. However, there were periods where I_p and multiplicity followed the same pattern but not to the same extent. After the storm made landfall, a logarithmic correlation of $r^2 = 0.441$ was noted for the flash rate versus I_p. Multiple regressions were determined for negative CG flash rate and multiplicity versus I_p ($r^2 = 0.435$, linear; $r^2 = 0.508$, logarithmic). The best fit equations are given in Appendix A.

The total (negative) CG flash rate increased as the storm made landfall. While the storm was over the water, the CG flash rate was 0.3 min^{-1}. After landfall was made, the CG flash rate increased to 0.32 min^{-1}. The mean negative multiplicity decreased from 2.8 to 2.4, while the median negative I_p increased from 70.4 kA to 75.9 kA.

2) Case 14

Case 14 occurred along the South Carolina coast near Charleston on 11 August. The first CG stroke associated with this case was at 0500. The geographic center of the lightning made landfall at 0645. The last CG flash occurred at 0935. The synoptic overview is in Appendix B.

As the storm moved onshore, the negative CG flash rate decreased (Fig. 6a). Prior to landfall, there was a sharp increase in the negative CG flash rate. During the T-30 and T-15 periods, the 15 minute negative CG flash rate increased from 16 to 49. It continued to increase during T-0 to 114. The negative CG flash rate decreased 16% to 96 during T+15. The negative multiplicity decreased after landfall from 3.6 to 3.5, a decrease of 3% (Fig. 6b). The negative first stroke peak current, I_p, increased slightly from 33.3 kA to 33.6 kA as the storm made landfall (Fig. 6c). During T+30, the negative CG flash rate continued to decrease an additional 20% to 77. The mean negative multiplicity increased to 3.6. The first stroke peak current increased 73% from 33.6 kA to 58.0 kA. The storm dissipated after this peak as it moved inland and CG activity ceased at 0935. Positive CG lightning was not examined because there was not enough data to provide a significant statistical basis.

Correlations were noted for the negative CG flash rate versus I_p before the storm made landfall ($r^2 = 0.569$, linear; $r^2 = 0.688$, logarithmic). Similarly, correlations were determined for negative CG flash rate versus multiplicity ($r^2 = 0.620$, logarithmic) and multiplicity versus I_p ($r^2 = 0.600$, linear; $r^2 = 0.490$, logarithmic). Multiple regressions were determined for negative CG flash rate and multiplicity versus

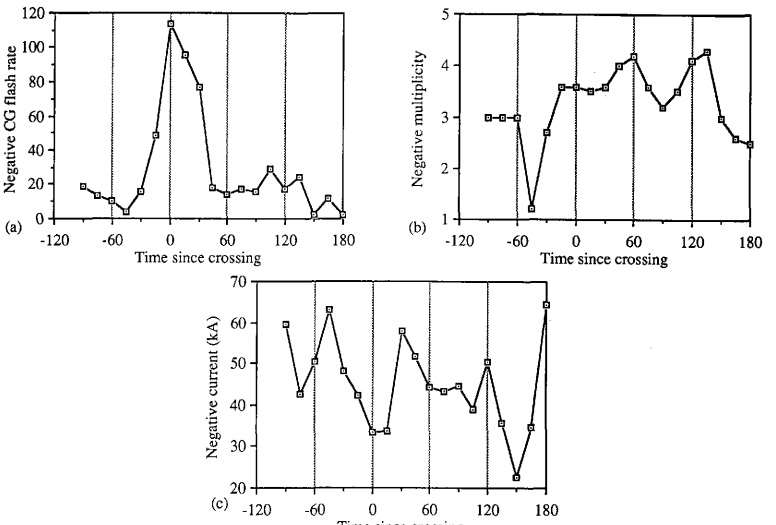

FIG. 6. Same as Fig. 4, except for Case 14.

I_p (r^2 = 0.728, linear; r^2 = 0.694, logarithmic). A set of correlations were also noted for negative CG flash rate and I_p versus multiplicity (r^2 = 0.601, linear; r^2 = 0.627, logarithmic). The best fit equations are given in Appendix A. After the storm made landfall, no correlations were found between any of the parameters.

The total and negative CG flash rates decreased as the storm made landfall. While the storm was over the water, the total CG flash rate was 2.15 min^{-1}. After landfall was made, the total CG flash rate decreased to 1.94 min^{-1}. The negative CG flash rate was 2.14 min^{-1} while over the water and decreased to 1.91 min^{-1} after crossing the coast. The mean negative multiplicity increased from 3.4 to 3.6, while the median negative I_p increased from 41.3 kA to 44.1 kA.

3) Case 22

Case 22 occurred along the Gulf coast of Florida near Tampa on 11 October. The first CG stroke associated with this case was at 1600. The geographic center of the lightning made landfall at 1800. The last CG flash occurred at 1945. The synoptic overview is in Appendix B.

As the storm moved onshore, the negative CG flash rate decreased. The negative CG flash rate peaked during the T-30 period at 43 (Fig. 7a). During T-15, the 15 minute negative CG flash rate decreased to 28. There was a slight decrease during T-0 to 27. The negative CG flash rate continued to decrease an additional 33% to 18 during T+15. The negative multiplicity decreased from 3.0 to 2.5, a decrease of 17% (Fig. 7b). The negative I_p decreased slightly from 29.5 kA to 26.3 kA as the storm made landfall (Fig. 7c). During T+30, the negative CG flash rate continued to decrease an additional 61% to 7. The mean negative multiplicity decreased slightly to 2.4. The first stroke peak current decreased 24% from 26.3 kA to 19.9 kA. The storm continued to dissipate as it moved inland. There was a secondary peak in negative CG flashes during the period 1830 - 1845 (T+45). The storm dissipated after this peak and CG activity ceased at 1945. Positive CG lightning was not examined because there was not enough data to provide a significant statistical basis.

No correlations were found between the parameters prior to the storm making landfall. After the storm made landfall, a linear correlation was noted for the negative CG flash rate versus percent positive (r^2 = 0.593). Correlations were determined for negative CG flash rate versus I_p (r^2 = 0.579, logarithmic), negative CG flash rate versus multiplicity (r^2 = 0.537, logarithmic) and multiplicity versus I_p (r^2 = 0.920, linear; r^2 = 0.865, logarithmic). A multiple correlation was attempted for negative CG

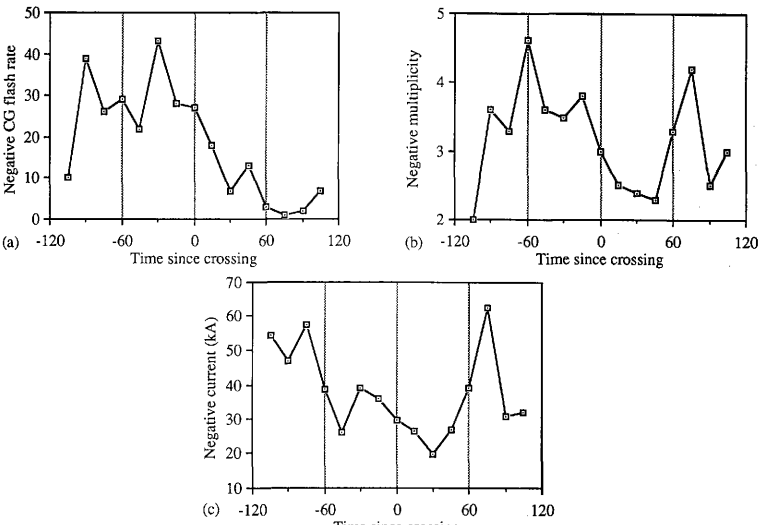

FIG. 7. Same as Fig. 4, except for Case 22.

flash rate, multiplicity and first stroke peak current. A linear correlation coefficient of $r^2 = 0.920$ was determined, but it was independent of the negative CG flash rate. Therefore, this correlation was not considered valid. The best fit equations are given in Appendix A.

The total and negative CG flash rates decreased as the storm made landfall. While the storm was over the water, the total CG flash rate was 2.44 min^{-1}. After landfall was made, the total CG flash rate increased to 2.90 min^{-1}. The negative CG flash rate was 2.44 min^{-1} while over the water and increased to 2.82 min^{-1} after crossing the coast. The mean negative multiplicity decreased from 3.3 to 3.2, while the median negative I_p decreased from 29.3 kA to 27.6 kA.

2. Land to sea transitions

a) Non-frontal

1) Case 8

Case 8 occurred along the Atlantic coast of Florida near Daytona Beach on 16 April. The first CG stroke associated with this case was at 2133. The geographic center of the lightning made landfall at 2245. The last CG flash occurred at 2359. The synoptic overview is in Appendix B.

As the storm moved offshore, the negative CG flash rate increased (Fig. 8a). This increase was a continuation of the increases experienced during the 30 minutes prior to crossing the coast. During T-0, there were 31 negative CG flashes. The negative CG flash rate increased 10% to 34 during T+15. The negative multiplicity increased from 1.6 to 2.9, an increase of 81% (Fig. 8b). The negative I_p also decreased 31.7 kA to 27.2 kA as the storm moved out to sea (Fig. 8c). During T+30, the negative CG flash rate decreased to 24, an reduction of 29%. The mean negative multiplicity did not change. The first stroke peak current increased from 27.2 kA to 32.0 kA. There was a secondary peak in the negative CG flash rate during T+45. The storm continued out to sea through the end of the case with a negative CG flash rate between 30 and 35. Both multiplicity and I_p increased through the T+60 period and then decreased until the end of the case. Positive CG lightning was not examined because there was not enough data to provide a significant statistical basis.

No correlations were found between any two of the parameters while over land. However, multiple regressions showed relationships between the negative CG flash rate, multiplicity, and I_p. A linear correlation was determined for the negative CG flash rate and multiplicity versus I_p ($r^2 = 0.534$). A linear correlation was also noted

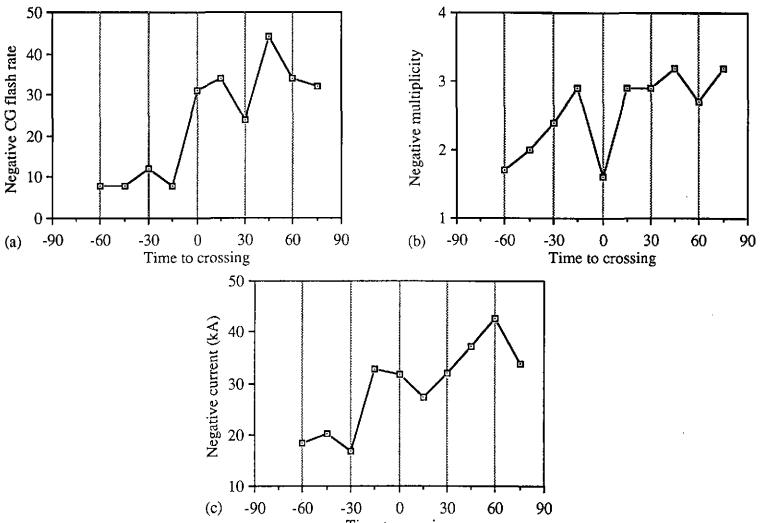

FIG. 8. Same as Fig. 4, except for Case 8.

for the negative CG flash rate and I_p versus multiplicity ($r^2 = 0.544$). No correlations were found between the parameters after the storm moved over the water. The best fit equations are given in Appendix A.

The total and negative CG flash rates increased as the storm moved out to sea. While the storm was over the land, the total CG flash rate was 0.94 min^{-1}. After the storm crossed the coast, the total CG flash rate increased to 2.31 min^{-1}. The negative CG flash rate was 0.93 min^{-1} while over the land and increased to 2.27 min^{-1} after crossing the coast. The mean negative multiplicity increased from 2.0 to 3.0, while the median negative I_p increased from 25.0 kA to 34.2 kA.

2) Case 12

Case 12 occurred along the Atlantic coast of Florida near Miami on 10 and 11 June. The first CG stroke associated with this case was at 2019 on 10 June. The geographic center of the lightning made landfall at 2315 on 10 June. The last CG flash occurred at 0156 on 11 June. The synoptic overview is in Appendix B.

As the storm moved offshore, the negative CG flash rate decreased (Fig. 9a). The storm intensified during the hour prior to crossing the coast. The negative CG flash rate increased from 269 during T-45 up to 488 during T-0. As the storm moved offshore, the negative CG flash rate during T+15 was almost the same as it was T-0. The negative CG flash rate increased to 489 during T+15. The negative multiplicity decreased from 4.2 to 3.8, a reduction of 10% after the storm moved over the water (Fig. 9b). The negative I_p increased 5% from 26.3 kA to 27.5 kA as the storm moved out to sea (Fig. 9c). During T+30, the negative CG flash rate decreased to 412, a reduction of 16%. The mean negative multiplicity increased 3% to 3.9 . The first stroke peak current increased from 27.5 kA to 28.3 kA. The storm dissipated as it moved to the southeast towards the Bahaman Islands. First stroke peak current steadily increased up to 37.2 kA through the T+135 period and then sharply increased at the end of the case.

The positive CG flash rate increased from 20 during T-45 to 26 during T-0 (Fig. 10a). As the storm moved offshore, the positive CG flash rate decreased 15% to 22 during T+15. The positive multiplicity stayed at 1.5 after the storm moved over the water (Fig. 10b). The positive I_p decreased 6% from 17.7 kA to 16.6 kA as the storm moved out to sea (Fig. 10c). During T+30, the positive CG flash rate decreased to 9, a reduction of 59%. The mean positive multiplicity decreased 33% to 1.0. The first stroke peak current increased from 16.6 kA to 19.9 kA. The percent positive through

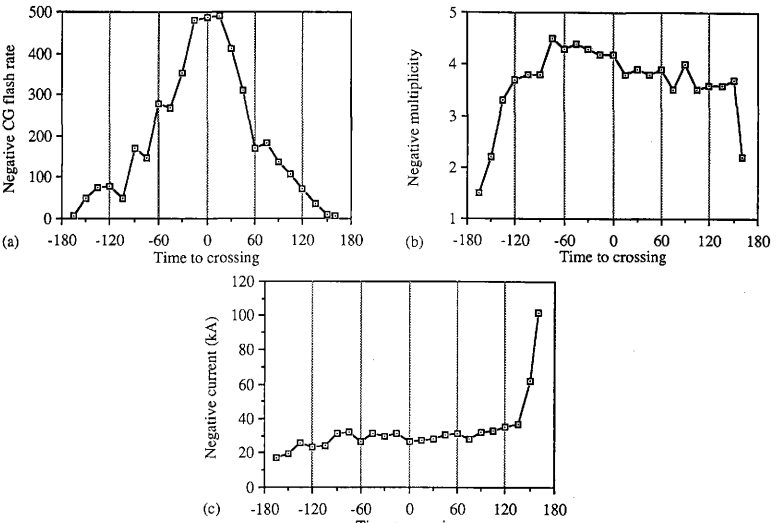

FIG. 9. Same as Fig. 4, except for Case 12.

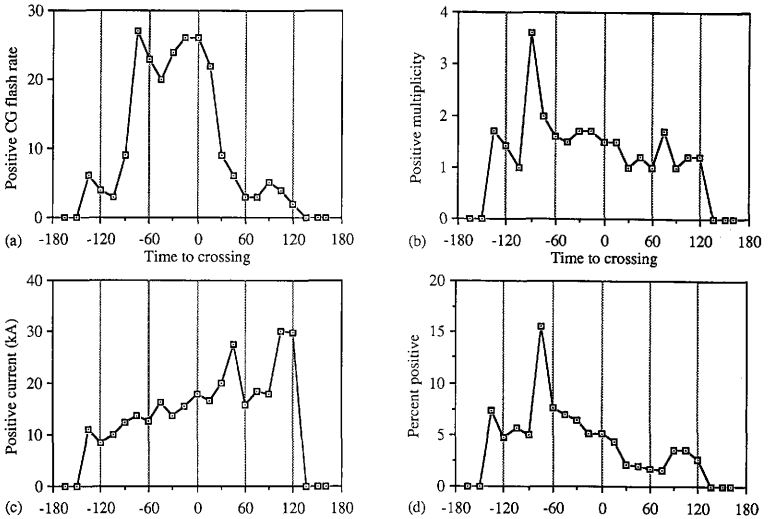

FIG 10. For Case 12, the lightning parameters (a) 15 minute positive CG flash rate, (b) mean positive multiplicity, (c) median positive first stroke peak current in kA, and (d) percent positive for the preceding 15 minute period versus the amount of time until/since the geographic center of the CG lightning activity crossed the coastline.

the life of the storm is shown in Fig. 10d. The positive CG activity ended by 0115 on 11 June.

Before the storm crossed the coastline, numerous correlations were noted. A logarithmic correlation was determined for the negative CG flash rate versus negative I_p ($r^2 = 0.708$). Similarly, correlations were determined for negative CG flash rate versus multiplicity ($r^2 = 0.413$, linear; $r^2 = 0.768$, logarithmic) and multiplicity versus negative I_p ($r^2 = 0.776$, linear; $r^2 = 0.816$, logarithmic). A set of multiple regressions were determined for negative CG flash rate and multiplicity versus negative I_p ($r^2 = 0.777$, linear; $r^2 = 0.827$, logarithmic). Correlations were also noted for negative CG flash rate and negative I_p versus multiplicity ($r^2 = 0.797$, linear; $r^2 = 0.862$, logarithmic). For positive CG activity, correlations were found for the positive CG flash rate versus positive I_p ($r^2 = 0.665$, linear; $r^2 = 0.740$, logarithmic). Multiple regressions were determined for positive CG flash rate and multiplicity versus positive I_p ($r^2 = 0.671$, linear; $r^2 = 0.741$, logarithmic).

After the storm crossed the coastline, some correlations remained. A logarithmic correlation was determined for the negative CG flash rate versus negative I_p ($r^2 = 0.860$). Similarly, correlations were determined for multiplicity versus negative I_p ($r^2 = 0.765$, linear; $r^2 = 0.687$, logarithmic). A set of multiple regressions was determined for the negative CG flash rate and multiplicity versus negative I_p ($r^2 = 0.794$, linear; $r^2 = 0.931$, logarithmic). A correlation was also noted for negative CG flash rate and negative I_p versus multiplicity, however it was independent of the flash rate making this correlation was invalid. The best fit equations are given in Appendix A.

The total, negative, and positive CG flash rates decreased as the storm moved out to sea. While the storm was over the land, the total CG flash rate was 14.86 min^{-1}. After the storm crossed the coast, the total CG flash rate decreased to 12.36 min^{-1}. The negative CG flash rate was 13.91 min^{-1} over the land and decreased to 12.02 min^{-1} after crossing the coast. The positive CG flash rate was 0.95 min^{-1}. After the storm crossed the coast, the positive CG flash rate decreased to 0.34 min^{-1}. As the storm moved offshore, the mean negative multiplicity decreased from 4.1 to 3.8, while the median negative I_p increased from 28.6 kA to 29.5 kA. The mean positive multiplicity decreased from 1.7 to 1.3, while the median positive I_p increased from 13.8 kA to 18.6 kA. The percent positive decreased from 6.42% to 2.71% as the storm moved over the water.

3) Case 13

Case 13 occurred along the Gulf coast of Florida near Fort Myers on 17 July. The first CG stroke associated with this case was at 2102. The geographic center of the lightning made landfall at 2230. The last CG flash occurred at 2323. The synoptic overview is in Appendix B.

The storm intensified during T-30 and had a negative CG flash rate of 41 (Fig. 11a). The negative CG flash rate decreased to 19 during T-15. During the T-0 period, the flash rate increased to 29. As the storm moved offshore, the negative CG flash rate during T+15 stayed at 29. The negative multiplicity decreased from 4.4 to 3.5, a decrease of 20% after the storm moved over the water (Fig. 11b). The negative I_p decreased 5% from 31.2 kA to 29.6 kA as the storm moved out to sea (Fig. 11c). During T+30, the negative CG flash rate decreased to 16. The mean negative multiplicity increased 3% to 3.6. The first stroke peak current increased from 29.6 kA to 46.0 kA. The last CG flash occurred 38 minutes after crossing the coast as it moved to the southwest into the Gulf of Mexico. The first stroke peak current increased to 73.8 kA during the end of the storm and the multiplicity decreased to 1.7.

The positive CG flash rate was 6 during T-30 and decreased to 1 during T-15. As the storm moved offshore, the positive CG flash rate decreased to zero during T+15. There was no more positive CG activity after the storm crossed the coast.

No correlations were found for the period that the storm was over land. No correlations could be calculated for when the storm was over the water because there were only three fifteen minute intervals of data after the storm moved offshore .

The total, negative, and positive CG flash rates decreased as the storm moved out to sea. While the storm was over the land, the total CG flash rate was 1.87 min^{-1}. After the storm crossed the coast, the total CG flash rate decreased to 1.53 min^{-1}. The negative CG flash rate was 1.66 min^{-1} while over the land and decreased to 1.45 min^{-1} after crossing the coast. Over land, the positive CG flash rate was 0.19 min^{-1}. As the storm moved offshore, the mean negative multiplicity decreased from 4.2 to 3.8, while the median negative I_p decreased from 38.5 kA to 34.0 kA. The percent positive decreased from 11.3% to 4.9%. After the storm crossed the coast, the positive CG flash rate decreased to 0.08 min^{-1}. Positive CG lightning parameters were not compared before and after the crossing because there were not enough data after the crossing to provide a significant statistical basis.

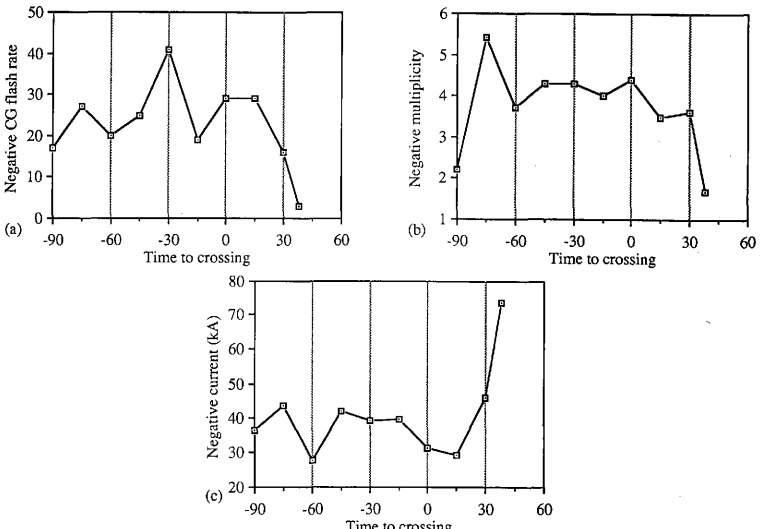

FIG. 11. Same as Fig. 4, except for Case 13.

4) Case 18

Case 18 occurred along the Georgia - South Carolina border on 9 September. The first CG stroke associated with this case was at 0000. The geographic center of the lightning made landfall at 0215. The last CG flash occurred at 0700. The synoptic overview is in Appendix B.

As the storm moved offshore, the negative CG flash rate decreased. This decrease was a continuation of the decreasing trend experienced during the 30 minutes prior to crossing the coast. During T-15, there were 85 negative CG flashes (Fig.12a). This was reduced to 62 during T-0. The negative CG flash rate decreased 18% to 51 during T+15. The negative multiplicity decreased 9% from 2.3 to 2.1 (Fig. 12b). The negative I_p increased from 26.0 kA to 28.7 kA as the storm moved out to sea (Fig. 12c). During T+30, the negative CG flash rate increased 4% to 53. The mean negative multiplicity increased 29% to 2.7. The first stroke peak current increased from 28.7 kA to 29.1 kA. There were secondary peaks in the negative CG flash rate as the storm moved out to sea and over the Gulf Stream.

The positive CG flash rate underwent a gradual decrease from 23 (T-75) to 8 (T-0). As the storm moved over the water, there was a significant increase in the flash rate up to 14, an increase of 75% (Fig. 13a). The positive multiplicity increased from 1.0 to 1.1 (Fig. 13b). The positive I_p increased from 47.3 kA to 58.9 kA as the storm moved out to sea (Fig. 13c). During T+30, the positive CG flash rate decreased 79% to 3. The mean positive multiplicity decreased 9% to 1.0. The first stroke peak current increased from 58.9 kA to 77.6 kA. The percent positive through the life of the storm is shown in Fig. 13d.

Before the storm crossed the coastline, some correlations were noted. A set of correlations was determined for the negative CG flash rate versus negative I_p ($r^2 = 0.412$, linear; $r^2 = 0.411$, logarithmic). Multiple regressions were determined for negative CG flash rate and multiplicity versus negative I_p ($r^2 = 0.425$, linear; $r^2 = 0.422$, logarithmic). After the storm moved over the water, a multiple correlation was noted for negative CG flash rate and multiplicity versus negative I_p ($r^2 = 0.461$, logarithmic).

The total, negative, and positive CG flash rates decreased as the storm moved out to sea. While the storm was over the land, the total CG flash rate was 7.56 min^{-1}. After the storm crossed the coast, the total CG flash rate decreased to 3.05 min^{-1}. This value is misleading because there was an hour when the storm was over the Gulf Stream that the negative CG flash rate increased to 5.97 min^{-1}. The negative CG flash

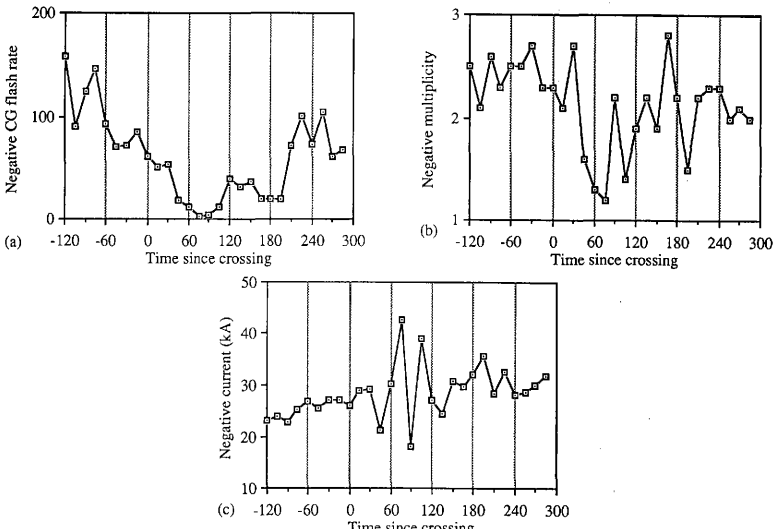

FIG. 12. Same as Fig. 4, except for Case 18.

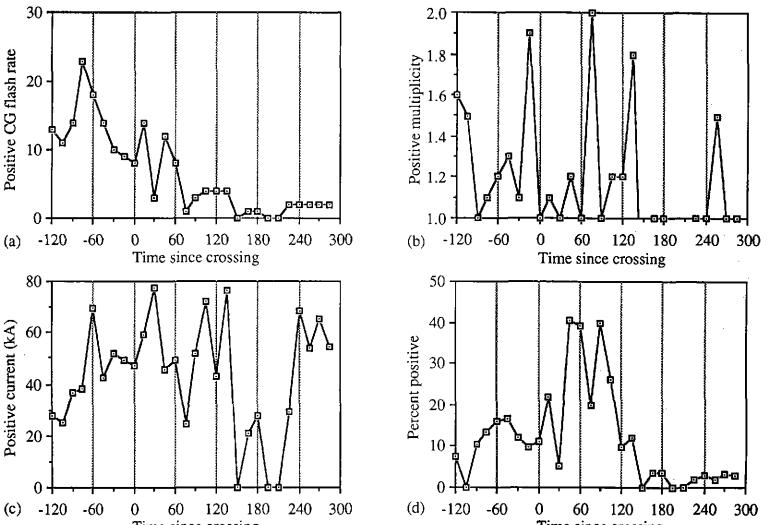

FIG. 13. Same as Fig. 10, except for Case 18.

rate was 6.67 min^{-1} while over the land and decreased to 2.82 min^{-1} after crossing the coast. The mean negative multiplicity decreased from 2.4 to 2.1, while the median negative I_p increased from 25.0 kA to 30.0 kA. The positive CG flash rate was 0.89 min^{-1} over the land and decreases to 0.23 min^{-1} while over the water. The mean positive multiplicity decreased from 1.3 to 1.2, while the median positive I_p increased from 41.0 kA to 48.5 kA.

5) Case 20

Case 20 occurred along the coast of Georgia north of Brunswick on 17 and 18 September. The first CG stroke associated with this case was at 2100 on 17 September. The geographic center of the lightning crossed the coastline at 0000 on 18 September. The last CG flash occurred at 0324 on 18 September. The synoptic overview is in Appendix B.

As the storm moved offshore, the negative CG flash rate increased. The storm intensified during the hour prior to crossing the coast. From T-45 until T-15, the negative CG flash rate increased from 113 to 196 (Fig. 14a). The negative CG flash rate decreased to 177 during T-0. After the storm crossed the coastline, the negative CG flash rate during T+15 increased 37% to 243. The negative multiplicity decreased from 3.3 to 3.2, a reduction of 3% after the storm moved over the water (Fig. 14b). The negative I_p decreased 5% from 34.3 kA to 32.6 kA as the storm moved out to sea (Fig. 14c). During T+30, the negative CG flash rate increased 37% to 334. The mean negative multiplicity continued to decrease to 3.1. The first stroke peak current increased from 32.6 kA to 34.0 kA. The storm had a secondary peak at 0130 on 18 September but dissipated over the following two hours.

The positive CG flash rate increased from 3 during T-30 up to 8 during T-0. As the storm moved offshore, the positive CG flash rate decreased 25% to 6 during T+15 (Fig. 15a). The positive multiplicity decreased from 1.1 to 1.0 after the storm moved over the water (Fig. 15b). The positive I_p increased 105% from 17.5 kA to 35.9 kA as the storm moved out to sea (Fig. 15c). During T+30, the positive CG flash rate stayed constant. The mean positive multiplicity increased to 1.2. The first stroke peak current decreased 57% to 15.39 kA. The positive CG activity continued through the end of the storm. The percent positive during the storm is shown on Fig. 15d.

After the storm crossed the coastline, some correlations were noted. A linear correlation was determined for the negative CG flash rate versus percent positive ($r^2 = 0.481$). Correlations were determined for the negative CG flash rate versus

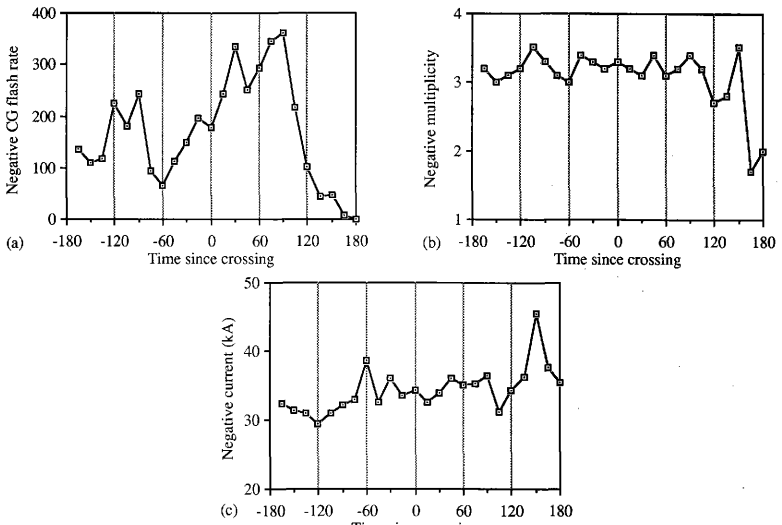

FIG. 14. Same as Fig. 4, except for Case 20.

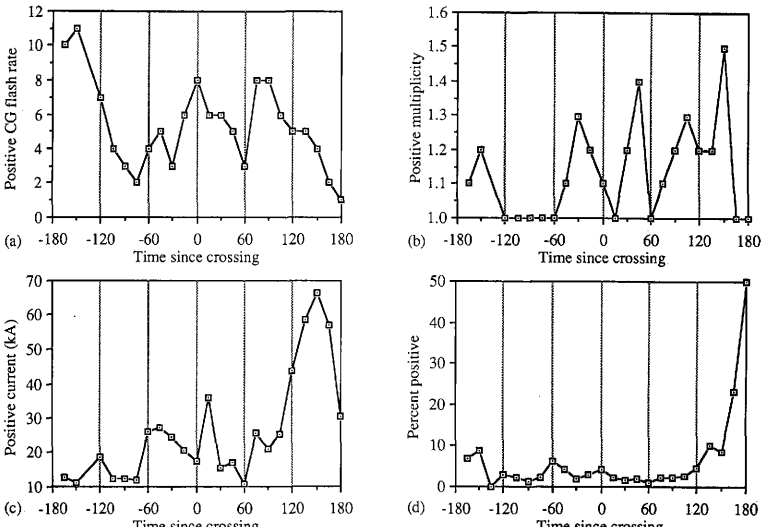

FIG. 15. Same as Fig. 10, except for Case 20.

multiplicity ($r^2 = 0.447$, linear; $r^2 = 0.695$, logarithmic). The logarithmic correlation for negative CG flash rate and negative I_p versus multiplicity yielded an $r^2 = 0.761$. No correlations were found between the parameters while the storm was over the land. The best fit equations are given in Appendix A.

The total and negative CG flash rates increased as the storm moved out to sea. While the storm was over the land, the total CG flash rate was 10.38 min^{-1}. After the storm crossed the coast, the total CG flash rate increased to 11.30 min^{-1}. The negative CG flash rate was 10.04 min^{-1} while over the land and increased to 11.00 min^{-1} after crossing the coast. The positive CG flash rate was 0.35 min^{-1}. After the storm crossed the coast, the positive CG flash rate decreased to 0.31 min^{-1}. As the storm moved offshore, the mean negative multiplicity remained the same, 3.2, while the median negative I_p increased from 32.4 kA to 34.7 kA. The mean positive multiplicity increased from 1.1 to 1.2 and the median positive I_p increased from 16.7 kA to 25.5 kA. The percent positive decreased from 3.37% to 2.73% as the storm moved out to sea.

b) Frontal

1) Case 1

Case 1 occurred along the Atlantic coast of Florida south of Jacksonville on 6 February. The first CG stroke associated with this case was at 1915. The geographic center of the lightning crossed the coastline at 2000. The last CG flash occurred at 2311. The synoptic overview is in Appendix B.

The negative CG flash rate peaked at 7 during the T-15 period. The negative CG flash rate decreased from 7 to 2 during T-0. As the storm moved offshore, the negative CG flash rate during T+15 increased 150% to 5 (Fig. 16a). The negative multiplicity decreased from 6.0 to 3.0, a reduction of 50% after the storm moved over the water (Fig. 16b). The negative I_p increased 58% from 35.1 kA to 55.3 kA as the storm moved out to sea (Fig. 16c). During T+30, the negative CG flash rate increased 40% to 7. The mean negative multiplicity continued to decrease to 2.4. The first stroke peak current increased from 55.3 kA to 64.6 kA. The negative CG flash rate had a secondary peak at 2100. The storm dissipated by 2311. Positive CG lightning was not examined because there was not enough data to provide a significant statistical basis.

Correlations were noted for the negative CG flash rate versus I_p ($r^2 = 0.455$, linear; $r^2 = 0.460$, logarithmic) after the storm moved out to sea. A set of multiple

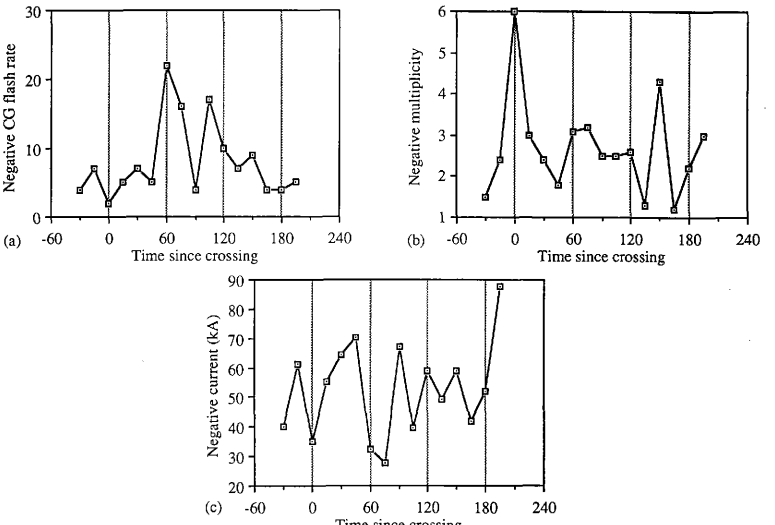

FIG. 16. Same as Fig. 4, except for Case 1.

regressions were determined for the negative CG flash rate and multiplicity versus I_p (r^2 = 0.553, linear; r^2 = 0.560, logarithmic). The best fit equations are given in Appendix A. No correlations could be calculated for while the storm was over land because there were only three fifteen minute intervals of data before the storm moved out to sea.

The total, negative, and positive CG flash rates increased as the storm moved out to sea. While the storm was over the land, the total CG flash rate was 0.31 min^{-1}. After the storm crossed the coast, the total CG flash rate increased to 0.63 min^{-1}. The negative CG flash rate was 0.29 min^{-1} while over the land and increased to 0.60 min^{-1} after crossing the coast. After the storm crossed the coast, the positive CG flash rate increased from 0.02 min^{-1} to 0.03 min^{-1}. As the storm moved offshore, the mean negative multiplicity remained the same (2.7), while the median negative I_p decreased from 61.0 kA to 48.5 kA. The percent positive decreased from 7.14% to 4.17% as the storm moved out to sea.

2) Case 3

Case 3 occurred along the coast of South Carolina near Myrtle Beach on 14 March. The first CG stroke associated with this case was at 0300. The geographic center of the lightning crossed the coastline at 0700. The last CG flash occurred at 0857. The synoptic overview is in Appendix B.

As the storm moved offshore, the negative CG flash rate decreased. The negative CG flash rate had increased in the hour prior to crossing the coast. It peaked at 27 during the T-15 period (Fig. 17a). The negative CG flash rate decreased slightly to 25 during T-0. After the storm crossed the coastline, the negative CG flash rate during T+15 decreased 44% to 14. The negative multiplicity stayed the same (1.6) after the storm moved over the water (Fig. 17b). The negative I_p increased 27% from 31.0 kA to 39.5 kA as the storm moved out to sea (Fig. 17c). During T+30, the negative CG flash rate increased 636% to 103. The mean negative multiplicity increased to 1.9. The first stroke peak current decreased 19% to 32.1 kA. The negative CG flash rate had a secondary peak during T+45. The multiplicity also peaked at 2.2 during the same period. The storm dissipated by 1000 as it moved out to sea.

After the storm crossed the coastline, the positive CG flash rate decreased. The positive CG flash rate was consistently in the 20 to 25 range in the hour prior to crossing the coast. It peaked at 24 during the T-30 period. The positive CG flash rate decreased slightly to 21 during T-0. As the storm moved offshore, the positive CG

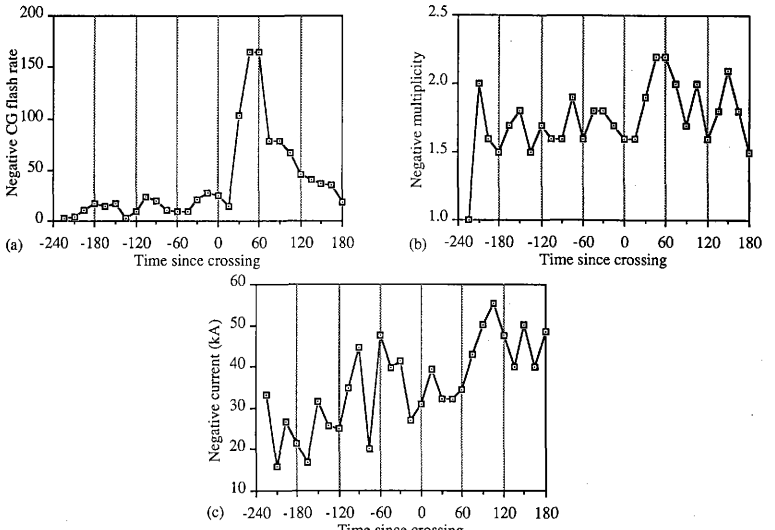

FIG. 17. Same as Fig. 4, except for Case 3.

flash rate during T+15 decreased 43% to 12 (Fig. 18a). The positive multiplicity increased from 1.3 to 1.5 after the storm moved over the water (Fig. 18b). The positive I_p decreased 4% from 61.8 kA to 59.2 kA as the storm moved out to sea (Fig. 18c). During T+30, the positive CG flash rate increased 25% to 15. The mean positive multiplicity decreased to 1.3. The first stroke peak current decreased 13% to 51.7 kA. The positive CG flash rate had a secondary peak of 18 during T+60. The multiplicity also peaked at 1.4 during the same period. Positive CG activity decreased sharply after the T+60 period. The percent positive through the life of the storm is shown in Fig. 20d.

Before the storm crossed the coast, a linear correlation was determined for the negative CG flash rate versus percent positive ($r^2 = 0.455$). After the storm moved out to sea, correlations were noted for the negative CG flash rate versus multiplicity ($r^2 = 0.555$, linear; $r^2 = 0.565$, logarithmic). Multiple regressions were determined for the negative CG flash rate and I_p versus multiplicity ($r^2 = 0.567$, linear; $r^2 = 0.566$, logarithmic). Additionally, a multiple regression was determined for the positive CG flash rate and multiplicity versus median positive I_p ($r^2 = 0.486$, logarithmic). The best fit equations are given in Appendix A.

The total and negative CG flash rates increased as the storm moved out to sea. While the storm was over the land, the total CG flash rate was 1.95 min^{-1}. After the storm crossed the coast, the total CG flash rate increased to 5.16 min^{-1}. The negative CG flash rate was 0.93 min^{-1} while over the land and increased to 4.7 min^{-1} after crossing the coast. As the storm moved offshore, the mean negative multiplicity increased from 1.7 to 2.0 and the median negative I_p increased from 28.5 kA to 40.0 kA. After the storm crossed the coast, the positive CG flash rate sharply decreased from 1.02 min^{-1} to 0.46 min^{-1}. After the storm moved over the water, the mean positive multiplicity stayed at 1.3 and the median positive I_p decreased from 60.8 kA to 53.5 kA. The percent positive decreased from 52.67% to 8.93% as the storm moved out to sea.

3) Case 5

Case 5 occurred along the coast of South Carolina near Myrtle Beach on 25 March. The first CG stroke associated with this case was at 0600. The geographic center of the lightning crossed the coastline at 0745. The last CG flash occurred at 1357. The synoptic overview is in Appendix B.

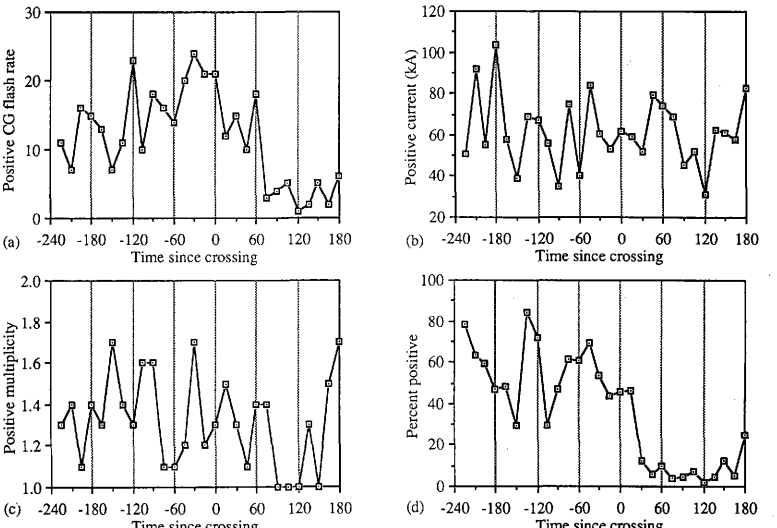

FIG. 18. Same as Fig. 10, except for Case 3.

As the storm moved offshore, the negative CG flash rate increased. The increase was a continuation of the trend during the hour prior to crossing the coast. It increased from 4 during T-30 to 66 during T-0 (Fig. 19a). After the storm crossed the coastline, the negative CG flash rate during T+15 stayed at 66. The negative multiplicity increased 35% from 2.0 to 2.7 after the storm moved over the water (Fig. 19b). The negative I_p increased 24% from 27.0 kA to 33.4 kA as the storm moved out to sea (Fig. 19c). During T+30, the negative CG flash rate increased 23% to 81. The mean negative multiplicity stayed at 2.7. The first stroke peak current increased 6% to 35.4 kA. The negative CG flash rate decreased to 29 during T+45, but then sharply increased to 107 during T+60. The negative CG flash rate continued to increase until T+90. The multiplicity also peaked at 2.9 during the same period. The storm continued its cycle of strengthening and weakening as it moved out to sea.

After the storm crossed the coastline, the positive CG flash rate decreased. The positive CG flash rate was varying in the hour prior to crossing the coast. It peaked at 15 during the T-30 period (Fig. 20a). The positive CG flash rate decreased to 6 during T-0. As the storm moved offshore, the positive CG flash rate during T+15 decreased to 5. The positive multiplicity stayed at 1.2 while the storm moved over the water (Fig. 20b). The positive I_p increased 91% from 22.0 kA to 42.1 kA as the storm moved out to sea (Fig. 20c). During T+30, the positive CG flash rate increased 38% to 8. The mean positive multiplicity increased to 1.3. The first stroke peak current increased 28% to 54.0 kA. The peak current increased an additional 49% during the T+45 period to 80.4 kA. The positive CG flash rate varied below 10 for the rest of the storm. The percent positive through the life of the storm is shown in Fig. 20d.

Before the storm crossed the coast, a linear correlation was determined between negative CG flash rate versus percent positive ($r^2 = 0.792$). A correlation was also noted for positive CG flash rate and positive I_p ($r^2 = 0.531$, logarithmic). Multiple regressions were determined for positive CG flash rate and multiplicity versus positive I_p ($r^2 = 0.555$, linear; $r^2 = 0.699$, logarithmic) and positive CG flash rate and positive I_p versus multiplicity ($r^2 = 0.471$, linear; $r^2 = 0.441$, logarithmic).

After the storm moved out to sea, a linear correlation was noted for negative CG flash rate versus percent positive ($r^2 = 0.563$). Correlations were determined for negative multiplicity versus negative I_p ($r^2 = 0.442$, linear; $r^2 = 0.663$, logarithmic). Multiple regression were determined for positive CG flash rate and multiplicity versus positive I_p ($r^2 = 0.448$, linear; $r^2 = 0.641$, logarithmic). The best fit equations are given in Appendix A.

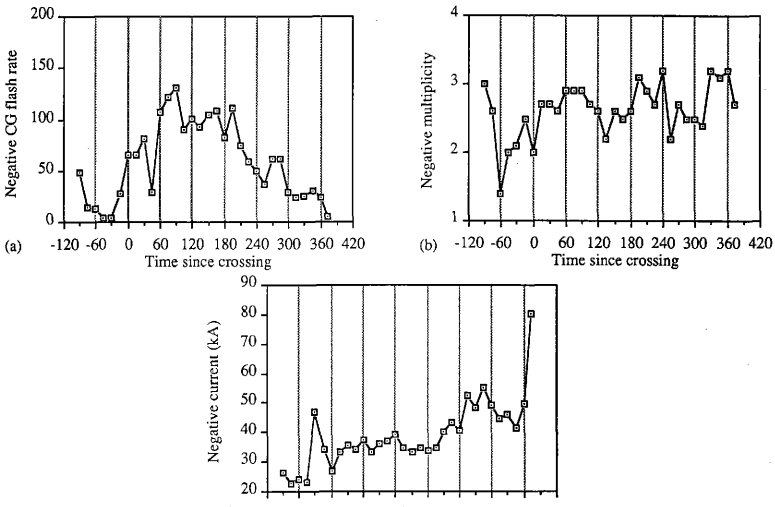

FIG. 19. Same as Fig. 4, except for Case 5.

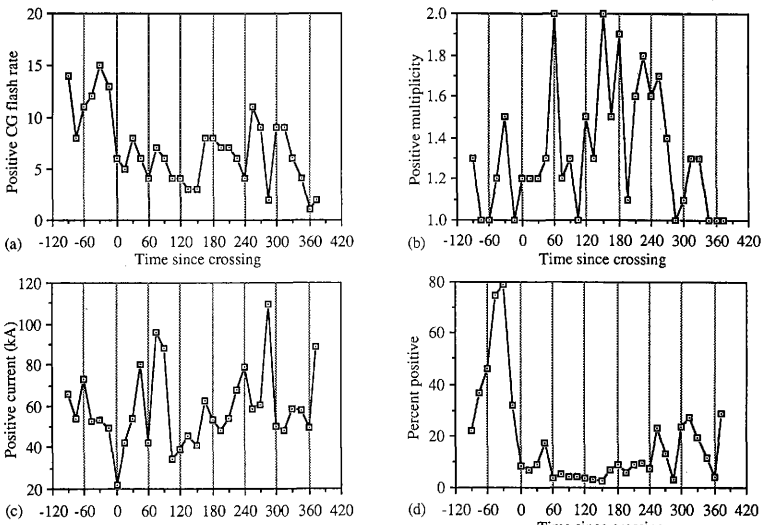

FIG. 20. Same as Fig. 10, except for Case 5.

There was an increase in the total and negative CG flash rates as the storm moved out to sea. While the storm was over the land, the total CG flash rate was 2.45 min^{-1}. After the storm crossed the coast, the total CG flash rate increased to 4.23 min^{-1}. The negative CG flash rate was 1.70 min^{-1} while over the land and increased to 3.90 min^{-1} after crossing the coast. As the storm moved offshore, the mean negative multiplicity increased from 1.2 to 1.4 and the median negative I_p increased from 26.5 kA to 37.9 kA. After the storm crossed the coast, the positive CG flash rate decreased from 0.75 min^{-1} to 0.33 min^{-1}. After the storm moved over the water, the mean positive multiplicity increased from 1.2 to 1.4 and the median positive I_p decreased from 53.5 kA to 52.7 kA. The percent positive decreased from 30.74% to 7.74% as the storm moved out to sea.

4) Case 6

Case 6 occurred along the Atlantic coast of Florida near Jacksonville on 14 April. The first CG stroke associated with this case occurred at 1900. The geographic center of the lightning crossed the coastline at 2130. The last CG flash associated this case occurred at 2204. The synoptic overview associated with this case is in Appendix B.

As the storm moved offshore, the negative CG flash rate decreased. The decrease was a continuation of the trend during the hour prior to crossing the coast. The negative CG flash rate decreased from 81 during T-60 to 34 during T-0 (Fig. 21a). After the storm crossed the coastline, the negative CG flash rate during T+15 decreased to 32. The negative multiplicity increased 20% from 3.5 to 4.2 after the storm moved over the water (Fig. 21b). The negative I_p decreased 14% from 30.9 kA to 26.6 kA as the storm moved out to sea (Fig. 21c). During T+30, the negative CG flash rate decreased 53% to 15. The mean negative multiplicity decreased to 2.5. The first stroke peak current increased 2% to 27.0 kA. The negative CG flash rate decreased to 1 during T+45 with the final CG flash at 2204. Positive CG lightning was not examined because there was not enough data to provide a significant statistical basis.

Before the storm moved out to sea, a logarithmic correlation was determined for negative CG flash rate versus negative I_p ($r^2 = 0.660$). Multiple regression determined correlations for positive CG flash rate and multiplicity versus positive I_p ($r^2 = 0.748$, logarithmic). No correlations could be calculated after the storm moved offshore because there were only three fifteen minute intervals of data. The best fit equations are given in Appendix A.

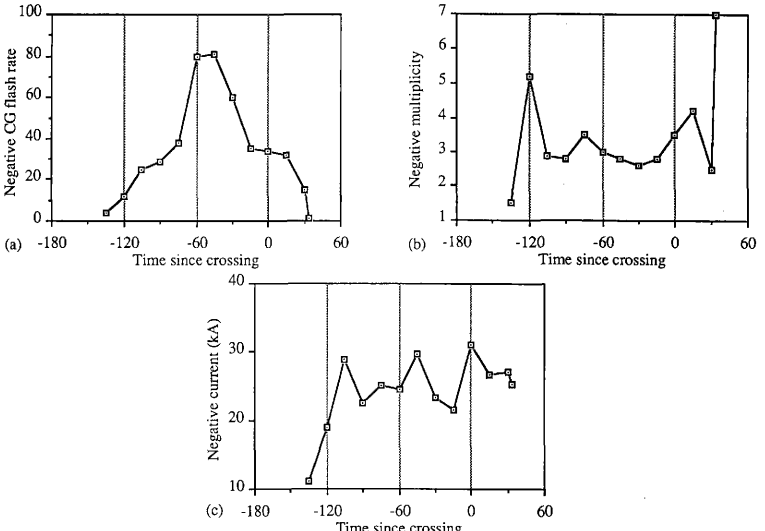

FIG. 21. Same as Fig. 4, except for Case 6.

There was a decrease in the total, negative, and positive CG flash rates as the storm moved out to sea. While the storm was over the land, the total CG flash rate was 2.71 min^{-1}. After the storm crossed the coast, the total CG flash rate decreased to 1.41 min^{-1}. The negative CG flash rate was 2.65 min^{-1} while over the land and decreased to 1.41 min^{-1} after crossing the coast. As the storm moved offshore, the mean negative multiplicity increased from 3.0 to 3.7 and the median negative I_p increased from 26.2 kA to 26.4 kA. After the storm crossed the coast, there were no positive CG flashes.

5) Case 7

Case 7 occurred along the east coast of Florida north of Daytona Beach on 14 April. The first CG stroke associated with this case was at 1930. The geographic center of the lightning crossed the coastline at 2130. The last CG flash occurred at 2359. The synoptic overview is in Appendix B.

As the storm moved offshore, the negative CG flash rate decreased. This flash rate decreased from 35 during T-45 to 17 during T-15 (Fig. 22a). The flash rate increased to 23 during T-0. After the storm crossed the coastline, the negative CG flash rate during T+15 decreased 52% to 11. The negative multiplicity increased from 2.5 to 4.2 as the storm moved over the water (Fig. 22b). The negative I_p increased slightly from 28.9 kA to 29.0 kA as the storm moved out to sea (Fig. 22c). During T+30, the negative CG flash rate increased 146% to 27. The mean negative multiplicity decreased to 2.5. The first stroke peak current increased 24% to 36.1 kA. During the first hour over the water, the negative CG flash rate fluctuated. After T+60, the negative CG flash rate increased up to 50. Positive CG lightning was not examined because there was not enough data to provide a significant statistical basis. There was no correlation between any of the parameters at any time during the storm.

There was an increase in the total and negative CG flash rates as the storm moved out to sea. While the storm was over the land, the total CG flash rate was 1.56 min^{-1}. After the storm crossed the coast, the total CG flash rate increased to 2.33 min^{-1}. The negative CG flash rate was 1.54 min^{-1} while over the land and increased to 2.31 min^{-1} after crossing the coast. As the storm moved offshore, the mean negative multiplicity decreased from 3.4 to 3.3 and the median negative I_p increased from 24.1 kA to 28.2 kA. The percent positive increased from 1.47% to 1.75%.

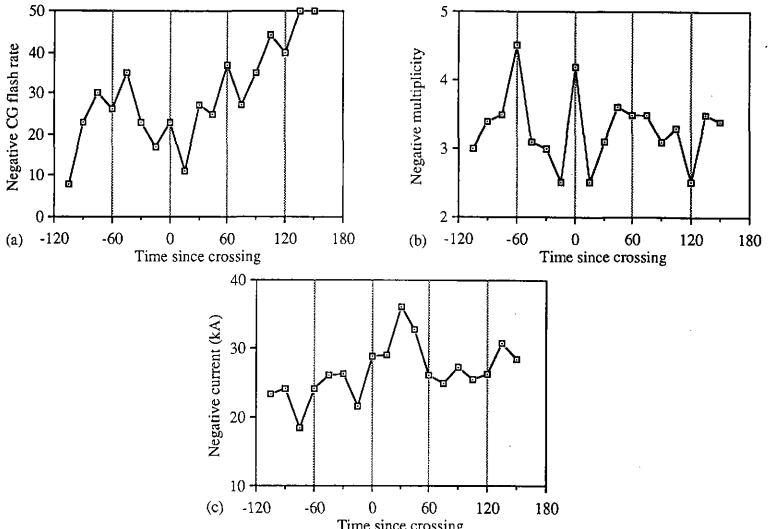

FIG. 22. Same as Fig. 4, except for Case 7.

6) Case 9

Case 9 occurred along the coast of South Carolina north of Savannah, Georgia on 2 May. The first CG stroke associated with this case was at 0000. The geographic center of the lightning crossed the coastline at 0130. The last CG flash occurred at 0351. The synoptic overview is in Appendix B.

As the storm moved offshore, the negative CG flash rate increased. This increase was continuation of the increases experienced during the 45 minutes prior to crossing the coast. The flash rate increased from 34 during T-30 to 68 during T-0 (Fig. 23a). After the storm crossed the coastline, the negative CG flash rate during T+15 increased 34% to 91. The negative multiplicity stayed at 3.8 as the storm moved over the water (Fig. 23b). The negative I_p decreased slightly from 29.3 kA to 28.9 kA as the storm moved out to sea (Fig. 23c). During T+30, the negative CG flash rate decreased 31% to 63. The mean negative multiplicity decreased to 3.4. The first stroke peak current decreased 18% to 23.7 kA. The negative CG flash rate was around 60 through the first hour over the water. After T+75, the negative CG flash rate decreased steadily through 0351. Positive CG lightning was not examined because there was not enough data to provide a significant statistical basis.

Before the storm crossed the coast, correlations were determined for the negative CG flash rate versus multiplicity ($r^2 = 0.700$, linear; $r^2 = 0.786$, logarithmic). A linear correlation was noted for multiplicity versus negative I_p ($r^2 = 0.417$). A set of multiple regressions were determined for negative CG flash rate and multiplicity versus negative I_p ($r^2 = 0.692$, linear; $r^2 = 0.666$, logarithmic) and negative CG flash rate and negative I_p versus multiplicity ($r^2 = 0.902$, linear; $r^2 = 0.921$, logarithmic).

After the storm moved out to sea, a logarithmic correlation was noted for negative CG flash rate versus negative I_p ($r^2 = 0.463$). Correlations were determined for negative CG flash rate versus multiplicity ($r^2 = 0.794$, linear; $r^2 = 0.562$, logarithmic). Multiple regressions were determined for negative CG flash rate and multiplicity versus negative I_p ($r^2 = 0.658$, linear; $r^2 = 0.849$, logarithmic) and negative CG flash rate and negative I_p versus multiplicity ($r^2 = 0.904$, linear; $r^2 = 0.877$, logarithmic). The best fit equations are given in Appendix A.

The total and negative CG flash rates increased as the storm moved out to sea. While the storm was over the land, the total CG flash rate was 2.44 min^{-1}. After the storm crossed the coast, the total CG flash rate increased to 2.90 min^{-1}. The negative CG flash rate was 2.44 min^{-1} while over the land and increased to 2.82 min^{-1} after crossing the coast. As the storm moved offshore, the mean negative multiplicity

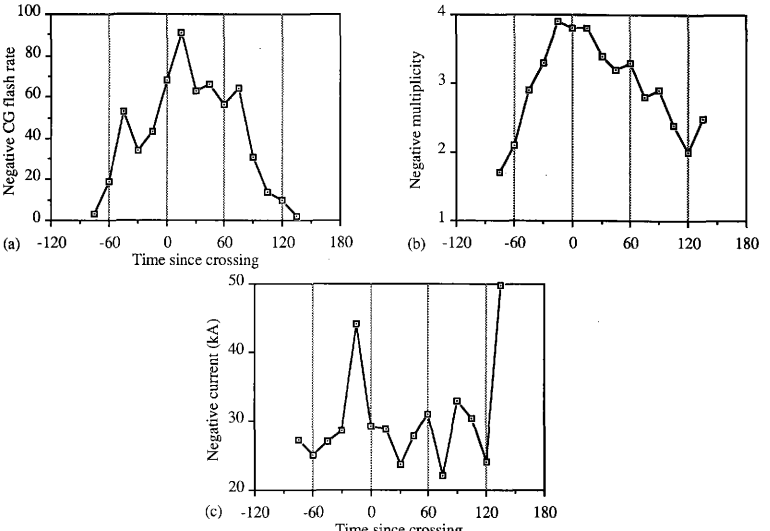

FIG. 23. Same as Fig. 4, except for Case 9.

decreased from 3.3 to 3.2 and the median negative I_p decreased from 29.3 kA to 27.6 kA.

7) Case 10

Case 10 occurred along the coast of South Carolina north of Savannah, Georgia on 4 May. The first CG stroke associated with this case was at 0941. The geographic center of the lightning crossed the coastline at 1115. The last CG flash occurred at 1359. The synoptic overview is in Appendix B.

As the storm moved offshore, the negative CG flash rate increased. This increase was a continuation of the increases experienced during the hour prior to crossing the coast. The flash rate increased from 83 during T-45 to 328 during T-0 (Fig. 24a). After the storm crossed the coastline, the negative CG flash rate during T+15 increased 24% to 408. The negative multiplicity increased from 3.9 to 4.4 as the storm moved over the water (Fig. 24b). The negative I_p increased from 29.0 kA to 34.2 kA as the storm moved out to sea (Fig. 24c). During T+30, the negative CG flash rate decreased 2% to 399. The mean negative multiplicity increased to 4.5. The first stroke peak current increased 2% to 35.0 kA. The negative CG flash rate continued to steadily decline through T+120.

The positive CG flash rate increased after the storm moved over the water. This increase was continuation of the increases experienced during the 30 minutes prior to crossing the coast. The flash rate increased from 3 during T-15 to 18 during T-0 (Fig. 25a). After the storm crossed the coastline, the positive CG flash rate during T+15 increased 139% to 43. The positive multiplicity increased from 1.5 to 1.7 as the storm moved over the water (Fig. 25b). The positive first stroke peak current increased from 14.6 kA to 14.9 kA as the storm moved out to sea (Fig. 25c). During T+30, the positive CG flash rate decreased 30% to 30. The mean positive multiplicity increased to 2.3. The first stroke peak current decreased to 14.7 kA. The percent positive through the life of the storm is shown in Fig. 25d. The positive CG flash rate continued to steadily decline through T+60 and positive CG activity was sporadic after 1215.

Before the storm crossed the coast, a logarithmic correlation was noted for negative CG flash rate versus negative I_p ($r^2 = 0.597$). A linear correlation was determined for the negative CG flash rate versus multiplicity ($r^2 = 0.782$). Multiple regressions were determined for negative CG flash rate and negative I_p versus multiplicity ($r^2 = 0.784$, linear; $r^2 = 0.650$, logarithmic).

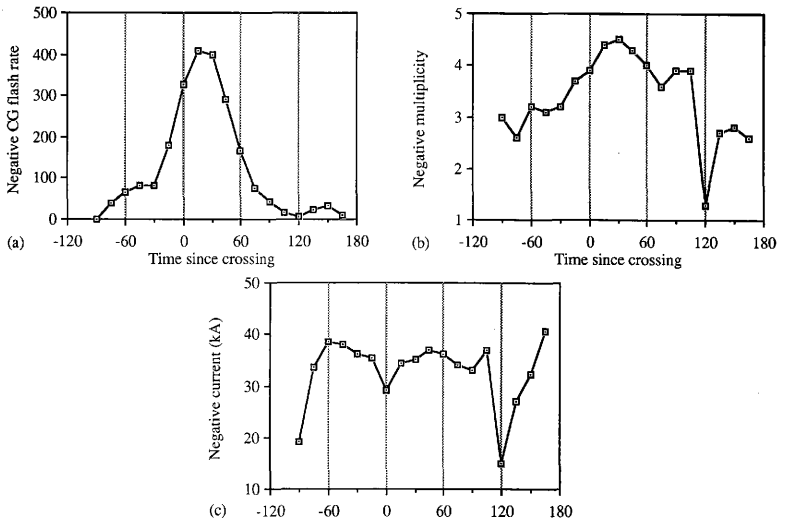

FIG. 24. Same as Fig. 4, except for Case 10.

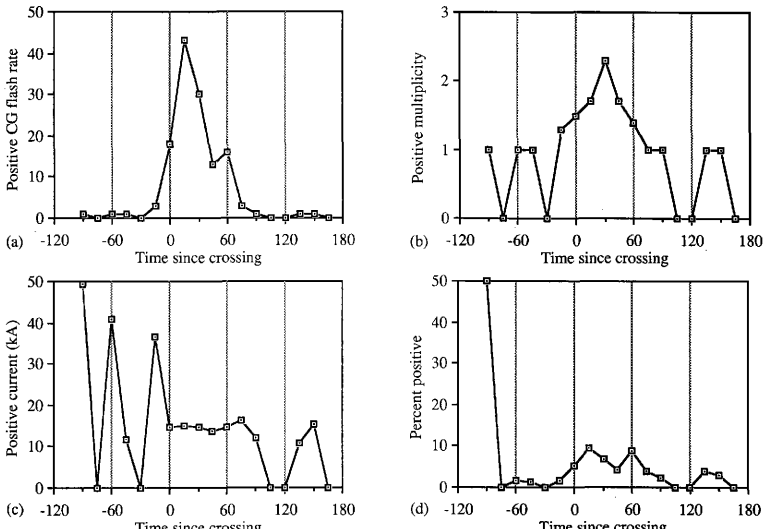

FIG. 25. Same as Fig. 10, except for Case 10.

After the storm moved out to sea, a logarithmic correlation was noted for negative CG flash rate versus percent positive (r^2 = 0.635). Correlations were determined for negative CG flash rate versus multiplicity (r^2 = 0.507, linear; r^2 = 0.628, logarithmic) and multiplicity versus negative I_p (r^2 = 0.496, linear; r^2 = 0.693, logarithmic). Multiple regression were determined for negative CG flash rate and multiplicity versus negative I_p (r^2 = 0.584, linear; r^2 = 0.782, logarithmic) and negative CG flash rate and negative I_p versus multiplicity (r^2 = 0.775, linear; r^2 = 0.895, logarithmic). Positive CG lightning was not examined for correlations because there was not enough data to provide a significant statistical basis. The best fit equations are given in Appendix A.

The total, negative, and positive CG flash rates increased as the storm moved out to sea. While the storm was over the land, the total CG flash rate was 8.52 min^{-1}. After the storm crossed the coast, the total CG flash rate increased to 9.56 min^{-1}. The negative CG flash rate was 8.27 min^{-1} while over the land and increased to 8.90 min^{-1} after crossing the coast. As the storm moved offshore, the mean negative multiplicity increased from 3.6 to 4.2 and the median negative I_p increased from 32.0 kA to 35.1 kA. The positive CG flash rate was 0.25 min^{-1} while over the land and increased to 0.66 min^{-1} after crossing the coast. As the storm moved offshore, the mean positive multiplicity increased from 1.4 to 1.7 and the median positive I_p decreased from 16.8 kA to 14.7 kA. The percent positive increased from 3.0% to 6.85%.

8) Case 11

Case 11 occurred along the Atlantic coast of Florida near Miami on 18 May. The first CG stroke associated with this case was at 2000. The geographic center of the lightning crossed the coastline at 2115. The last CG flash occurred at 2259. The synoptic overview is in Appendix B.

As the storm moved offshore, the negative CG flash rate increased. This increase was a continuation of the increases experienced during the 30 minutes prior to crossing the coast. The flash rate increased from 84 during T-15 to 180 during T-0 (Fig. 26a). After the storm crossed the coastline, the negative CG flash rate during T+15 increased 2% to 184. The negative multiplicity increased from 3.0 to 3.2 as the storm moved over the water (Fig. 26b). The negative I_p decreased from 26.7 kA to 23.9 kA as the storm moved out to sea (Fig. 26c). During T+30, the negative CG flash rate increased 7% to 196. The mean negative multiplicity increased to 3.3. The first stroke peak current increased 7% to 25.5 kA. The negative CG flash rate continued to

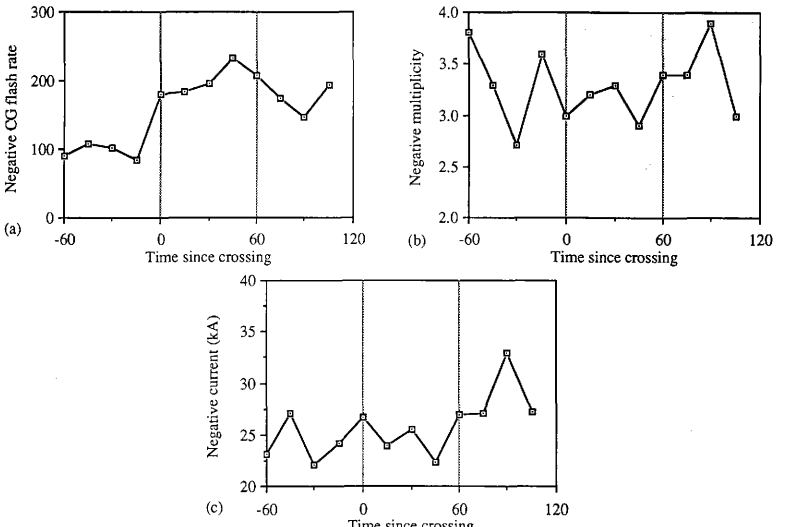

FIG. 26. Same as Fig. 4, except for Case 11.

steadily increase through T+45. After that period, the negative CG flash rate decreases through T+75.

The positive CG flash rate increased after the storm moved over the water. This increase was a continuation of the increases experienced during the 30 minutes prior to crossing the coast. The flash rate increased from 2 during T-15 to 11 during T-0. After the storm crossed the coastline, the positive CG flash rate during T+15 increased 9% to 12 (Fig. 27a). The positive multiplicity decreased from 1.2 to 1.0 as the storm moved over the water (Fig. 27b). The positive I_p increased from 11.7 kA to 13.7 kA as the storm moved out to sea (Fig. 27c). During T+30, the positive CG flash rate decreased 50% to 6. The mean positive multiplicity stayed at 1.0. The first stroke peak current increased to 24.6 kA. The positive CG flash rate was steady at about 6 through the T+75 period. The percent positive through the life of the storm is shown in Fig. 27d.

Before the storm crossed the coast, a linear correlation was noted for negative CG flash rate versus percent positive ($r^2 = 0.615$). Multiple regressions were determined for negative CG flash rate and multiplicity versus negative I_p ($r^2 = 0.481$, linear; $r^2 = 0.556$, logarithmic) and negative CG flash rate and negative I_p versus multiplicity ($r^2 = 0.466$, logarithmic).

After the storm moved out to sea, correlations were noted for negative CG flash rate versus negative I_p ($r^2 = 0.679$, linear; $r^2 = 0.701$, logarithmic). Correlation were determined for negative CG flash rate versus multiplicity ($r^2 = 0.689$, linear; $r^2 = 0.711$, logarithmic) and multiplicity versus negative I_p ($r^2 = 0.747$, linear; $r^2 = 0.717$, logarithmic). Multiple regressions were determined for negative CG flash rate and multiplicity versus negative I_p ($r^2 = 0.784$, linear; $r^2 = 0.770$, logarithmic) and negative CG flash rate and negative I_p versus multiplicity ($r^2 = 0.790$, linear; $r^2 = 0.777$, logarithmic). The best fit equations are given in Appendix A.

The total and negative CG flash rates increased as the storm moved out to sea. While the storm was over the land, the total CG flash rate was 7.81 min^{-1}. After the storm crossed the coast, the total CG flash rate increased to 8.37 min^{-1}. The negative CG flash rate was 7.51 min^{-1} while over the land and increased to 8.11 min^{-1} after crossing the coast. As the storm moved offshore, the mean negative multiplicity increased from 3.2 to 3.3 and the median negative I_p increased from 25.3 kA to 26.1 kA. The positive CG flash rate was 0.30 min^{-1} while over the land and decreased to 0.26 min^{-1} after crossing the coast. As the storm moved offshore, the mean positive

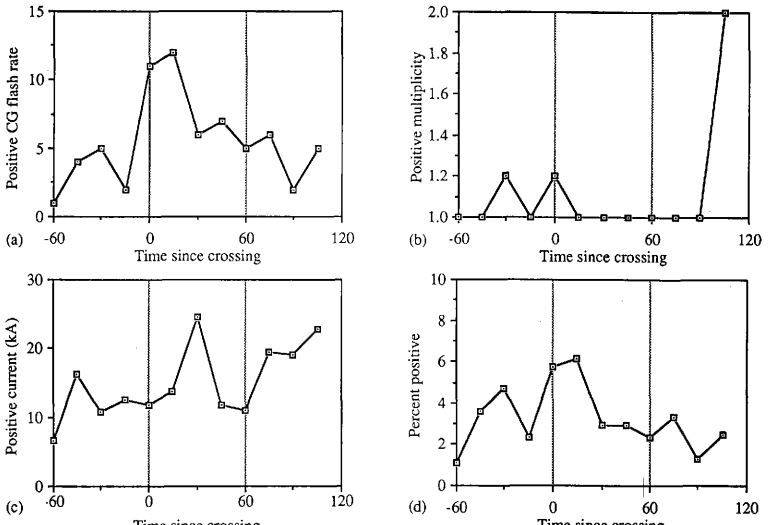

FIG. 27. Same as Fig. 10, except for Case 11.

multiplicity stayed at 1.1 and the median positive I_p increased from 11.5 kA to 14.4 kA. The percent positive decreased from 3.92% to 3.11%.

9) Case 15

Case 15 occurred along the Atlantic coast of Florida near Daytona Beach on 21 and 22 August. The first CG stroke associated with this case was at 2200 on 21 August. The geographic center of the lightning crossed the coastline at 0030 on 22 August. The last CG flash occurred at 0559. The synoptic overview is in Appendix B.

As the storm approached the coastline, the negative CG flash rate decreased. The flash rate decreased from 376 during T-15 to 268 during T-0 (Fig. 28a). After the storm crossed the coastline, the negative CG flash rate decreased during T+15 to 264. The negative multiplicity stayed at 3.6 as the storm moved over the water (Fig. 28b). The negative I_p decreased from 25.7 kA to 24.2 kA as the storm moved out to sea (Fig. 28c). During T+30, the negative CG flash rate increased 8% to 286. The mean negative multiplicity decreased to 3.4. The first stroke peak current increased 10% to 26.7 kA. The negative CG flash rate was variable through T+45. After that period, the negative CG flash rate increased during T+60 and peaked during T+90.

The positive CG flash rate increased after the storm moved over the water. The flash rate decreased from 18 during T-30 to 5 during T-0. After the storm crossed the coastline, the positive CG flash rate remained 5 (Fig. 29a). The positive multiplicity decreased from 1.2 to 1 as the storm moved over the water (Fig. 29b). The positive I_p increased from 10.2 kA to 15.4 kA as the storm moved out to sea (Fig. 29c). During T+30, the positive CG flash rate increased to 10. The mean positive multiplicity increased to 1.2. The first stroke peak current increased 2% to 15.7 kA. The positive CG flash rate continued to increase through T+90. After that period, the positive CG flash rate decreased and followed the pattern of the negative CG flash rate. The percent positive through the life of the storm is shown in Fig. 29d.

Before the storm crossed the coast, no correlations were determined among the parameters. After the storm moved out to sea, correlations were noted for negative CG flash rate versus multiplicity ($r^2 = 0.665$, linear; $r^2 = 0.649$, logarithmic). Multiple regression determined correlations for negative CG flash rate and negative I_p versus multiplicity ($r^2 = 0.707$, linear; $r^2 = 0.696$, logarithmic). The best fit equations are given in Appendix A.

The total, negative, and positive CG flash rates increased as the storm moved out to sea. While the storm was over the land, the total CG flash rate was 17.21 min^{-1}.

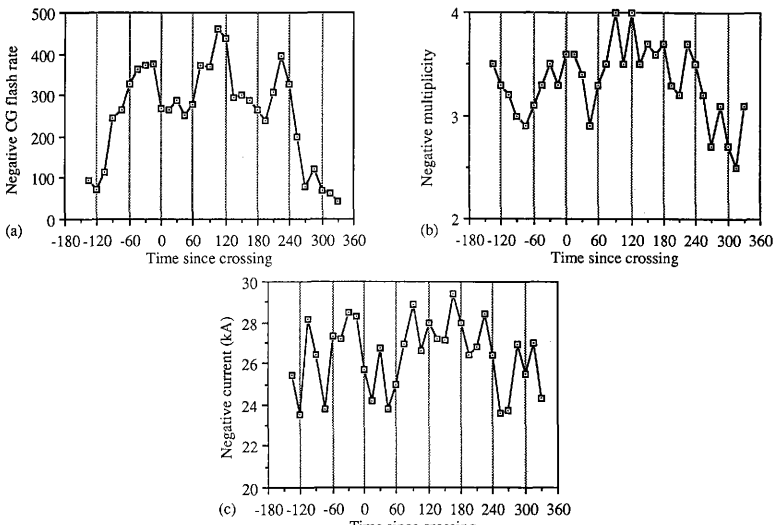

FIG. 28. Same as Fig. 4, except for Case 15.

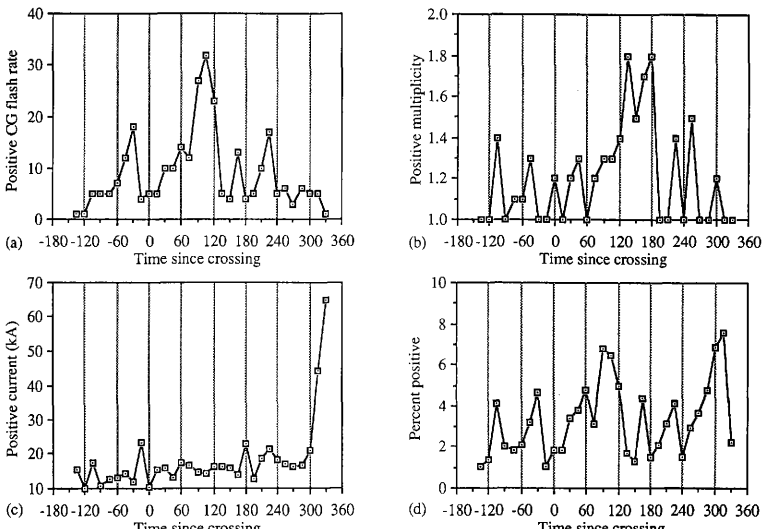

FIG. 29. Same as Fig. 10, except for Case 15.

After the storm crossed the coast, the total CG flash rate increased to 17.97 min^{-1}. The negative CG flash rate was 16.79 min^{-1} while over the land and increased to 17.30 min^{-1} after crossing the coast. As the storm moved offshore, the mean negative multiplicity increased from 3.3 to 3.5 and the median negative I_p stayed at 27.0 kA. The positive CG flash rate was 0.42 min^{-1} while over the land and increased to 0.67 min^{-1} after crossing the coast. As the storm moved offshore, the mean positive multiplicity increased from 1.1 to 1.3 and the median positive I_p increased from 11.5 kA to 27.0 kA. The percent positive decreased from 2.44% to 3.74%.

10) Case 16

Case 16 occurred along the South Carolina coast north of Charleston on 2 and 3 September. The first CG stroke associated with this case was at 2000 on 2 September. The geographic center of the lightning crossed the coastline at 2215 on 2 September. The last CG flash occurred at 0159 on 3 September. The synoptic overview is in Appendix B.

As the storm moved offshore, the negative CG flash rate increased. The flash rate had decreased from 189 during T-30 to 120 during T-0 (Fig. 30a). After the storm crossed the coastline, the negative CG flash rate increased during T+15 to 134. The negative multiplicity increased from 2.9 to 3.0 as the storm moved over the water (Fig. 30b). The negative I_p increased from 34.6 kA to 41.2 kA as the storm moved out to sea (Fig. 30c). During T+30, the negative CG flash rate decreased 6% to 126. The mean negative multiplicity increased to 3.3. The first stroke peak current decreased 15% to 34.9 kA. The negative CG flash rate was variable through T+75. After that period, the negative CG flash rate increased and peaked during T+90.

The positive CG flash rate was the same after the storm moved over the water. The flash rate decreased from 6 during T-30 to 3 during T-0. After the storm crossed the coastline, the positive CG flash rate remained 3 (Fig. 31a). The positive multiplicity increased from 1.2 to 1.3 as the storm moved over the water (Fig. 31b). The positive I_p decreased from 54.7 kA to 43.6 kA as the storm moved out to sea (Fig. 31c). During T+30, the positive CG flash rate remained 3. The mean positive multiplicity remained 1.3. The first stroke peak current increased 106% to 89.7 kA. The positive CG flash rate was variable below 5 through the rest of the storm. The percent positive through the life of the storm is shown in Fig. 31d.

Before the storm crossed the coast, a set of regressions were determined for the negative CG flash rate versus multiplicity ($r^2 = 0.629$, linear; $r^2 = 0.510$, logarithmic).

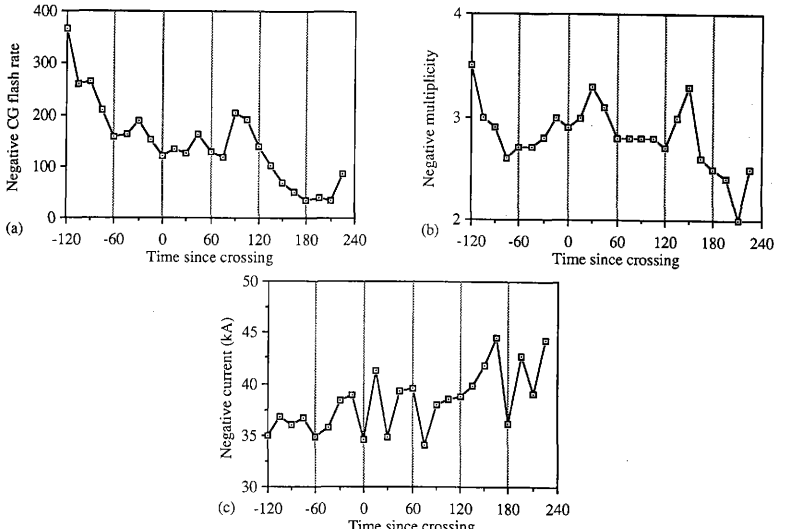

FIG. 30. Same as Fig. 4, except for Case 16.

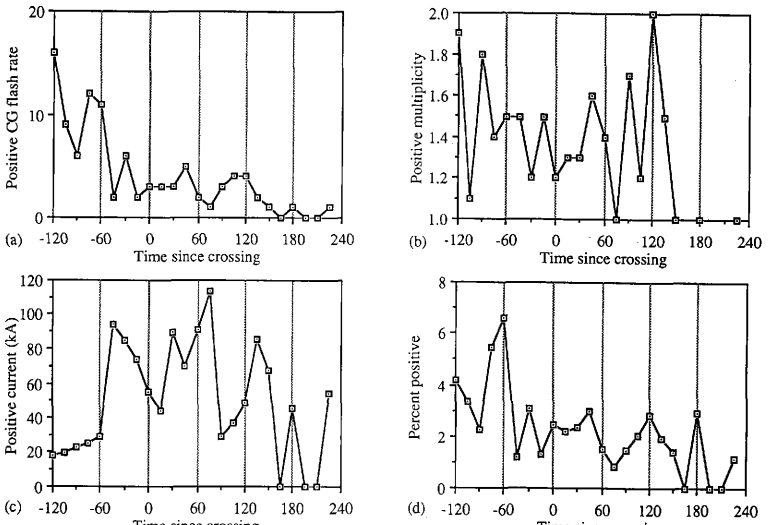

FIG. 31. Same as Fig. 10, except for Case 16.

A correlation was noted for the positive CG flash rate versus positive I_p ($r^2 = 0.612$, linear; $r^2 = 0.678$, logarithmic). Multiple regressions were determined for negative CG flash rate and negative I_p versus multiplicity ($r^2 = 0.668$, linear; $r^2 = 0.534$, logarithmic) and positive CG flash rate and multiplicity versus negative I_p ($r^2 = 0.619$, linear; $r^2 = 0.715$, logarithmic).

After the storm moved out to sea, a logarithmic correlation was noted for negative CG flash rate versus multiplicity ($r^2 = 0.404$). Correlations were determined for positive CG flash rate versus multiplicity ($r^2 = 0.479$, linear; $r^2 = 0.589$, logarithmic). Multiple regression determined correlations for negative CG flash rate and negative I_p versus multiplicity ($r^2 = 0.405$, logarithmic) and positive CG flash rate and positive I_p versus multiplicity ($r^2 = 0.590$, logarithmic). The best fit equations are given in Appendix A.

The total, negative, and positive CG flash rates decreased as the storm moved out to sea. While the storm was over the land, the total CG flash rate was 14.4 min^{-1}. After the storm crossed the coast, the total CG flash rate decreased to 7.32 min^{-1}. The negative CG flash rate was 13.9 min^{-1} while over the land and decreased to 7.18 min^{-1} after crossing the coast. As the storm moved offshore, the mean negative multiplicity decreased from 3.0 to 2.9 and the median negative I_p increased from 36.5 kA to 39.0 kA. The positive CG flash rate was 0.5 min^{-1} while over the land and decreased to 0.13 min^{-1} after crossing the coast. As the storm moved offshore, the mean positive multiplicity decreased from 1.5 to 1.4 and the median positive I_p increased from 24.0 kA to 47.0 kA. The percent positive decreased from 3.45% to 1.82%.

11) Case 17

Case 17 occurred along the Gulf coast near the Texas - Louisiana border on 6 and 7 September. The first CG stroke associated with this case was at 2200 on 6 September. The geographic center of the lightning crossed the coastline at 0200 on 7 September. The last CG flash occurred at 0251 on 7 September. The synoptic overview is in Appendix B.

As the storm moved offshore, the negative CG flash rate increased. The flash rate had decreased from 45 during T-45 to 12 during T-0 (Fig. 32a). After the storm crossed the coastline, the negative CG flash rate increased during T+15 to 22. The negative multiplicity increased from 2.9 to 3.9 as the storm moved over the water (Fig 32b). The negative I_p increased from 54.1 kA to 54.6 kA as the storm moved out to sea (Fig. 32c). During T+30, the negative CG flash rate increased 77% to 39. The

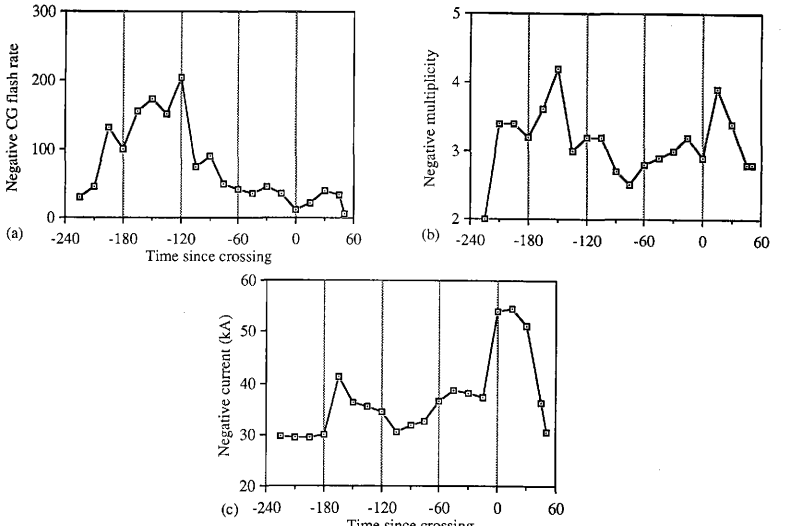

FIG. 32. Same as Fig. 4, except for Case 17.

mean negative multiplicity decreased to 3.4. The first stroke peak current decreased 6% to 51.2 kA. The negative CG flash rate decreased to 33 during T+45 and to 5 during T+60. Both the mean multiplicity and median first stroke peak current decreased through the remainder of the storm. There was no positive CG flash rate during the 30 minutes prior to the storm crossing the coastline. There was one positive CG flash during T+15 and then one more during T+45.

Before the storm crossed the coast, multiple regressions were determined for negative CG flash rate and negative I_p versus multiplicity ($r^2 = 0.434$, logarithmic). No correlations could be calculated for while the storm was over the water because there were only four fifteen minute intervals of data before the storm moved out to sea. The best fit equation is given in Appendix A.

The total, negative, and positive CG flash rates decreased as the storm moved out to sea. While the storm was over the land, the total CG flash rate was 6.38 min^{-1}. After the storm crossed the coast, the total CG flash rate decreased to 1.98 min^{-1}. The negative CG flash rate was 5.71 min^{-1} while over the land and decreased to 1.94 min^{-1} after crossing the coast. As the storm moved offshore, the mean negative multiplicity stayed at 3.3 and the median negative I_p increased from 34.5 kA to 48.5 kA. The positive CG flash rate was 0.67 min^{-1} while over the land and decreased to 0.04 min^{-1} after crossing the coast. Positive CG lightning parameters were not examined because there was not enough data to provide a significant statistical basis. The percent positive decreased from 10.51% to 1.98%.

12) Case 21

Case 21 occurred along the Atlantic coast near the North Carolina - South Carolina border on 18 and 19 September. The first CG stroke associated with this case was at 2000 on 18 September. The geographic center of the lightning crossed the coastline at 2200 on 18 September. The last CG flash occurred at 0459 on 18 September. The synoptic overview is in Appendix B.

As the storm moved offshore, the negative CG flash rate increased. The flash rate had increased from 503 during T-45 to 676 during T-0 (Fig. 33a). After the storm crossed the coastline, the negative CG flash rate increased 25% during T+15 to 844. The negative multiplicity decreased from 3.2 to 3.1 as the storm moved over the water (Fig 33b). The negative I_p decreased from 33.1 kA to 32.9 kA as the storm moved out to sea (Fig. 33c). During T+30, the negative CG flash rate decreased 6% to 797. The mean negative multiplicity decreased to 2.9. The first stroke peak current decreased 3%

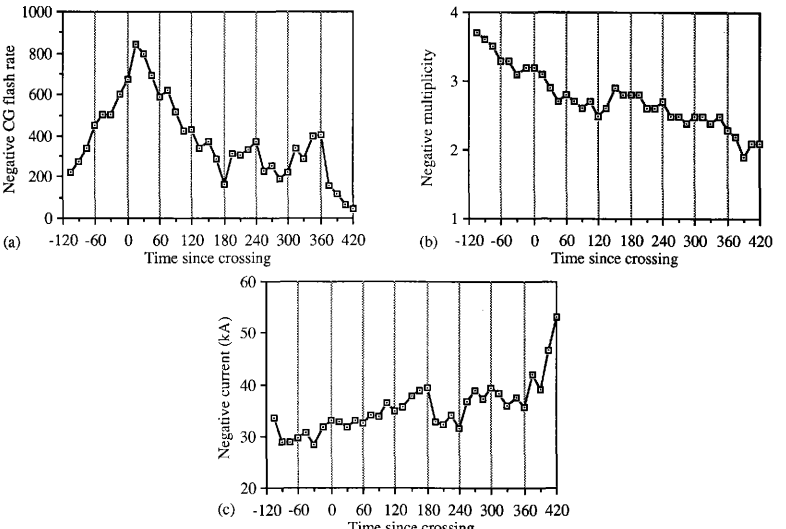

FIG. 33. Same as Fig. 4, except for Case 21.

to 31.8 kA. The negative CG flash rate decreased to 695 during T+45 and to 591 during T+60. The storm continued with a large amount of negative CG activity through the rest of the case.

As the storm moved offshore, the positive CG flash rate decreased. The flash rate had increased from 19 during T-45 to 23 during T-0. After the storm crossed the coastline, the positive CG flash rate stayed at 23 (Fig. 34a). The positive multiplicity decreased from 1.4 to 1.3 as the storm moved over the water (Fig. 34b). The positive I_p decreased from 22.0 kA to 19.3 kA as the storm moved out to sea (Fig. 34c). During T+30, the positive CG flash rate decreased 26% to 17. The mean positive multiplicity decreased to 1.2. The first stroke peak current increased 24% to 24.0 kA. The positive CG flash rate decreased to 12 during T+60 and to 7 during T+75. The positive CG flash rate fluctuated through the rest of the case and was no greater than 13. The percent positive through the life of the storm is shown in Fig. 34d.

Before the storm crossed the coast, a linear correlation was determined for the negative CG flash rate versus percent positive ($r^2 = 0.767$). A correlation was also noted for the negative CG flash rate versus multiplicity ($r^2 = 0.814$, linear; $r^2 = 0.870$, logarithmic). Multiple regressions were determined for the negative CG flash rate and multiplicity versus negative I_p ($r^2 = 0.571$, linear) and negative CG flash rate and negative I_p versus multiplicity ($r^2 = 0.917$, linear; $r^2 = 0.909$, logarithmic). For positive CG activity, correlations were determined for the multiplicity versus positive I_p ($r^2 = 0.588$, linear; $r^2 = 0.537$, logarithmic). Multiple regressions were determined for the positive CG flash rate and multiplicity versus positive I_p ($r^2 = 0.725$, linear; $r^2 = 0.648$, logarithmic) and positive CG flash rate and positive I_p versus multiplicity ($r^2 = 0.725$, linear; $r^2 = 0.648$, logarithmic).

After the storm crossed the coast, correlations were determined for the negative CG flash rate versus negative I_p ($r^2 = 0.502$ linear; $r^2 = 0.766$, logarithmic). Correlations were also noted for the negative CG flash rate versus multiplicity ($r^2 = 0.502$, linear; $r^2 = 0.576$, logarithmic) and multiplicity versus negative I_p ($r^2 = 0.413$, linear; $r^2 = 0.435$, logarithmic). Multiple regressions were determined for the negative CG flash rate and multiplicity versus negative I_p ($r^2 = 0.571$, linear; $r^2 = 0.909$, logarithmic) and negative CG flash rate and negative I_p versus multiplicity ($r^2 = 0.917$, linear; $r^2 = 0.909$, logarithmic).

The total, negative, and positive CG flash rates decreased as the storm moved out to sea. While the storm was over the land, the total CG flash rate was 31.63 min^{-1}. After the storm crossed the coast, the total CG flash rate decreased to 24.57 min^{-1}. The

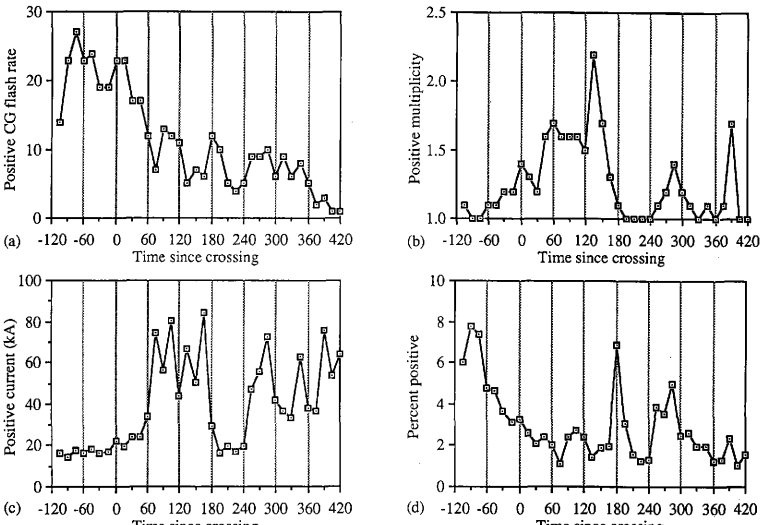

FIG. 34. Same as Fig. 10, except for Case 21.

negative CG flash rate was 30.19 min^{-1} while over the land and decreased to 24.14 min^{-1} after crossing the coast. As the storm moved offshore, the mean negative multiplicity decreased 3.3 to 2.7, while the median negative I_p increased from 30.8 kA to 35.0 kA. The positive CG flash rate was 1.44 min^{-1} while over the land and decreased to 0.43 min^{-1} after crossing the coast. As the storm moved offshore, the mean positive multiplicity increased 1.2 to 1.3, while the median positive I_p increased from 17.6 kA to 36.6 kA. The percent positive decreased from 4.58% to 2.25%.

13) Case 23

Case 23 occurred along the Georgia coast north of Brunswick on 30 October. The first CG stroke associated with this case was at 1315. The geographic center of the lightning crossed the coastline at 1645. The last CG flash occurred at 1959. The synoptic overview is in Appendix B.

As the storm moved offshore, the negative CG flash rate decreased. The flash rate had increased from 46 during T-15 to 82 during T-0 (Fig. 35a). After the storm crossed the coastline, the negative CG flash rate decreased 54% during T+15 to 38. The negative multiplicity decreased from 3.6 to 3.4 as the storm moved over the water (Fig. 35b). The negative I_p increased from 34.2 kA to 39.4 kA as the storm moved out to sea (Fig. 35c). During T+30, the negative CG flash rate decreased 5% to 36. The mean negative multiplicity decreased to 2.9. The first stroke peak current decreased 5% to 37.4 kA. The negative CG flash rate decreased to 24 during T+45 and to 16 during T+60. There was a secondary peak in the negative CG flash rate at T+120.

The positive CG flash rate varied both before and after the storm passed over the coast. After the storm moved over the water, the positive CG flash rate never exceeded 6. There was no correlation between any of the parameters at any time during the storm.

There was a decrease in the total, negative, and positive CG flash rates as the storm moved out to sea. While the storm was over the land, the total CG flash rate was 3.93 min^{-1}. After the storm crossed the coast, the total CG flash rate decreased to 2.28 min^{-1}. The negative CG flash rate was 3.6 min^{-1} while over the land and decreased to 2.17 min^{-1} after crossing the coast. As the storm moved offshore, the mean negative multiplicity increased 3.0 to 3.6, while the median negative I_p increased from 30.3 kA to 34.1 kA. The positive CG flash rate was 0.33 min^{-1} while over the land and decreased to 0.11 min^{-1} after crossing the coast. As the storm moved

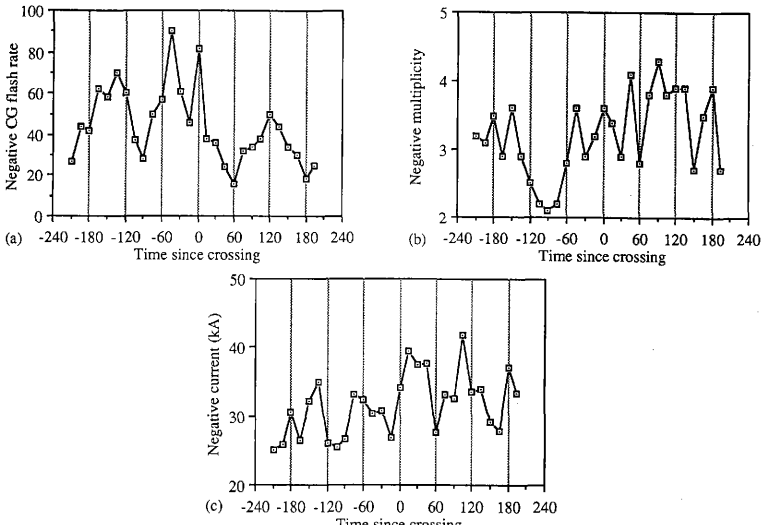

FIG. 35. Same as Fig. 4, except for Case 23.

offshore, the mean positive multiplicity decreased 1.3 to 1.1 and the median positive I_p decreased from 26.6 kA to 23.8 kA. The percent positive decreased from 8.9% to 6.0%.

6) Case 24

Case 24 occurred along the coast of Georgia north of Brunswick on 11 November. The first CG stroke associated with this case was at 0500. The geographic center of the lightning crossed the coastline at 0715. The last CG flash occurred at 1159. The synoptic overview is in Appendix B.

The storm intensified during the hour prior to crossing the coast. The negative CG flash rate increased from 12 during T-45 up to 25 during T-0. As the storm moved offshore, the negative CG flash rate during T+15 increased 28% to 32 (Fig. 36a). The negative multiplicity increased from 2.2 to 2.6, an increase of 18% after the storm moved over the water (Fig. 36b). The negative I_p decreased 10% from 34.3 kA to 30.9 kA as the storm moved out to sea (Fig. 36c). During T+30, the negative CG flash rate decreased sharply 66% to 11. The mean negative multiplicity increased 8% to 2.4. The first stroke peak current increased from 30.9 kA to 38.9 kA. The storm had secondary peaks at 0900 and 1159 while the storm continued out to sea.

The positive CG flash rate increased from 1 during T-30 up to 7 during T-0. As the storm moved offshore, the positive CG flash rate decreased to 1 during T+15 (Fig. 37a). The mean positive multiplicity stayed at 1.0 as the storm moved over the water (Fig. 37b). The positive I_p decreased 50% from 34.7 kA to 17.2 kA as the storm moved out to sea (Fig. 37c). During T+30, the positive CG flash rate stayed constant. The mean positive multiplicity did not change, while the first stroke peak current increased 90% to 32.7 kA. The positive CG activity continued through the end of the storm. The percent positive through the life of the storm is shown in Fig. 37d.

Before the storm crossed the coastline, numerous correlations were noted. A correlation was determined between the negative CG flash rate versus percent positive ($r^2 = 0.588$, linear). The logarithmic correlation for negative CG flash rate versus multiplicity yielded an $r^2 = 0.698$. A set of multiple regressions were determined using negative CG flash rate and negative I_p versus multiplicity ($r^2 = 0.603$, linear; $r^2 = 0.711$, logarithmic).

After the storm crossed the coastline, some of the correlations remained. Correlations were determined for the negative CG flash rate versus multiplicity ($r^2 = 0.437$, linear; $r^2 = 0.531$, logarithmic). Multiple regressions were determined

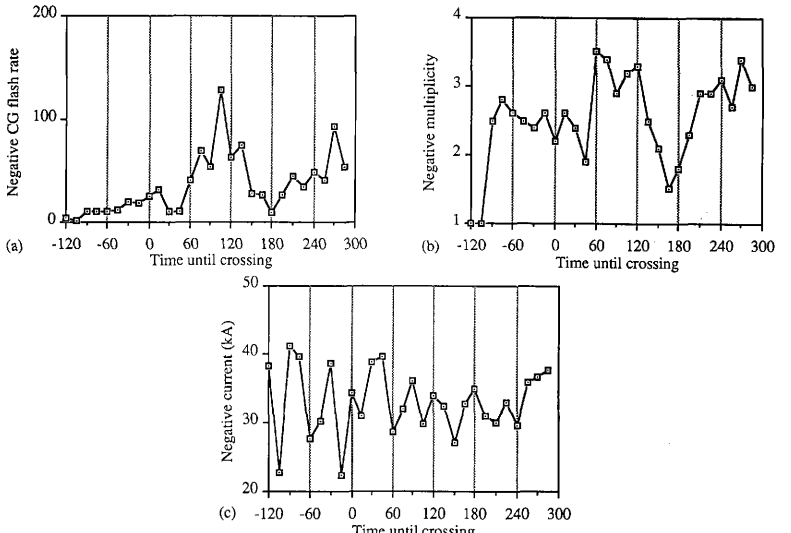

FIG. 36. Same as Fig. 4, except for Case 24.

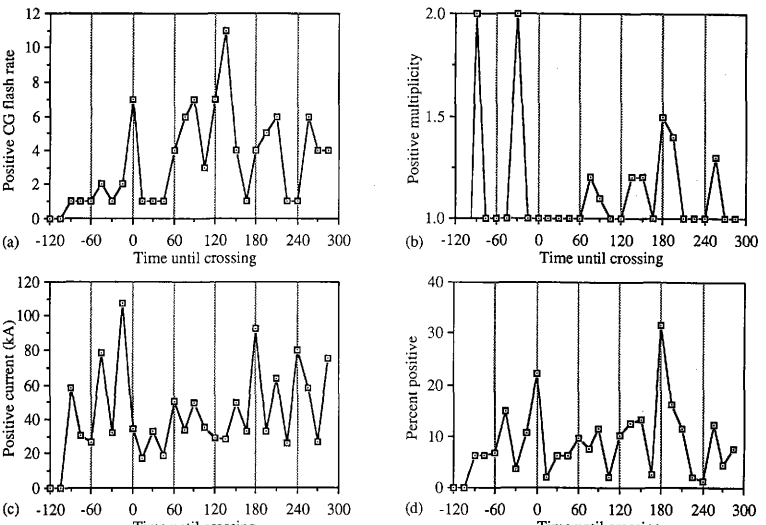

FIG. 37. Same as Fig. 10, except for Case 24.

for negative CG flash rate and negative I_p versus multiplicity ($r^2 = 0.439$, linear; $r^2 = 0.536$, logarithmic). The best fit equations are given in Appendix A.

The total, negative, and positive CG flash rates increased as the storm moved out to sea. While the storm was over the land, the total CG flash rate was 0.93 min^{-1}. After the storm crossed the coast, the total CG flash rate increased to 3.37 min^{-1}. The negative CG flash rate was 0.82 min^{-1} while over the land and increased to 3.11 min^{-1} after crossing the coast. The positive CG flash rate increased after the storm crossed the coast. The positive CG flash rate was 0.11 min^{-1} while over the land. After the storm crossed the coast, the positive CG flash rate increased to 0.27 min^{-1}. As the storm moved offshore, the mean negative multiplicity increased from 2.4 to 2.9, while the median negative I_p increased from 31.8 kA to 32.8 kA. The mean positive multiplicity stayed at 1.1 and the median positive I_p decreased from 55.0 kA to 33.5 kA. The percent positive decreased from 11.9% to 8.0% as the storm moved out to sea.

CHAPTER VII
DISCUSSION

The analysis examined twenty-three cases of storms which moved from over the land to over the water or vice versa. These storms were categorized and analyzed based on their method of formation and the direction of their movement across the coastline. There were four storms which moved onshore, one of which was formed by non-frontal mechanisms. The remaining nineteen storms moved offshore, fourteen of which were generated by frontal mechanisms.

The examination of these twenty-three storms considered trends in both negative and positive CG lightning activity as the individual storms moved onshore. The parameters of interest included the 15 minute flash rate, mean multiplicity, median first stroke peak current and the percent positive. The values for these parameters were also examined for the portion of the storm before and after crossing the coast. Finally, linear and logarithmic correlation coefficients and their associated equations of best fit were examined for before and after the storm crossed the coastline.

1. Sea to land transitions

a) Non-frontal

Since there was only one case, Case 19, in which a storm formed by non-frontal mechanisms moved onshore, no generalizations can be made. However, the data does allow for some discussion. When the storm moved onshore, there was a sharp increase (91%) in the negative CG flash rate. However, the associated multiplicity and peak current decreased 31% and 15%, respectively. During the next fifteen minutes, the negative CG flash rate continued to increase. The multiplicity and peak current also increased. Through the remainder of the storm, all three parameters decreased. There was not enough positive CG activity to draw any conclusions.

There are two possible, but not exclusive, explanations for the increase in negative CG flash rate. First, as the storm moved onshore, it entered more convectively unstable air. The higher surface temperature found in southeastern Texas at 1930 would yield a larger CAPE. With more CAPE available, there are stronger updrafts and consequently, a higher negative CG flash rate. Second, the storm's motion was controlled by the southeasterly synoptic flow and the evolving sea breeze. The increase in the negative CG flash rate may be linked to the storm passing through

the convergence zone along the sea breeze front. The lifting along the sea breeze front combined with the existing lifting within the storm enhanced the updraft, yielding a higher CG flash rate. The synoptic flow advected the storm past the sea breeze front and caused the sharp decrease in the flash rate.

The unexpected decrease in the multiplicity during the first fifteen minutes the storm was onshore may be associated with a time lag between the increase in flash rate and the anticipated increase in multiplicity. The amount of charge in the mid-level charge centers increases with an increasing updraft because of a larger mixed-phase region. But the amount of charge may not increase as fast as the CG flash rate. Since the charge source of subsequent strokes is adjacent charge centers, a higher CG flash rate will lead to a lower multiplicity because there is a finite amount of charge available. A higher CG flash rate would also lead to lower values of first stroke peak current. During the remainder of the storm, all three parameters followed the same downward pattern.

b) Frontal

1) Negative CG lightning

There were three storms which were caused by frontal passages that moved from sea to land. In all cases, there was not enough positive CG activity to allow for a sufficient analysis. Of these three storms, the negative CG flash rate decreased in two (Cases 14 and 22) during the thirty minutes after the coastal crossing. In both cases, there was a strong offshore peak in the flash rate. In Case 14, the CG flash rate peaked during the fifteen minutes prior to landfall. In Case 22, the peak occurred during the T-30 period. The decrease experienced after crossing the coast may have been associated with the natural cycle of storm evolution rather than the coastal transition.

The other case, Case 2, had a slight increase in the negative CG flash rate as the storm moved onshore. During the first fifteen minutes, the multiplicity decreased 23%, while the peak current increased only 0.7%. For the following fifteen minutes, the CG flash rate continued to increase. The multiplicity increased 4% but peak current decreased 17%. The lag in the increase of multiplicity may be similar to the time lag seen in Case 14. However, the trends in the flash rate may not be significant because of their low levels.

For the first thirty minutes of the cases, the trend in multiplicity followed the trend of the flash rate during 67% (4 of 6) of the intervals. For the first stroke peak

current, its trend followed the trend of the flash rate during 33% (2 of 6) of the intervals; two intervals had current changes of less than 1%.

Because of the low sample size, no definite trends in the parameters can be defined as the storms made landfall. These decreases may be a continuation of declining trends in the CG flash rate that started before the storms moved onshore. For the case where there was an increase in flash rate, the flash rate was low (< 5 per 15 minutes) and these trends may not be significant.

2) Correlations

During two of the cases (Cases 2 and 22), there were correlations among parameters after the storms made landfall. In the remaining storm (Case 14), the correlations occurred only while it was over the water. For all three cases, the equations of best fit had similar exponents for negative CG flash rate versus peak current. The equations of best fit were:

- Case 2 (After) : $I_p = 114.78\ FR^{-0.235}$ (5)
- Case 22 (Before): $I_p = 48.716\ FR^{-0.265}$ (6)
- Case 14 (Before): $I_p = 77.48\ FR^{-0.167}$. (7)

The closeness of exponents between cases 2 and 22 should be especially noted because these are correlations that occurred over land. The differences in the constant are related to difference in flash rates used to develop the relationships. The similarity between the equations are shown in Figure 38.

Reasonable logarithmic correlations ($r^2 > 0.530$) between the negative CG flash rate and multiplicity were found in Cases 14 and 22. However, there are two discrepancies between the cases. In Case 14, the correlation occurred before landfall and the parameters are positively correlated. However during Case 22, it occurred over the land and the parameters are negatively correlated.

- Case 14 (Before) : $Mult = 1.223\ FR^{0.273}$ (8)
- Case 22 (After) : $Mult = 3.607\ FR^{-0.154}$. (9)

These relationships are shown graphically on Figure 39.

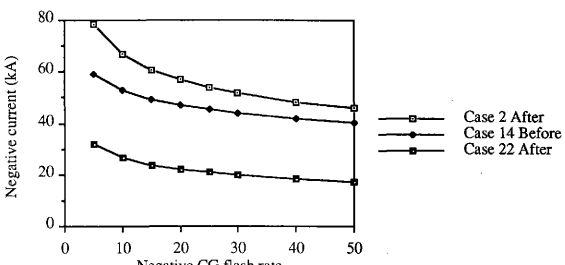

FIG. 38. Graphical representation of the logarithmic equations of best fit for negative CG flash rate versus negative current. These cases were frontal storms which moved from sea to land.

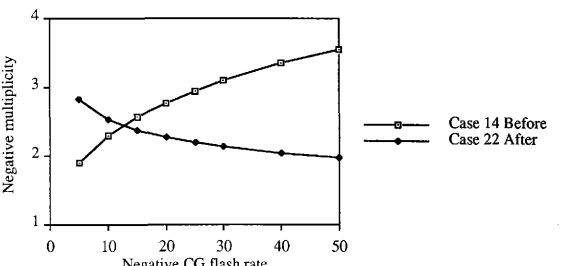

FIG. 39. Graphical representation of the logarithmic equations of best fit for negative CG flash rate versus negative multiplicity. These cases were frontal storms which moved from sea to land.

Similarly, linear correlations ($r^2 > 0.600$) between the multiplicity versus first stroke peak current for the negative flashes were determined for Cases 14 and 22. As above, the same two discrepancies occur between the cases.

- Case 14 (Before): Ip = -9.917(Mult) + 76.891 (10)
- Case 22 (After) : Ip = 19.617(Mult) - 22.68. (11)

These relationships are shown graphically in Figure 40. For Case 22 over land, multiplicity and peak current are positively correlated, while for Case 14 over the water, these parameters are negatively correlated.

For Cases 2 and 14, there were multiple regressions, both linear and logarithmic, for negative CG flash rate and negative multiplicity versus negative first stroke peak current for which $r^2 > 0.500$. For Case 2, the best fit was logarithmic and occurred while the storm was over the land, while Case 14 had a linear best fit and occurred before the storm moved onshore. In both cases, the flash rate and multiplicity were negatively correlated.

There were three sets of correlations which were found in at least two of the three cases. The negative correlation between flash rate and first stroke peak current was consistent across all three cases. However, the correlations between flash rate and multiplicity, and multiplicity and peak current varied from case to case. In one case, flash rate and multiplicity were found to be positively correlated when over the water, yet in another case they were negatively correlated when over the land. Similarly, in one case, multiplicity and peak current were negatively correlated when over the water, but correlated when over the land in the other case.

2. Land to sea transitions

a) Non-frontal

1) Negative CG lightning

There were five storms which were caused by non-frontal mechanisms that moved from land to sea. Of the five storms, the negative CG flash rate had a decreasing trend in four cases for the thirty minute period following crossing the coastline. Notably, there were three cases (Cases 8, 12, and 13) in which the flash rate either increased or leveled off for the first fifteen minutes offshore and then decreased at least 15% during T+30. In these three cases, there had been a pattern of increasing

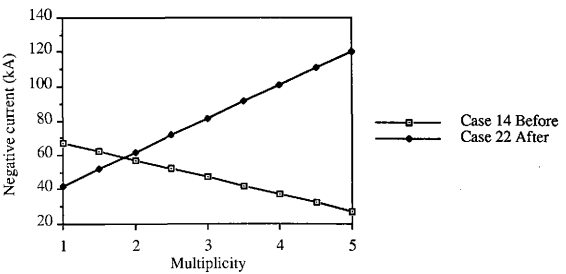

FIG. 40. Graphical representation of the linear equations of best fit for negative multiplicity versus negative current. These cases were frontal storms which moved from sea to land.

negative CG flash rates while over land in the thirty minutes prior to crossing the coastline.

In the remaining case, Case 20, the negative CG flash rate increased 37% during the first two fifteen minute periods after the storm crossed the coast. The flash rate decreased during the next period, but then increased again and peaked during T+90.

The decrease in the negative CG flash rate in four of the five storms is expected. As a non-frontal storm moves offshore, the buoyancy, which is caused by the warm ground, is diminished. The CG flash rate is related to the strength of the updraft, so as the updraft changes, the flash rate changes in a similar manner.

For the thirty minutes after the storm moved offshore, the trend in negative multiplicity followed the trend of the negative CG flash rate during only 20% (2 of 10) of the intervals. For the negative first stroke peak current, its trend followed the trend of the negative CG flash rate during 20% (2 of 10) of the intervals.

2) Positive CG lightning

For these five cases where non-frontal thunderstorms moved from land to sea, there was sufficient positive CG lightning activity for analysis in three cases. In all cases, there was a decreasing trend in the CG flash rate in the first thirty minutes over the water.

These decreases in the positive CG flash rate occurred as the storms moved offshore and dissipated. This result is surprising because increased positive CG activity is associated with the dissipation phase of storms (Williams 1989). Typically, the positive activity occurs in the stratiform region of the storm. Non-frontal storms do not have an extensive stratiform region, because of their structure, which may preclude the occurrence of positive CG lightning.

For the thirty minutes after the storm moved offshore, the trend in positive multiplicity followed the trend of the positive CG flash rate during 66% (4 of 6) of the intervals. For the positive first stroke peak current, its trend followed the trend of the positive CG flash rate during 33% (2 of 6) of the intervals.

3) Correlations

Since there were five cases in which non-frontal storms moved from land to sea, there were ten periods for which correlations could be calculated. There was

sufficient negative CG lightning in all ten periods to have statistically significant values. In calculating the equations of best fit for the positive parameters, there were no equations defined which had a $r^2 \geq 0.400$.

The calculation of logarithmic correlation for the negative CG flash rate versus multiplicity yielded correlations of greater than 0.500 for two of the ten periods. These occurred in Cases 12 and 20 while over land. In all cases, the equations of best fit were:

- Case 12 (Before): $\text{Mult} = 1.15\ FR^{0.232}$ (12)
- Case 20 (After): $\text{Mult} = 1.83\ FR^{0.101}$ (13)

These relationships are shown graphically in Figure 41. In both of these periods, the flash rate is positively correlated to the multiplicity, regardless of whether the storm was over land or over water. These results are consistent with the results of Goodman and MacGorman (1986) and Studwell and Orville (1995).

While there were only two periods, both during Case 12, in which the correlation coefficient for negative multiplicity versus first stroke negative peak current was greater than 0.400, the results are notable. Similar to the pattern seen in frontal sea to land storms, when the storm was over the water, the multiplicity was negatively correlated to the peak current. However, when the storm was over the land, the two parameters were positively correlated. These best fit equations are shown in Figure 42.

There are four possible negative multiple correlation combinations: flash rate and multiplicity versus first stroke peak current, and flash rate and first stroke peak current versus multiplicity, linear and logarithmic. There were three which had four or five periods with correlation coefficients of greater than 0.400. The fourth combination was valid for only three periods, but the results are significant.

The results seen for negative CG flash rate and multiplicity versus first stroke negative peak current were the same for linear and logarithmic equations of fit. Since the correlation coefficients were higher for the logarithmic equations ($r^2 \geq 0.827$), these are the results which will be discussed. For Case 12, the results were similar to those seen for the correlation between negative multiplicity and first stroke peak current. When Case 12 was over the land, both independent parameters, flash rate and multiplicity, were positively correlated to the first stroke peak current. After the storm crossed the coast, the independent parameters were negatively correlated to the peak

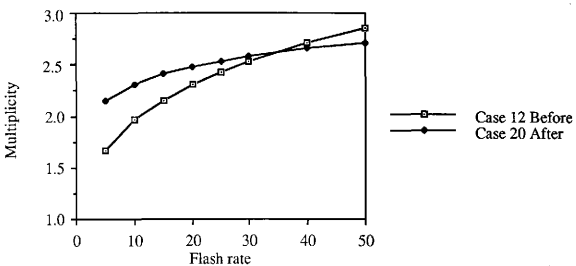

FIG. 41. Graphical representation of the logarithmic equations of best fit for negative flash rate versus negative multiplicity. These cases were non-frontal storms which moved from land to sea.

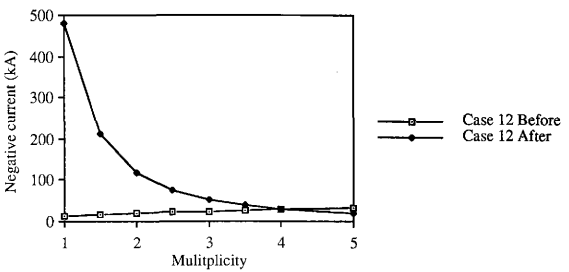

FIG. 42. Graphical representation of the logarithmic equations of best fit for negative multiplicity versus negative current. These cases were non-frontal storms which moved from land to sea.

current. However during Case 18 while the storm was over the land, the flash rate was negatively correlated but the multiplicity was positively correlated.

In the two cases (Cases 8 and 12) that there was a correlation while the storm was over land, the peak current was positively correlated in both cases. The flash rate was negatively correlated during Case 8, but positively correlated during Case 12.

- Case 8 (Before): Mult = -0.043 FR + 0.043 I_p + 1.645 (14)
- Case 12 (Before) : Mult = 0.001 FR + 0.150 I_p - 0.534 (15)

For the multiple regression of negative CG flash rate and median first stroke peak current versus mean negative multiplicity, the peak current was positively correlated while the storm was over the land. It became negatively correlated to the multiplicity after the storm move offshore.

There were two cases which had a significant correlation between negative CG flash rate and the mean negative multiplicity. During Case 12, the relationship between the negative multiplicity and the first stroke peak current changed, similar to the pattern seen for frontal storms which moved from land to sea. When the storm was over land, these parameters were positively correlated. But when the storm moved offshore, they became negatively correlated. This pattern was consistent through most of the multiple regressions.

b) Frontal

1) Negative CG lightning

There were fourteen storms which were caused by the passage of a front that moved from land to sea. Of the fourteen storms which had sufficient negative lightning, six cases had an increasing trend in the negative CG flash rate thirty minutes after crossing the coastline and eight storms had a decreasing trend in the flash rates.

There were five cases during which the negative CG flash rate decreased during the fifteen minutes after crossing the coastline. The decrease in one case (Case 6) was part of a continuing trend of decreasing flash rates. In three other cases (Cases 3, 7 and 23), there was a peak in the flash rate within the thirty minutes prior to crossing the coast. In the remaining case (Case 15), the decrease in negative CG flash rate was only 1%.

There were eight cases in which the negative CG flash rate increased as the storm moved offshore. The increases in five of these eight cases (Cases 9, 10, 11, 21 and 24) were the result of continuing upward trend in flash rate. In the remaining three cases (Cases 1, 16, and 17), there had been a minimum in flash rate within the thirty minutes prior to crossing the coast, but then increased as the storm moved offshore. In the five cases where there was a increasing trend in negative CG flash rate while over the land that continued through the first fifteen minutes while over the water, the flash rate decreased during the T+30 period in four of the cases (Cases 9, 10, 21 and 24).

Case 11 was the only case in which there was increasing trend in the negative CG flash rate while over the land and this trend continued as the storm moved over the water. In two of the remaining three cases (Cases 1, 16, and 17) where the negative CG flash rate increased as the storm moved offshore, the flash rate increased during the T+30 period.

There was little continuity in the trends noted in the lightning parameters or the correlations between the parameters for frontal storms which moved from land to sea. There were no specific patterns in the changes in the negative CG flash rate. This variability is because there are no changes in the mechanisms that cause updrafts. For negative CG activity during the first thirty minutes after a storm has moved over the water, the trends in mean multiplicity followed the trend of the flash rate during 44% (12 of 28) of the intervals. For the median first stroke peak current, its trend followed the trend of the flash rate during 54% (15 of 28) of the intervals.

2) Positive CG lightning

Of the thirteen frontal storms which moved from land to sea, eight had sufficient positive CG lightning for analysis. Of these eight storms, the positive CG flash rate had an increasing in two cases and a decreasing trend in five cases after thirty minutes. There was no change in the remaining case.

Similar to the findings for the negative lightning, there was no continuity in the seven cases for the pattern of positive CG flash rate as a storm moved over the water. For positive CG activity during the first thirty minutes after a storm has moved over the water, the trends in mean multiplicity followed the trend of the flash rate during 37% (6 of 16) of the intervals. For the median first stroke peak current, its trend followed the trend of the flash rate during 44% (7 of 16) of the intervals. There was also no patterns detected in the examination of the correlations for the positive parameters.

3) Correlations

There were fourteen storms which were formed by frontal mechanisms and moved from land to sea. This means that there were twenty-eight possible periods for which correlations could be examined. However, there was sufficient negative CG lightning in twenty-five periods to have statistically significant values. The calculation of linear correlation for the negative CG flash rate versus mean multiplicity yielded values of $r^2 \geq 0.400$ for eleven of the twenty-five periods. The logarithmic correlations resulted in $r^2 \geq 0.400$ for twelve of the periods. During ten of the periods, the mean multiplicity was positively correlated to the flash rate. In the remaining two periods, one period was while the storm was over the land (Case 21), while for Case 11, the negative correlation occurred while the storm was over the water. The slope of the linear fit varied by a factor of 15 which shows the variability in the mechanism associating flash rate to multiplicity. The equations of best fit will not be listed or plotted because of the large amount of periods for these correlations.

The calculation of the linear correlation for the negative CG flash rate versus the median negative first stroke peak current yielded only three periods which had $r^2 \geq 0.400$. These three periods were Cases 1, 11, and 21 after the storm moved over the water. In all three periods, the peak current was negatively correlated to the flash rate. The calculation of logarithmic correlation for these parameters yielded eight cases which had $r^2 \geq 0.400$. But for the three periods which had a linear fit of the data, the correlation coefficient was greater for the linear cases. In six of the eight periods, the peak current was negatively correlated. All of the six periods occurred while the storm was over the water. The remaining two periods during Cases 6 and 10 when the peak current and flash rate were positively correlated occurred while the storm was over land.

The calculation of the linear correlation for the percent positive versus negative CG flash rate yielded correlation coefficients greater than 0.400 in seven of the possible twenty-five periods. During five of these seven periods, the percent positive and the flash rate were negatively correlated. There was no pattern for whether the correlation was positive or negative compared to when a storm was over land or water.

The logarithmic and linear correlation of mean negative multiplicity versus mean first stroke peak current yielded correlation coefficients greater than 0.400 in three of the possible twenty-five periods. In all three cases, the parameters were positively correlated.

Linear and logarithmic multiple regressions were used to compare the negative CG flash rate and mean multiplicity versus the median negative first stroke peak current. There were correlation coefficients greater than 0.400, both linear and logarithmic, for nine of the twenty-five possible periods. The correlation coefficient was greater for the logarithmic fit in seven of the nine periods. The flash rate was positively correlated for a logarithmic calculation in two of the nine periods (Cases 6 and 11 over land). For logarithmic calculations, the negative correlations for flash rate occurred in six periods over the water and one period over land. The multiplicity was negatively correlated for a logarithmic calculation in only one of the nine periods (Case 5 over water). The positive correlations for multiplicity occurred in five periods over the water and three periods over land. The results for the linear correlations were the same as the logarithmic calculations except that the linear r^2 for Case 6 over land was less than 0.400. Also, Case 21 over land had a $r^2 = 0.571$, while the logarithmic correlation coefficient was less than 0.400. During this period, the flash rate was negatively correlated, which is not consistent with the other findings for multiplicity in this multiple correlation.

Linear and logarithmic multiple regressions were also used to compare the negative CG flash rate and the median negative first stroke peak current versus mean multiplicity. There were correlation coefficients greater than 0.400 for eleven periods with linear equations of best fit and fourteen periods with logarithmic equations of best fit. The logarithmic correlation coefficient was equal to or greater than the linear fit in eight of the fourteen periods. The flash rate was negatively correlated for a logarithmic calculation in three of the fourteen periods (Cases 11 and 21 over land, Case 11 over water). The positive logarithmic correlations for flash rate occurred in six periods over the water and five periods over land. The negative first stroke peak current was negatively correlated for a logarithmic calculation in only two of the fourteen periods (Cases 10 and 24 over land). The positive correlations for multiplicity occurred in five periods over the water and seven periods over land.

The results for the linear correlations are different than what was determined for the logarithmic calculations. The linear r^2 for Cases 11, 17, and 24 over land were less than 0.400 which yielded eleven periods for examination. The flash rate was negatively correlated in three of the eleven periods (Cases 11 and 15 over water, Case 21 over land). Of the remaining eight periods which were positively correlated, three periods were over land and five periods were over the water. The first stroke peak

current was also negatively correlated during three periods (Cases 15 and 21 over water, Case 10 over land).

In examining the correlations between the positive parameters, there were sixteen possible intervals. However, there was sufficient positive CG lightning in twelve periods to have statistically significant values. There were no two parameter correlations which had more than three intervals with correlation coefficients greater than 0.400. For multiple regressions, the only case which had more than three intervals with $r^2 > 0.400$ was the logarithmic flash rate and multiplicity versus peak current. The flash rate and multiplicity were negatively correlated for one interval (Case 16 over land). For the remaining intervals, which occurred over both the land and the water, the flash rate and multiplicity were positively correlated.

The correlations seen for other types of storms for mean negative multiplicity versus the median first stroke peak current did not occur in frontal land to sea storms. What had occurred in other scenarios was that these parameters were positively correlated over land and negatively correlated over water. For frontal storms which moved from land to water, there were four periods which had significant correlations. Of these four periods, three periods had positive correlations. One of the period was over land, while the other two occurred over water. The negatively correlated period occurred over the water.

However, there were correlations which were reasonably consistent with those for other storm types. The negative CG flash rate and the mean negative multiplicity were positively correlated in ten of twelve cases. This results is consistent with the results of Goodman and MacGorman (1986) and Studwell and Orville (1995). Additionally, the correlations between the flash rate and the median negative first stroke peak current were consistent. These parameters were positively correlated when over the land and negatively correlated when over the water.

3. Flash rate changes less than 10%

This section examines the seven cases in which there were changes in negative CG flash rate of less than 10% during the first fifteen minutes after the storm crossed the coastline. In cases in which the flash rate changed by a small amount, the changes in the lightning parameters may be associated with the storm moving to a new ambient environment. All seven of the cases in which there was a low change in the flash rate

occurred during cases which moved from land to sea. Three of the storms were formed by non-frontal mechanisms, while the remaining four were generated by a front.

For the non-frontal storms, the flash rate increased in one case (Case 8) and did not change in the remaining two cases (Cases 12 and 13). In all three cases, both the mean negative multiplicity and median negative first stroke peak current decreased.

For the frontal storms, the negative CG flash rate decreased in two cases (Cases 6 and 15), increased in Case 11, and did not change in Case 5. In the two cases in which the flash rate decreased, the multiplicity decreased in one case and had no change in the other. The peak current decreased in both cases. In the case with the increasing CG flash rate, the multiplicity increased, while the peak current decreased. For the case where there was no change in the flash rate, both the multiplicity and first stroke peak current increased.

The decrease in negative multiplicity after the non-frontal storms moved over the water may be associated with the reduction in development and continuance of the mid-level charge centers. This reduction may be due to a lessening in the intensity of the updrafts. As a non-frontal storm moves over the water, it loses its source of generation, the warm ground. However, a reduction in the magnitude of the updraft should also result in a decrease in the negative CG flash rate, which was not seen. Therefore, a change in the updraft may not be the only reason for changes in multiplicity.

However for frontal storms, the trend of the negative multiplicity matched that of the negative CG flash rate. During these storms, the generation of the mid-level charge centers would depend on the storm's lifecycle. This yields a pattern similar to that seen for the entire set of frontal storms where the variability in the multiplicity and flash rate are associated with the storm's lifecycle.

The median first stroke peak current decreased in six of the seven cases. The only case in which it increased was during a period when there was no change in the flash rate and an increase in the multiplicity. There is not enough known about the mechanisms which govern the magnitude of the peak current to determine why changes are occurring. However, there has to be some kind of change to alter the peak currents in such a consistent manner.

CHAPTER VIII
CONCLUSIONS

1. Lightning parameters

a) Negative CG flash rate

The negative CG flash rate changed in a more predictable manner for the thirty minutes after crossing the coast in airmass storms than in frontal storms. In the airmass storm which moved onshore, the flash rate increased, while in the 80% of the storms which moved offshore, the flash rate had a decreasing trend. This is expected because as a storm moved over land, it encounters more convectively unstable air and the convergence zone along the sea breeze front. Conversely, as an airmass storm moves over the water, the uplifting, which is caused by the warm ground, is diminished. The negative CG flash rate is related to the strength of the updraft, so as the updraft changes, the flash rate changes in a similar manner.

In the storms caused by the passage of fronts, there was no identifiable pattern in the changes of the flash rate. For storms which moved from land to sea, the negative CG flash rate had an increasing trend in 43% and a decreasing trend in 57% of the cases after thirty minutes. This variability is because there are no changes in the updrafts due to a change in the storm's driving force as it moves offshore. The lifting in frontal storms is caused by the denser cold air acting as a wedge and yields convective lifting ahead of the front. There would be little thermodynamic difference between the air over the land and water. The variability seen in the flash rate is associated with the natural variability of the storm.

b) Negative multiplicity and first stroke peak current

The negative multiplicity did not show a strong relationship with the negative CG flash rate. The trend of the negative multiplicity showed a direct relationship with the negative CG flash rate during the thirty minutes after crossing the coast only for frontal storms which moved from sea to land. The multiplicity tracked the flash rate during 67% of the intervals. In the remaining three categories of storms, the multiplicity only tracked the flash rate a maximum of 44% of the fifteen minute intervals. (For the sea to land airmass storm, multiplicity followed the flash rate 50% of the time, but there were only two intervals.) A lag may exist between an increase (decrease) in the negative CG flash rate and associated increase (decrease) in the

multiplicity. It may occur because the variability of the updrafts, which cause changes in the CG flash rate and multiplicity, may not influence the magnitude of charge in charge centers as quickly as changes in the rate of charge separation.

Similar to the negative multiplicity, the negative first stroke peak current did not show a strong relationship with the negative CG flash rate. Frontal storms which moved from land to sea were the only cases that the trend of the negative peak current showed a tendency for a direct relationship with the negative CG flash rate during the thirty minutes after crossing the coast. In this situation, the peak current tracked the flash rate during 54% of the intervals. In the other three types of storms, the peak current only tracked the flash rate a maximum of 33% of the fifteen minute intervals. (For the sea to land airmass storm, peak current followed the flash rate 50% of the time, but there were only two intervals.) The same argument used for multiplicity may apply to the first stroke peak current. Changes in the magnitude of the current may have a time lag behind changes in the flash rate.

c) Positive CG flash rate *

The positive CG flash rate changed in a more predictable manner for the thirty minutes after crossing the coast in airmass storms than in frontal storms. In the airmass storms which moved offshore, the flash rate had a decreasing trend in all of the cases, while in the frontal storms, the changes in flash rate did not show any pattern.

This was not expected because as an airmass storm moves over water, the storm starts to dissipate. The occurrence of positive CG lightning has been associated with the end of electrically active storms. However, there was a peak in the percent positive at the end of the storm in only one of the four cases. Positive lightning during a storm's dissipation typically occurs in the stratiform region. Airmass storms do not usually develop a stratiform region. The lack of stratiform regions may account for the decrease in positive CG lightning.

In the storms caused by the passage of fronts, the positive CG flash rate increased in 25%, decreased in 63% and stayed the same in 12% of the cases during the first thirty minutes over the water. This variability is because the storm may not necessarily dissipate as it moves offshore. Different storms would be in various stages

* There was only a statistically significant amount of positive CG activity in the storms which moved from land to sea, both airmass and frontal.

of development. So the variability seen in the positive CG flash rate is associated with the natural variability of the storm.

d) Positive multiplicity and first stroke peak current *

The positive multiplicity showed a strong relationship with the positive CG flash rate for airmass storms. The trend of the positive multiplicity showed a direct relationship with the positive CG flash rate during the thirty minutes after crossing the coast and moving across the water in non-frontal storms; the multiplicity tracked the flash rate during 66% of the intervals. In the frontal storms, the multiplicity only tracked the flash rate during 37% of the fifteen minute intervals.

The positive first stroke peak current did not show a strong relationship with the positive CG flash rate. The fifteen minute trend in peak current did not follow in either airmass or frontal storms in more than 50% of the intervals.

2. Correlations

The negative CG flash rate and the mean negative multiplicity were positively correlated during 81% (13 of 16) of the periods which had correlation coefficients greater than 0.400. This is consistent with previous findings.

An unexpected result was that for frontal storms which moved from land to sea, the negative CG flash rate and first stroke peak current were positively correlated for 67% (2 of 3) of the intervals over the land and always negatively correlated over the water. However for frontal storms which moved from sea to land, the negative CG flash rate and first stroke peak current were always negatively correlated over the land. There was one case of negative correlation for a storm over the water. In airmass storms which moved from land to sea, there was little pattern in the correlations for these three cases.

However, this seeming contradiction between the direction of travel does show a pattern when all fourteen periods are examined. In 79% (11 of 14) of the intervals, the negative CG flash rate and the first stroke peak current were positively correlated during the early part of the storm and negatively correlated for the latter periods of the storms. Further breakdown shows for the beginning of the storm, there was positive correlation between the parameters in 50% (3 of 6) of the intervals. During the end of the storm, the parameters were negatively correlated in 100% (8 of 8) of the intervals.

As a storm dissipates, the CG flash rate decreases. The increase in the peak current would result from fewer flashes using the mid-level charge centers.

3. Flash rate changes less than 10%

The airmass storms which had changes in the negative CG flash rate less than 10% exhibited consistent changes in the mean negative multiplicity. In all three airmass storms, the mean multiplicity decreased as the storms moved over the water. The reductions occurred even though the negative CG flash rate increased in one case and did not change in the remaining two cases. As stated in earlier conclusions, these decreases may be the results of reduction in the updraft. Even though the flash rate may increase, the level of charge generation lessens.

The frontal storms which had less than 10% changes in the negative CG flash rate also exhibited consistent changes in the mean multiplicity. However, the consistency for the mean multiplicity is different than what was seen for the airmass storms. For cases where the flash rate decreased, the multiplicity also decreased or had no change. When the flash rate increased, the multiplicity increased. However, when there was no change in the flash rate, the multiplicity increased.

The median first stroke peak current decreased in six of the seven cases. The only case in which it increased was during a period when there was no change in the flash rate and an increase in the multiplicity. There is not enough known about the mechanisms which govern the magnitude of the peak current to determine why changes are occurring. However, there has to be some kind of change to alter the currents in such a consistent manner.

4. Further research

Additional research in the changes of lightning parameters as the storms cross over a coastline could be conducted. By using five minute instead of fifteen minute intervals, a better fit may be determined for the correlations. Smaller trends in the negative CG flash rate may also be seen. However, a drawback for decreasing the length of the intervals is that more "noise" would be introduced into the analysis.

The use of infrared satellite data and radar data from sites near the individual cases would be useful. These tools would provide another reference point for clues into changes in the storms as they moved across a coastline.

REFERENCES

Atkinson, B.W. 1981: *Mesoscale Atmospheric Circulations*. Academic Press., 125-127.

Barnes, S.L., and E.W. Newton, 1986: Thunderstorms in a synoptic setting. *Thunderstorm Morphology and Dynamics*, E. Kessler, Ed. University of Oklahoma Press., 81-82.

Bell, G.D., and L.F. Bosart, 1988: Appalachian cold-air damming. *Mon. Wea. Rev.*, **116**, 137-161.

Biswas, K.R., and P.V. Hobbs, 1990: Lightning over the Gulf Stream. *Geophys. Res. Lett.*, **17**, 941-943.

Blanchard, D.O., and R.E. Lopez, 1985: Spatial patterns of convection in south Florida. *Mon. Wea. Rev.*, **113**, 1283-1299.

Brook, M., M. Nakano, P. Krehbiel, and T. Takeuti, 1982: The electrical structure of the Hokuriku winter thunderstorms. *J. Geophys. Res.*, **87**, 1207-1215.

Colucci, S.J., 1976: Winter cyclone frequencies over the eastern United States and adjacent western Atlantic. *Bull. Amer. Meteor. Soc.*, **57**, 548-553.

Cotton, W.R., 1990: *Storms*. ASTeR Press., 39-40.

Dirks, R.A., J.P. Kuettner, and J.A. Moore, 1988: Genesis of Atlantic Lows Experiment (GALE): An Overview. *Bull. Amer. Meteor. Soc.*, **69**, 148-160.

Dodge, P.P., and R.W. Burpee, 1993: Characteristics on rainbands, radar echoes, and lightning near the North Carolina coast during GALE. *Mon. Wea. Rev.*, **121**, 1936-1955.

Dong, Y., and J. Hallett, 1992: Charge separation by ice and water drops during growth and evaporation. *J. Geophys. Res.*, **97**, 20361-20371.

Engholm, C.D., E.R. Williams, and R.M. Dole, 1990: Meteorological and electrical conditions associated with positive cloud-to-ground lightning. *Mon. Wea. Rev.*, **118**, 470-487.

Gilmore, M.S., A.H. Perez, R.E. Orville, and L.J. Wicker, 1994: XLIGHT, An interactive lightning analysis and display system. Preprints, *10th International Conference on Interactive and Processing Systems for Meteorology, Oceanography, and Hydrology*, Nashville, TN, American Meteorological Society, 44-47.

Goodman, S.J., and D.R. MacGorman, 1986: Cloud-to-ground lightning activity in mesoscale convective complexes. *Mon. Wea. Rev.*, **114**, 2320-2328.

Holle, R.H., and R.E. Lopez, 1993: Overview of real-time lightning detection systems and their meteorological uses. NOAA Technical Memorandum ERL NSSL-102, Norman, OK.

Huburt, P., and G. Mouget, 1981: Return stroke velocity measurements in two triggered lightning flashes. *J. Geophys. Res.*, **87**, 5253-5261.

Idone, V.P., and R.E. Orville, 1982: Lightning return stroke velocities in the Thunderstorm Research International Program. *J. Geophys. Res.*, **87**, 4903-4915.

Idone, V.P., R.E. Orville, P. Hubert, L. Barret, and A. Eybert-Berard, 1984: Correlated observations of three triggered lightning flashes. *J. Geophys. Res.*, **89**, 1385-1394.

Kraus, K., and J. Canniff, 1995: Incorporating lightning data into automated weather observations. Preprints, *6th Conference on Aviation Weather Systems*, Dallas, TX, American Meteorological Society, 466-469.

Krehbiel, P.R., M. Brook, and R.A. McCrory, 1979: An analysis of the charge structure of lightning discharges to ground. *J. Geophys. Res.*, **84**, 2432-2456.

Krehbiel, P.R., 1986: The electrical structure of thunderstorms. *The Earth's Electrical Environment*, E.P. Krider and R.G. Roble, Ed., National Academy Press, 90-113.

Krider, E.P., 1986: Physics of lightning. *The Earth's Electrical Environment*, E.P. Krider and R.G. Roble, Ed., National Academy Press, 30-40.

Lapenta, W.M., and N.L. Seaman, 1990: A numerical investigation of East Coast cyclogenesis during the cold-air damming event of 27-28 February 1982. Part I: Dynamic and thermodynamic structure. *Mon. Wea. Rev.*, **118**, 2668-2695.

Lapenta, W.M., and N.L. Seaman, 1992: A numerical investigation of East Coast cyclogenesis during the cold-air damming event of 27-28 February 1982. Part II: Importance of physical mechanisms. *Mon. Wea. Rev.*, **120**, 52-76.

Lhermitte, R., and E. Williams, 1985: Thunderstorm electrification: A case study. *J. Geophys. Res.*, **90**, 6071-6078.

Lundholm, R., 1957: Induced overvoltage surges on transmission lines. *Chalmers Tek. Hoegsk. Handl.*, **188**, 1-117.

MacGorman, D.R., D.W. Burgess, V. Mazur, W.D. Rust, W.L. Taylor, and B.C. Johnson, 1989: Lightning rates relative to tornadic storm evolution on 22 May 1981. *J. Atmos. Sci.*, **46**, 221-250.

MacGorman, D.R., 1993: Lightning in tornadic storms: A review. *The Tornado: Its structure, dynamics, predictions, and hazards*, AGU Monograph No. 79, American Geophysical Union, 173-182.

Malan, D.J., and B.F.J. Schonland, 1951: The electrical processes in the intervals between the strokes of a lightning discharge. *Proc. Roy. Soc. London, A*, **206**, 145-163.

Nicholls, M.E., R.A. Pielke, and W.R. Cotton, 1991. A two-dimensional numerical investigation of the interaction between sea breezes and deep convection over the Florida peninsula. *Mon. Wea. Rev.*, **119**, 298-323.

Orville, R.E., R.W. Henderson, and L.F. Bosart, 1983: An east coast lightning detection network. *Bull. Amer. Meteor. Soc.*, **64**, 1029-1037.

Orville, R.E., and R.W. Henderson, 1986: Global distribution of midnight lightning: September 1977 to August 1978. *Mon. Wea. Rev.*, **114**, 2640-2653.

Orville, R.E., R.A. Weisman, R.B. Pyle, R.W. Henderson, and R.E. Orville, Jr., 1987: Cloud-to-ground lightning flash characteristics from June 1984 through May 1985. *J. Geophys. Res.*, **92**, 5640-5644.

Orville, R.E., R.W. Henderson, and L.F. Bosart, 1988: Bipole patterns revealed by lightning locations in mesoscale storm systems. *Geophys. Res. Lett.*, **15**, 129-132.

Orville, R.E., 1990a: Winter lightning along the East Coast. *Geophys. Res. Lett.*, **17**, 713-715.

Orville, R.E., 1990b: Peak-current variations of lightning return strokes as a function of latitude. *Nature*, **342**, 149-151.

Orville, R.E., 1991: Calibration of a magnetic direction finding network using measured triggered lightning return stroke peak currents. *J. Geophys. Res.*, **96**, 17135-17142.

Orville, R.E., 1993: Cloud-to-ground lightning in the Blizzard of '93. *Geophys. Res. Lett.*, **20**, 1367-1370.

Petersen, W.A. and S.A. Rutledge, 1992: Some characteristics of cloud-to-ground lightning in tropical northern Australia. *J. Geophys. Res.*, **97**, 11553-11560.

Pyle, R., 1995: National network status. Preprints, *International Lightning Detection Conference*, Tucson, AZ.

Rakov, V.A., M.A. Uman, and R. Thottappillil, 1994: Review of lightning properties from electric field and TV observations. *J. Geophys. Res.*, **99**, 10745-10750.

Reap, R.M., and D.R. MacGorman, 1989, Cloud-to-ground lightning: Climatological characteristics and relationships to model fields, radar observations, and severe local storms. *Mon. Wea. Rev.*, **117**, 518-535.

Reap, R.M., 1994: Analysis and prediction of lightning strike distributions associated with synoptic map types over Florida. *Mon. Wea. Rev.*, **122**, 1698-1715.

Reible, D.D., J.E. Simpson, and P.F. Linden, 1993: The sea breeze and gravity-current frontogenesis. *Quart. J. Roy. Meteor. Soc.*, **119**, 1-16.

Rutledge, S.A. and D.R. MacGorman, 1988: Cloud-to-ground lightning activity in the 10-11 June 1985 mesoscale convective system observed during the Oklahoma-Kansas PRE-storm Project. *Mon. Wea. Rev.*, **116**, 1393-1408.

Rutledge, S.A. and W.A. Peterson, 1994: Vertical radar reflectivity structure and cloud-to-ground lightning in the stratiform region of MCSs: Further evidence for in situ charging in the stratiform region. *Mon. Wea. Rev.*, **122**, 1760-1776.

Samsury, C.E., and R.E. Orville, 1994: Cloud-to-ground lightning in tropical cyclones: A study of hurricanes Hugo (1989) and Jerry (1989). *Mon. Wea. Rev.*, **122**, 1887-1896.

Silver, A.C., and R.E. Orville, 1995: A climatology of cloud-to-ground lightning for the contiguous United States: 1992-1993. Preprints, *9th Conference on Applied Climatology*, Dallas, TX, American Meteorological Society, 325-330.

Studwell, A.M., and R.E. Orville, 1995: Characteristics of cloud-to-ground lightning in a severe winter storm, 9-12 February 1994. Preprints, *6th Conference on Aviation Weather Systems*, Dallas, TX, American Meteorological Society, 176-181.

Vorphal, J.A., J.G. Sparrow, and E.P. Ney, 1970: Satellite Observations of Lightning. *Science*, **169**, 860-862.

Wagner, C.F., 1963: The relation between stroke current and the velocity of the return stroke, *Trans. AIEE Power Appl Syst.*, **82**, 609-617.

Wallace, J.M., and P.V. Hobbs, 1977: *Atmospheric Science: An Introductory Survey.* Academic Press Inc., 350 pp.

Williams, E.R. 1989: The tripole structure of thunderstorms. *J. Geophys. Res.*, **94**, 13151 - 13167.

Williams, E.R., R. Zhang, and J. Rydock, 1991: Mixed-phase microphysics and cloud electrification. *J. Atmos. Sci.*, **48**, 2195 - 2203.

Winn, W.P., G.W. Schwede, and C.B. Moore, 1974: Measurements of electric fields in thunderclouds. *J. Geophys. Res.*, **79**, 1761 - 1767.

Zipser, E.J., and K.R. Lutz, 1994: The vertical profile of radar reflectivity of convective cells: A strong indicator of storm intensity and lightning probability?. *Mon. Wea. Rev.*, **122**, 1751-1759.

APPENDIX A

EQUATIONS OF BEST FIT

• Case 1 (After) n=13:

- Negative CG flash rate (FR) vs. negative median first stroke peak current I_p

$I_p = 71.141 - 1.906(FR)$ $r^2 = 0.460$

$I_p = 108.64\ FR^{-0.369}$ $r^2 = 0.455$

- Negative multiple regressions

$I_p = 57.552 - 2.26(FR) + 6.566(Mult)$ $r^2 = 0.553$

$\ln I_p = -0.453 \ln (FR) + 0.324 \ln (Mult) + 4.573$ $r^2 = 0.560$

• Case 2 (After) n=9:

- Negative CG flash rate vs. negative median first stroke peak current I_p

$I_p = 114.78\ FR^{-0.235}$ $r^2 = 0.441$

- Negative multiple regressions

$I_p = 138.548 - 5.838(FR) - 10.262(Mult)$ $r^2 = 0.435$

$\ln I_p = -0.211 \ln (FR) - 0.191 \ln (Mult) + 4.743$ $r^2 = 0.508$

• Case 3 (Before) n=16:

- Negative CG flash rate vs. percent positive

$PP = 78.798 - 1.656(FR)$ $r^2 = 0.435$

• Case 3 (After) n=12:

- Negative CG flash rate vs. multiplicity (Mult)

$Mult = 1.622 + 0.003\ FR$ $r^2 = 0.555$

$Mult = 1.13\ FR^{0.124}$ $r^2 = 0.565$

- Negative multiple regressions

$Mult = 1.421 + 0.004(FR) + 0.004(I_p)$ $r^2 = 0.567$

$\ln Mult = 0.121 \ln (FR) + 0.658 \ln (I_p) + 0.226$ $r^2 = 0.566$

-Positive multiple regressions

$\ln I_p = 0.124 \ln (FR) + 0.658 \ln (Mult) + 3.729$ $r^2 = 0.486$

• Case 5 (Before) n=7:

- Negative flash rate vs. percent positive

$PP = 67.529 - 0.979(FR)$ $r^2 = 0.792$

- Positive flash rate vs. positive median first stroke peak current

$I_p = 6.54\ FR^{0.856}$ $r^2 = 0.531$

- Positive multiple regressions

$I_p = 57.677 + 4.114(FR) - 43.631(Mult)$ $r^2 = 0.555$

$\ln I_p = 1.042 \ln (FR) + 1.09 \ln (Mult) + 1.596$ $r^2 = 0.699$

$Mult = 1.005 + 0.049(FR) - 0.007(I_p)$ $r^2 = 0.471$

$\ln Mult = 0.452 \ln (FR) + 0.328 \ln (I_p) + 0.358$ $r^2 = 0.441$

• Case 5 (After) n=25:

- Negative flash rate vs. percent positive

$PP = 21.714 - 0.165(FR)$ $r^2 = 0.563$

- Negative flash rate vs. negative median first stroke peak current

$I_p = 54.871 - 0.190(FR)$ $r^2 = 0.442$

$I_p = 99.88\ FR^{-0.222}$ $r^2 = 0.663$

- Negative multiple regressions

$I_p = 62.839 - 0.190(FR) - 2.903(Mult)$ $r^2 = 0.448$

$\ln I_p = -0.223 \ln (FR) - 0.183 \ln (Mult) + 4.791$ $r^2 = 0.641$

• Case 6 (Before) n=10:

- Negative flash rate vs. negative median first stroke peak current

$I_p = 9.40\ FR^{0.261}$ $r^2 = 0.660$

- Negative multiple regressions

$\ln I_p = 0.230 \ln (FR) + 0.294 \ln (Mult) + 2.030$ $r^2 = 0.748$

• Case 8 (Before) n=5:

- Negative multiple regressions

$I_p = -3.529 + 0.622(FR) + 9.008(Mult)$ $r^2 = 0.534$

$Mult = 1.645 - 0.043(FR) + 0.043(I_p)$ $r^2 = 0.544$

• Case 9 (Before) n=6:

- Negative CG flash rate vs. multiplicity

$Mult = 1.773 + 0.032\ FR$ $r^2 = 0.700$

$Mult = 1.21\ FR^{0.260}$ $r^2 = 0.786$

- Multiplicity vs. negative median first stroke peak current

$I_p = 15.392 + 5.031(Mult)$ $r^2 = 0.417$

- Negative multiple regressions

$I_p = 7.457 - 0.287(FR) + 11.285(Mult)$ $r^2 = 0.692$

$\ln I_p = -0.202 \ln (FR) + 0.987 \ln (Mult) + 3.024$ $r^2 = 0.666$

$Mult = 0.138 + 0.028(FR) + 0.060(I_p)$ $r^2 = 0.902$

$\ln Mult = 0.225 \ln (FR) + 0.639 \ln (I_p) - 1.863$ $r^2 = 0.921$

• Case 9 (After) n=9:

- Negative flash rate vs. negative median first stroke peak current

$I_p = 45.33\ FR^{-0.131}$ $r^2 = 0.463$

- Negative CG flash rate vs. multiplicity

$Mult = 2.204 + 0.016\ FR$ $r^2 = 0.794$

$Mult = 1.92\ FR^{0.120}$ $r^2 = 0.562$

- Negative multiple regressions

$I_p = -8.514 - 0.467(FR) + 20.258(Mult)$ $r^2 = 0.658$

$\ln I_p = -0.267 \ln (FR) + 1.127 \ln (Mult) + 3.079$ $r^2 = 0.849$

$Mult = 1.249 + 0.020(FR) + 0.026(I_p)$ $r^2 = 0.904$

$\ln Mult = 0.204 \ln (FR) + 0.637 \ln (I_p) - 1.777$ $r^2 = 0.877$

• Case 10 (Before) n=7:

- Negative flash rate vs. negative median first stroke peak current

$I_p = 21.46\ FR^{0.102}$ $r^2 = 0.597$

- Negative CG flash rate vs. multiplicity

$Mult = 2.855 + 0.003\ FR$ $r^2 = 0.782$

- Negative multiple regressions

$Mult = 2.931 + 0.004(FR) - 0.002(I_p)$ $r^2 = 0.784$

$\ln Mult = 0.091 \ln (FR) - 0.497 \ln (I_p) + 2.533$ $r^2 = 0.650$

Case 10 (After) n=11:

- Negative flash rate vs. percent positive

$PP = 1.627 + 0.017(FR)$ $r^2 = 0.635$

- Negative CG flash rate vs. multiplicity

$Mult = 2.861 + 0.004(FR)$ $r^2 = 0.507$

$Mult = 1.50\,FR^{0.194}$ $r^2 = 0.628$

- Multiplicity vs. negative median first stroke peak current

$I_p = 4.849(Mult) + 16.041$ $r^2 = 0.496$

$I_p = 15.36\,Mult^{0.614}$ $r^2 = 0.693$

- Negative multiple regressions

$I_p = 11.322 - 0.018(FR) + 6.916(Mult)$ $r^2 = 0.584$

$\ln I_p = -0.089 \ln (FR) + 0.902 \ln (Mult) + 2.748$ $r^2 = 0.782$

$Mult = -0.411 + 0.003(FR) + 0.079(I_p)$ $r^2 = 0.775$

$\ln Mult = 0.125 \ln (FR) + 0.796 \ln (I_p) - 2.073$ $r^2 = 0.895$

• Case 11 (Before) n=5:

- Negative CG flash rate vs. percent positive

$PP = -0.718 + 0.037(FR)$ $r^2 = 0.615$

- Negative multiple regressions

$I_p = 13.531 + 0.044(FR) + 1.863(Mult)$ $r^2 = 0.481$

$\ln I_p = 0.251 \ln (FR) + 0.314 \ln (Mult) + 1.665$ $r^2 = 0.556$

$\ln Mult = -0.394 \ln (FR) + 0.925 \ln (I_p) - 0.065$ $r^2 = 0.466$

• Case 11 (After) n=7:

- Negative flash rate vs. negative median first stroke peak current

$I_p = 46.654 - 0.105(FR)$ $r^2 = 0.679$

$I_p = 1199.91\,FR^{-0.728}$ $r^2 = 0.663$

- Negative CG flash rate vs. multiplicity

$Mult = 5.255 - 0.010(FR)$ $r^2 = 0.689$

$Mult = 67.09\,FR^{-0.575}$ $r^2 = 0.711$

- Multiplicity vs. negative median first stroke peak current

$I_p = 8.953(Mult) - 2.988$ $r^2 = 0.747$

$I_p = 7.30\,Mult^{1.08}$ $r^2 = 0.717$

• Case 11 (After) n=7: (cont.)

- Negative multiple regressions

$I_p = 15.054 - 0.044(FR) + 6.014(Mult)$ $r^2 = 0.784$

$\ln I_p = -0.370 \ln (FR) + 0.622 \ln (Mult) + 4.476$ $r^2 = 0.770$

$Mult = 2.718 - 0.005(FR) + 0.054(I_p)$ $r^2 = 0.790$

$\ln Mult = -0.306 \ln (FR) + 0.370 \ln (I_p) + 1.586$ $r^2 = 0.777$

• Case 12 (Before) $n_{negative}=12$, $n_{positive}=10$:

- Negative CG flash rate vs. negative median first stroke peak current I_p

$I_p = 13.87\ FR^{0.132}$ $r^2 = 0.708$

- Negative CG flash rate vs. multiplicity

$Mult = 2.955 + 0.004\ FR$ $r^2 = 0.413$

$Mult = 1.15\ FR^{0.232}$ $r^2 = 0.768$

- Multiplicity vs. negative median first stroke peak current

$I_p = 4.535(Mult) + 9.92$ $r^2 = 0.776$

$I_p = 13.34\ Mult^{0.534}$ $r^2 = 0.816$

- Negative multiple regressions

$I_p = 10.254 + 0.002(FR) + 4.361(Mult)$ $r^2 = 0.777$

$\ln I_p = 0.034 \ln (FR) + 0.423 \ln (Mult) + 2.570$ $r^2 = 0.827$

$Mult = -0.514 + 0.001(FR) + 0.150(I_p)$ $r^2 = 0.797$

$\ln Mult = 0.105 \ln (FR) + 0.963 \ln (I_p) - 2.390$ $r^2 = 0.862$

- Positive CG flash rate vs. median positive first stroke peak current

$I_p = 0.232(FR) + 9.162$ $r^2 = 0.665$

$I_p = 13.07\ FR^{0.229}$ $r^2 = 0.740$

- Positive multiple regressions

$I_p = 8.620 + 0.232(FR) + 0.302(Mult)$ $r^2 = 0.671$

$\ln I_p = 0.231 \ln (FR) - 0.025 \ln (Mult) + 1.968$ $r^2 = 0.741$

• Case 12 (After) $n_{negative}=11$, $n_{positive}=8$:

- Negative CG flash rate vs. negative median first stroke peak current

$I_p = 120.06\ FR^{-0.259}$ $r^2 = 0.860$

- Multiplicity vs. negative median first stroke peak current I_p

$I_p = -40.07(Mult) + 184.446$ $r^2 = 0.765$

$I_p = 481.55\ Mult^{-2.025}$ $r^2 = 0.687$

• Case 12 (After) $n_{negative}$=11, $n_{positive}$=8: (cont.)

- Negative multiple regressions

$I_p = 174.341 - 0.027(FR) - 35.938(Mult)$ $r^2 = 0.794$

$\ln I_p = -0.189 \ln (FR) - 0.894 \ln (Mult) + 5.603$ $r^2 = 0.931$

• Case 14 (Before) n=7:

- Negative CG flash rate vs. negative median first stroke peak current

$I_p = 54.883 - 0.201(FR)$ $r^2 = 0.569$

$I_p = 77.48\ FR^{-0.167}$ $r^2 = 0.668$

- Negative CG flash rate vs. multiplicity

$Mult = 1.223\ FR^{0.273}$ $r^2 = 0.620$

- Multiplicity vs. negative median first stroke peak current

$I_p = -9.917(Mult) + 76.891$ $r^2 = 0.600$

$I_p = 71.31\ Mult^{-0.406}$ $r^2 = 0.490$

- Negative multiple regressions

$I_p = 70.697 - 0.12(FR) - 6.416(Mult)$ $r^2 = 0.728$

$\ln I_p = -0.147 \ln (FR) - 0.072 \ln (Mult) + 4.365$ $r^2 = 0.508$

$Mult = 5.614 - 0.001(FR) - 0.057(I_p)$ $r^2 = 0.601$

$\ln Mult = -0.23 \ln (FR) - 0.26 \ln (I_p) + 1.330$ $r^2 = 0.627$

• Case 15 (After) n=22:

- Negative CG flash rate vs. multiplicity

$Mult = 2.648 + 0.003\ FR$ $r^2 = 0.665$

$Mult = 1.50\ FR^{0.148}$ $r^2 = 0.649$

- Negative multiple regressions

$Mult = 1.266 + 0.002(FR) - 0.056(I_p)$ $r^2 = 0.707$

$\ln Mult = 0.127 \ln (FR) + 0.464 \ln (I_p) - 1.004$ $r^2 = 0.696$

• Case 16 (Before) n=8:

- Negative CG flash rate vs. multiplicity

$Mult = 2.231 + 0.003\ FR$ $r^2 = 0.629$

$Mult = 0.92\ FR^{0.215}$ $r^2 = 0.510$

- Negative multiple regressions

$Mult = 0.650 + 0.003(FR) + 0.042(I_p)$ $r^2 = 0.668$

$\ln Mult = 0.232 \ln (FR) + 0.383 \ln (I_p) - 1.56$ $r^2 = 0.534$

• Case 16 (Before) n=8: (cont.)

- Positive CG flash rate vs. positive median first stroke peak current I_p

$I_p = 86.955 - 5.146(FR)$ $r^2 = 0.612$

$I_p = 1042.31\ FR^{-0.731}$ $r^2 = 0.678$

- Positive multiple regressions

$I_p = 100.91 - 5.003(FR) - 10.153(Mult)$ $r^2 = 0.619$

$\ln I_p = -0.719 \ln (FR) - 0.736 \ln (Mult) + 5.218$ $r^2 = 0.715$

• Case 16 (After) $n_{negative}=16$, $n_{positive}=13$:

- Negative CG flash rate vs. multiplicity

$Mult = 1.49\ FR^{0.135}$ $r^2 = 0.404$

- Negative multiple regressions

$\ln Mult = 0.133 \ln (FR) - 0.062 \ln (I_p) + 0.641$ $r^2 = 0.405$

- Positive CG flash rate vs. multiplicity

$Mult = 0.912 + 0.162\ FR$ $r^2 = 0.479$

$Mult = 1.03\ FR^{0.291}$ $r^2 = 0.589$

- Positive multiple regression

$\ln Mult = 0.295 \ln (FR) + 0.020 \ln (I_p) - 0.056$ $r^2 = 0.590$

• Case 17 (Before) n=16:

- Negative multiple regressions

$\ln Mult = 0.148 \ln (FR) + 0.422 \ln (I_p) - 1.008$ $r^2 = 0.434$

• Case 18 (Before) n=9:

- Negative CG flash rate vs. negative median first stroke peak current

$I_p = 28.328 - 0.031(FR)$ $r^2 = 0.412$

$I_p = 45.38\ FR^{-0.129}$ $r^2 = 0.411$

- Negative multiple regressions

$I_p = 25.832 - 0.031(FR) + 1.041(Mult)$ $r^2 = 0.425$

$\ln I_p = -0.13 \ln (FR) + 0.09 \ln (Mult) + 3.740$ $r^2 = 0.422$

• Case 18 (After) n=19:

- Negative multiple regression

$\ln Mult = 0.125 \ln (FR) - 0.487 \ln (I_p) + 1.892$ $r^2 = 0.461$

• Case 20 (After) n=12:

- Negative CG flash rate vs. percent positive (PP)

$PP = 22.577 - 0.072(FR)$ $r^2 = 0.481$

- Negative CG flash rate vs. multiplicity

$Mult = 2.433 + 0.003\ FR$ $r^2 = 0.447$

$Mult = 1.83\ FR^{0.101}$ $r^2 = 0.695$

- Negative multiple regressions

$Mult = -0.101 + 0.003(FR) - 0.067(I_p)$ $r^2 = 0.593$

$\ln Mult = 0.111 \ln (FR) - 0.653 \ln (I_p) - 1.772$ $r^2 = 0.761$

• Case 21 (Before) n=8:

- Negative CG flash rate vs. percent positive

$PP = 9.541 - 0.01(FR)$ $r^2 = 0.767$

- Negative CG flash rate vs. multiplicity

$Mult = 3.908 - 0.001\ FR$ $r^2 = 0.814$

$Mult = 8.356\ FR^{-0.151}$ $r^2 = 0.870$

- Negative multiple regressions

$I_p = -32.747 - 0.022(FR) + 15.928(Mult)$ $r^2 = 0.571$

$Mult = 2.883 - 0.001(FR) + 0.035(I_p)$ $r^2 = 0.917$

$\ln Mult = -0.154 \ln (FR) + 0.191 \ln (I_p) + 1.485$ $r^2 = 0.909$

- Positive multiplicity vs. positive median first stroke peak current

$I_p = 13.305(Mult) + 2.165$ $r^2 = 0.588$

$I_p = 15.502\ Mult^{0.836}$ $r^2 = 0.537$

- Positive multiple regressions

$I_p = -3.98 + 0.214(FR) + 14.658(Mult)$ $r^2 = 0.725$

$\ln I_p = 0.209 \ln (FR) + 0.908 \ln (Mult) + 2.094$ $r^2 = 0.648$

$Mult = 0.561 - 0.012(FR) + 0.049(I_p)$ $r^2 = 0.725$

$\ln Mult = -0.183 \ln (FR) + 0.699 \ln (I_p) - 1.306$ $r^2 = 0.648$

• Case 21 (After) n=28:

- Negative CG flash rate vs. negative median first stroke peak current

$I_p = 42.783 - 0.016(FR)$ $r^2 = 0.502$

$I_p = 86.488\ FR^{-0.151}$ $r^2 = 0.411$

• Case 21 (After) n=28: (cont.)

- Negative CG flash rate vs. multiplicity

$Mult = 2.220 + 0.001\ FR$ $r^2 = 0.502$

$Mult = 1.265\ FR^{0.123}$ $r^2 = 0.576$

- Negative multiple regressions

$I_p = 53.638 - 0.012(FR) - 4.890(Mult)$ $r^2 = 0.542$

$\ln I_p = -0.152 \ln (FR) + 0.012 \ln (Mult) + 4.457$ $r^2 = 0.766$

$Mult = 2.919 + 0.001(FR) - 0.016(I_p)$ $r^2 = 0.542$

$\ln Mult = 0.125 \ln (FR) + 0.019 \ln (I_p) + 0.151$ $r^2 = 0.576$

- Multiplicity vs. positive median first stroke peak current

$I_p = -11.127(Mult) + 65.371$ $r^2 = 0.413$

$I_p = 70.598\ Mult^{-0.703}$ $r^2 = 0.435$

- Positive multiple regression

$\ln Mult = 0.140 \ln (FR) + 0.256 \ln (I_p) - 0.983$ $r^2 = 0.424$

• Case 22 (After) n=7:

- Negative CG flash rate vs. percent positive

$PP = 56.878 - 3.88(FR)$ $r^2 = 0.593$

- Negative CG flash rate vs. negative median first stroke peak current I_p

$I_p = 48.716\ FR^{-0.265}$ $r^2 = 0.579$

- Negative CG flash rate vs. multiplicity

$Mult = 3.607\ FR^{-0.154}$ $r^2 = 0.537$

- Multiplicity vs. negative median first stroke peak current I_p

$I_p = 19.617(Mult) - 22.68$ $r^2 = 0.920$

$I_p = 6.411\ Mult^{1.547}$ $r^2 = 0.865$

• Case 24 (Before) n=9:

- Negative CG flash rate vs. percent positive

$PP = 0.74(FR) - 1.279$ $r^2 = 0.588$

- Negative CG flash rate vs. multiplicity

$Mult = 0.94\ (FR)^{0.349}$ $r^2 = 0.698$

- Negative multiple regression

$\ln Mult = 0.366 \ln (FR) - 0.209 \ln (I_p) + 0.622$ $r^2 = 0.711$

• Case 24 (After) n=19:

- Negative CG flash rate vs. multiplicity

$Mult = 2.102 + 0.013\ FR$	$r^2 = 0.437$
$Mult = 1.10\ FR^{0.242}$	$r^2 = 0.531$

- Negative multiple regressions

$Mult = 2.351 + 0.013(FR) - 0.007(I_p)$	$r^2 = 0.439$
$\ln Mult = 0.171 \ln (FR) + 0.25 \ln (I_p) - 0.536$	$r^2 = 0.536$

APPENDIX B

SYNOPTIC OVERVIEW

The following discussion provides the synoptic overview of the cases examined in this research. The time of the crossing of the geographic center of the lightning is given in the section title. The format is date and time in UTC. Hereafter, all times are given in UTC.

1. Cases 1 (06/2000) and 2 (06/2300)

The geographic centers of the lightning of these two frontal storms crossed the coastline within three hours of one another. However on 6 September, Case 1 crossed the east coast of Florida at 2000, while Case 2 moved onshore north of Tampa, Florida at 2300. A surface low was off of the North Carolina coast near Cape Hatteras. A cold front extended across the Florida panhandle from Jacksonville parallel to the Gulf coast to near Mobile, Alabama. There was a steady westerly upper-level flow at all levels. There were no upper-level troughs in the region.

2. Case 3 (14/0700)

Case 3 was a frontal storm that moved offshore near Myrtle Beach, South Carolina on 14 March. A low in southern Quebec had a cold front extending along the western edge of the Appalachian Mountains. At 14/0300, a trough was on the east side of the mountain. By 14/0600, the trough was analyzed as a cold front from the low center and had past Columbia, South Carolina. The geographic center of the case passed over the coastline at 14/0700. After 14/0900, the cold front passed Charleston, South Carolina.

At the 850 mb level, there was a low over western Ontario. There was an associated trough extending southeastward across North Carolina. During the 14/0000 sounding, the 850 mb flow was 35 knots from 290° at Charleston. At the 700 mb level, the low was in northern Manitoba with a trough through Tennessee and western Georgia. The 700 mb flow at Charleston was 25 knots from 250°. At the 500 mb level, there was no low identified but there was a sharp trough southward through North Carolina and South Carolina. The 500 mb flow at Charleston was 65 knots from 290°.

3. Case 5 (25/0745)

Case 5 was a frontal storm that moved offshore near Myrtle Beach, South Carolina on 25 March. At 25/1200, there was a surface low in southern Quebec and the cold front extended along the east side of the Appalachian Mountains. A second low was near Charlotte, North Carolina along the front. The storms associated with this case may have been generated by outflow boundaries.

At 25/1200, there was an 850 mb trough analyzed near the Tennessee / North Carolina border extending southward to near Mobile, Alabama. The 850 mb flow at Charleston, South Carolina was 40 knots from 260°. The 500 mb and 750 mb charts were not available.

4. Cases 6 (14/2130) and 7 (14/2130)

Cases 6 and 7 were frontal storms that moved offshore during 14 April. These cases were associated with the same frontal system. Case 6 moved offshore near Jacksonville, Florida, while Case 7 crossed the coast north of Daytona Beach, Florida. At 14/1800, the surface low was centered over central Quebec with an associated cold front extending along the Atlantic seaboard. The front crossed the coastline between Jacksonville and Cape Kennedy, Florida.

At 15/0000, there was an 850 mb low located north of Hudson Bay. The 850 mb flow at Daytona Beach was 230° at 10 knots. At the 700 mb level, the upper-level low was north of Hudson Bay. There was a sharp trough extending southeastward across New England. The 700 mb flow at Daytona Beach, Florida was 250° at 10 knots. At the 500 mb level, the upper-level low was southeast of James Bay. The 500 mb flow at Daytona Beach, Florida was 260° at 25 knots.

5. Case 8 (16/2245)

Case 8 was a non-frontal storm that moved offshore near Daytona Beach, Florida on 16 April. At 16/2100, there was a surface low south of James Bay. A cold front extended over the Atlantic and curved back to cross the eastern Florida coast south of St. Augustine. By 17/0000, the cold front moved south past Melbourne.

The upper-level data was not available for the 700 mb and 850 mb levels at 17/0000. At the 500 mb level, there was a low center southwest of James Bay with a trough to the southeast across Virginia. At Daytona Beach, the 500 mb flow was 280° at 20 knots.

6. Case 9 (02/0130)

Case 9 was a frontal storm which moved offshore north of Savannah, Georgia on 2 May. There were no surface analysis charts available for this time period. The Weather Depiction charts generated at the National Meteorological Center were used. These charts showed a cold front off of the Georgia - South Carolina coast at 02/1900. (The previous Weather Depiction charts did not have any frontal analysis.) There were no upper-level charts available for this time period.

7. Case 10 (04/1115)

Case 10 was a frontal storm which moved offshore north of Savannah, Georgia on 4 May. At 04/0900, there were two surface lows identified in the area of the storm. One was north of Wilmington, North Carolina and the second was west of Brunswick, Georgia. A cold front connected the low centers and extend to the southwest into the Gulf of Mexico. By 04/1200, the low that was over Georgia moved offshore along with the cold front. There was no upper-level data available for this case.

8. Case 11 (18/2115)

Case 11 was a frontal storm which moved offshore near Miami, Florida on 18 May. At 18/2100, there was a surface low north of Tampa, Florida. A stationary front was analyzed across the Florida peninsula. The front crossed the Atlantic coast north of West Palm Beach, Florida. There was no upper-level data available.

9. Case 12 (10/2100)

Case 12 was a non-frontal storm that moved offshore near Miami, Florida on 10 June. At 10/2100, there was a surface low over eastern Kentucky and an associated stationary front through southern South Carolina. There was also a cold front westward across Arkansas.

At 11/0000, there was an upper-level high centered over the Gulf of Mexico. At Daytona Beach, Florida, the 700 mb and 850 mb flow was 350° at 15 knots. At 500 mb, the flow was 350° at 10 knots.

10. Case 13 (17/2100)

Case 13 was a non-frontal storm that moved offshore near Fort Myers, Florida on 17 July. There was a high pressure center over the Gulf of Mexico south of Mississippi. There were no fronts analyzed in the southeastern United States. At

18/0000, there was high pressure center at 700 mb over the eastern Gulf of Mexico near the Florida coast. At Tampa, Florida, the 850 mb flow was 070° at 10 knots. The 700 mb flow was 040° at 10 knots, while the 500 mb data were not available.

11. Case 14 (11/0645)

Case 14 was a frontal storm that moved from sea to land near Charleston, South Carolina on 11 August. At 11/0600, there was a surface low to the southeast of Charleston. An associated coastal front was parallel to the coastline. The front moved onshore by 1000.

At 11/0000, there was an 850 mb high over northern Arkansas. The 850 mb flow at Charleston was 090° at 10 knots. At 700 mb, the high center was over northeastern Arkansas and the upper-level winds were 080° at 10 knots. There were no upper-level circulation center identified at 500 mb and the 500 mb winds at Charleston were 180° at 10 knots.

12. Case 15 (22/0030)

Case 15 was a frontal storm that moved offshore near Daytona Beach, Florida on 22 August. At 22/0000, a low pressure was analyzed over the Atlantic Ocean east of New Jersey. An associated cold front was located along the Atlantic seaboard south into northern Georgia. Outflow boundaries were analyzed in northern Florida.

At 22/0000, there was a low center east of Hudson Bay at both the 700 mb and 850 mb levels. A trough extended to the southwest through northeastern Alabama. The 700 mb and 850 mb flow at Waycross, Georgia were 260° at 25 and 15 knots, respectively. At 500 mb, there was a low center in southern Ohio. The associated trough extended through central Alabama. The 500 mb flow at Waycross was 270° at 25 knots.

13. Case 16 (02/2215)

Case 16 was a frontal storm that moved offshore north of Charleston, South Carolina on 2 September. At 02/2100, a surface low was analyzed near Savannah, Georgia. There was an associated cold front extending along the Atlantic coast. At the 850 mb level, there was a low center over northern Alabama and a high center over Texas at 03/0000. The 850 mb flow at Charleston, South Carolina was 250° at 5 knots. At 700 mb, there was a high center over Texas. The 700 mb flow at Charleston was 300° at 15 knots. At the 500 mb level, there was a weak trough through

northwestern Alabama. There were also high centers over Texas and the Gulf of Mexico west of Tampa, Florida. The 500 mb flow at Charleston was 300° at 15 knots.

14. Case 17 (07/0200)

Case 17 was a frontal storm that moved offshore near the Texas - Louisiana border on 7 September. At 07/0300, there was a surface low over northern Virginia with an associated cold front parallel extending southward. The front became parallel to the Gulf coast in Louisiana and eastern Texas.

There were no 850 mb level data available for any time period. Additionally, for 07/0000, there was no sounding data from Lake Charles, Louisiana because the storm was over the station. At 06/1200, the 850 mb flow was 010° at 5 knots. There was high center near Houston, Texas. At 700 mb, there was a high center over Corpus Christi, Texas and the flow at Lake Charles was calm. At 500 mb, the high center was south of Lake Charles and the flow was 280° at 5 knots.

15. Case 18 (09/2215)

Case 18 was a non-frontal storm that moved offshore near the Georgia - South Carolina border on 9 September. At 09/0300, there was a surface low southwest of Roanoke, Virginia. The associated cold front extended to the south and curved to lie parallel to the Gulf Coast across the Florida panhandle.

At the 700 mb and 850 mb levels, there were no distinguishable upper-level features at 09/0000. At Charleston, South Carolina, the 700 mb flow was calm, while the 850 mb flow was 230° at 15 knots. At 500 mb, there was a trough in western Georgia. The 500 mb flow at Charleston was 260° at 20 knots.

16. Case 19 (14/1930)

Case 19 was a non-frontal storm which moved from over the water to over land near Galveston, Texas on 14 September. At 14/1800, there was a surface high over western North Carolina. The prevailing winds at Galveston were 130° at 10 knots, while the surface temperature was 28°C. At the 850 mb level, there was a low center over the Yucatan peninsula. The 850 mb flow was 110° at 15 knots. The 500 mb and 700 mb flows were 5 knots from 90° and 110°, respectively.

17. Case 20 (18/0000)

Case 20 was a non-frontal storm that moved offshore north of Brunswick, Georgia during 17 and 18 September. At 17/2100, there were surface lows over eastern Mississippi and central New York. A cold front connected the two centers and extended into Louisiana.

At 18/0000, there was a 850 mb trough which extended through Kentucky to southern Mississippi. The 850 mb flow at Waycross, Georgia was 270° at 30 knots. At the 700 mb level, there was a low over Arkansas, while there was a high off of the Georgia / South Carolina coast. The 700 mb flow at Waycross was 270° at 15 knots. At the 500 mb level, there was a low east of Hudson Bay. There was also an associated trough through eastern Alabama. The 500 mb flow at Waycross was 230° at 20 knots.

18. Case 21 (18/2200)

Case 21 was a frontal storm which moved offshore near the North Carolina - South Carolina border on 18 September. At 18/2100, there were surface lows analyzed over Charleston, South Carolina and the Florida panhandle. There was a cold front connecting the two cyclones. At 19/0000, there was 850 mb low over the South Carolina coast. The 850 mb flow at Charleston, South Carolina was 270° at 25 knots. At the 700 mb level, there was a trough extending southward through central South Carolina and eastern Georgia. The 700 mb flow was 260° at 20 knots. At the 500 mb level, the trough was over western South Carolina and central Georgia. The 500 mb flow was 270° at 30 knots.

19. Case 22 (11/1800)

Case 22 was a frontal storm that moved onshore near Tampa, Florida on 11 October. At 11/1500, there was a surface low south of Applachicola with a warm front extending east across the panhandle. There was an associated cold front trailing to the south across the Gulf of Mexico.

At 11/1200, there was an 850 mb lows southeast of Lake Charles, Louisiana. At Tallahassee, Florida, the 850 mb flow was 100° at 10 knots. There was a 700 mb low near Beaumont, Texas. The 700 mb flow was 180° at 5 knots. There were no 500 mb data available.

20. Case 23 (30/1200)

Case 23 was a frontal storm which moved offshore near Brunswick, Georgia on 30 October. At 30/1200, there were surface lows located south of Panama City and east of the South Carolina coast. A stationary front connected the lows. By 30/1500, the front was analyzed as a cold front moving south across the Florida peninsula.

At 30/1200, there were no 700 mb or 850 mb data available. The 500 mb flow at Waycross, Georgia was 190° at 30 knots.

21. Case 24 (11/0715)

Case 24 was a frontal storm that moved offshore north of Brunswick, Georgia on 11 November. At 0900, the surface low center was south of Jacksonville, Florida. There was an associated stationary front analyzed across the Florida peninsula.

At 1200, there was a 850 mb low over the Mississippi - Alabama border. The 850 mb flow at Waycross, Georgia was 200° at 5 knots. There was a 700 mb low north of Pensicola. The 700 mb flow at Waycross was 260° at 25 knots. The 500 mb level data was not available.

APPENDIX C

ABBREVIATIONS

B_{peak} - peak magnetic field
c - speed of light
CAPE - convective available potential energy
CG - cloud-to-ground
DF - direction finder
DMSP - Defense Meteorological Satellite Program
FR - flash rate
IC - intercloud
IDL - Interactive Data Language
i_{peak} - peak current
I_p - first stroke peak current
LCL - lifted condensation level
LFC - level of free convection
LLJ - low level jet
LWC - liquid water content
mb - millibar
MCC - mesoscale convective complex
MDF - magnetic direction finder
Mult - multiplicity
NLDN - National Lightning Detection Network
PJ - polar jet
r - range from the detector to the ground strike point of the CG flash
r^2 - correlation coefficient
SJ - subtropical jet
TOA - time-of-arrival system
UTC - universal time code
v - velocity of the return stroke
V_{rs} - return stroke propagation speed
W - empirical constant
μ_o - conductivity of free space
Θw - wet bulb potential temperature

VITA

AARON MARK STUDWELL

EDUCATION:

1995	M. S. degree in Meteorology, Texas A&M University
1989 - 1990	Graduate courses in Aerospace Engineering, University of Maryland
1987	B. S. Eng. degree in Aerospace Engineering, University of Michigan

EMPLOYMENT:

1993 - Present	Research Assistant, Texas A&M University, Department of Meteorology
1991 - 1993	Mechanical Systems Design Engineer - Antilock Braking Systems, Delco Chassis Division - General Motors
1989 - 1991	Defense Systems Engineer - Strategic Defense Initiative, Teledyne Brown Engineering
1988 - 1989	Associate Engineer - NASA - Goddard Space Flight Center, Computer Sciences Corporation

MAJOR FIELD OF SPECIALIZATION:

Cloud physics and mesoscale phenomena

PERMANENT MAILING ADDRESS:

1515 Rudel Road, Apt. #1101
Tomball, Texas 77375